Biomass gasification in small scale plants: experimental and modelling analysis

Elisa Pieratti

UNIVERSITÀ DEGLI STUDI DI TRENTO
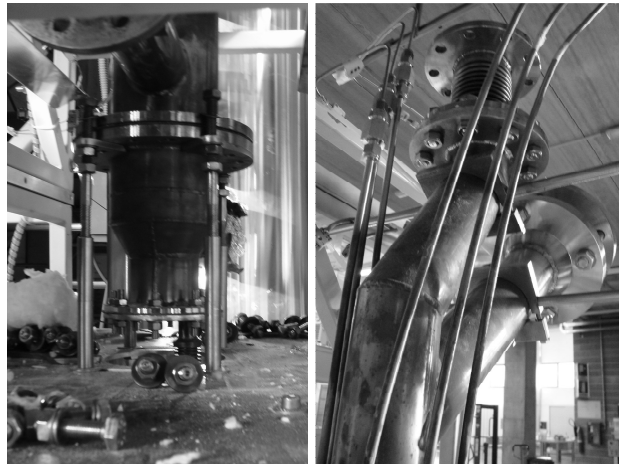Dipartimento di Ingegneria Civile
e Ambientale

2011

Biomass gasification in small scale plants:

experimental and modelling analysis

Elisa Pieratti

2011

"Life is not waiting for the storm to pass but learning to dance in the rain"
Anonymous

A te, che colori la mia vita

Acknowledgements

Three years have gone and a lot of things have happened. There have been difficult moments, but others of fun and real happiness. I have met a lot of people, gaining new friends. I'd like to thank all the people that for months, days or only for few hours have walked with me during these three years.

Thanks to:

Paolo Baggio, for giving me the possibility of doing this PhD and for being always helpful in spite of his busy activity,

My friend and colleague Alessandro; he has shared not only the office but also the desk with me, every day for three years. Thank you for your kindness, your help and for making me laughs every day,

Lorenzo Tognana for his precious help during the experimental activity and for the time spent answering to all my questions, especially in the last months,

Giulia that has shared with me several PhD courses, a lot of coffee breaks and lunches. She has always time for everyone. Thanks to be so nice,

Marco Baratieri, who has patiently explained to me the secrets of its code,

Sergio Ceschini and all the people of Sofcpower for their support in the experimental activity

Prof. Klas Engvall for his interest and support towards my thesis,

Thomas and Vera, for the time spent together during my stay in Stockholm,

Damiano for the GC measurement and Elisa Carlon, for her help in the modeling activity,

Laura Martuscelli and Elena Uber for their precious work,

Thanks to all the people that have shared the time with me at the conferences:
Marco, Alessandro, Daniele, Francesca, Andrea, Luca, Maurizio, Anna…
§
I'd like to thank Michele who, in spite of the distance and the hard work, finds the time to wake me up and to be present in my life every day,

Chiara, which is the best friend one can have, always smiling and happy,

Stefano, thanks for your nice mails and messages,

DenisSS, Riccardo, Elena, Pino, Giorgio, Nicola
the time spent with you, my friends, is always the best,
§
Denis, my husband, for his care and love, for walking every day with me, hand in hand,

And to my mum and all my family for beings always with me, with love.

Contents

List of symbols and acronyms

Roman

A	Area [m²]
a_{ik}	Number of atoms of the *k- th* element found in the molecule of the *i-th* specie
A_k	Total number of atoms of the *k- th* element *(k = 1, …, M)*
C	Carbon
c_p	Specific heat at constant pressure [kJ kg^{-1} K^{-1}]
C_p	Molar heat capacity at constant pressure [kJ kmol^{-1} K^{-1}]
F_{se}	Stoichiometric air to fuel ratio
G	Molar Gibbs energy [kJ kmol^{-1}]
h	Heat transfer convective coefficient [W m^{-2}·K^{-1}]
$H(T)$	Heat source [kJ kmol^{-1}]
H_{in}	Reactants entalphy (in input)
H_{out}	Products entalphy (in output)
i	*i-th* species
L	Lagrange function
m	Mass [kg]
m_b	feeding rate [kg s^{-1}]
$\dot{m}$	Mass flow [kg s^{-1}] or [kmol s^{-1}]
M	Molar mass [kg kmol^{-1}]
n	Number of moles
$\vec{n}^0$	Initial composition vector
N^0_{input}	Initial input vector
N^1_{input}	Modified initial input vector
N^*_{input}	Modified initial input vector
P	Pressure [bar]
Q	Heat source [W m^{-3}]
r	Radial coordinate [m]
R	Gas constant
R_d	Radius
S	Molar entropy [kJ kmol^{-1} K^{-1}]
t	Time [s]
T	Temperature [K] or [°C]
U	Molar internal energy [kJ kmol^{-1}]
U	velocity [m s^{-1}]
V	Molar volume [m³ kmol^{-1}]
V_b	Volume of the biomass treated
x	Molar fraction
Y	Specific gaseous yield [Nm³ kg^{-1}]
z	Axial coordinate [m]

Greek

ΔH	Molar enthalpy change [kJ kmol^{-1}]
ΔH^0	Standard molar enthalpy change [kJ kmol^{-1}]
ΔH_f^0	Standard molar enthalpy change of formation [kJ kmol^{-1}]
ΔH^T	Molar enthalpy change at fixed temperature [kJ kmol^{-1}]
β	Correction parameter for the converted biomass

ε	Efficiency
ϕ	porosity
θ	Heating rate [K s^{-1}]
λ	Thermal conductivity [W m^{-1}·K^{-1}]
λ_b	Biomass thermal conductivity [W m^{-1}·K^{-1}]
λ_k	Lagrange multiplier for the *k- th* element
η_c	Carbon conversion efficiency
μ	Chemical potential [kJ kmol^{-1}]
ν_j	Stoichiometric coefficients
ξ_j	Extents of the reaction
ρ	Density [kg m^{-3}]
ρ	Biomass density [kg m^{-3}]
τ_0	time constant [s]

Acronyms

AFC	Alkaline Fuel Cells
ar	As Received
B-IGFC	Biomass Integrated gasification fuel cell system
BFB	Bubbling Fluidized Bed gasifier
CHP	Combined Heat and Power generation
CFB	Circulating Fluidized Bed gasifier
CFD	Computational fluid Dynamics
daf	Dry Ash Free
DMFC	Direct Methanol Fuel Cells
EF	Entrained Flow gasifier
ER	Equivalence Ratio
EFQ	Engine Fuel Quality
FEM	Finite Element Method
GC	Gas-Chromatograph
HHV	Higher Heating Value [kJ kmol^{-1}] or [kJ Nm^{-3}] or [kJ kg^{-3}]
HNN	Hybrid Neural network
HRSG	Heat Recovery Steam Generator
HV	Heating Value [kJ kmol^{-1}] or [kJ Nm^{-3}] or [kJ kg^{-3}]
IGCC	Integrated Gasification Combined Cycles
LHV	Low Heating Value [kJ kmol^{-1}] or [kJ Nm^{-3}] or [kJ kg^{-3}]
MCFC	Molten Carbonate Fuel Cells
NN	Neural network
PAH	Polyciclic Aromatics Hydrocarbons
PAFC	Phosphoric Acid Fuel Cells
PEMFC	Proton Exchange Membrane Fuel Cells
PFD	Process Flow Diagram
*RMS*error	Root mean square error
rpm	Revolutions Per Minute
RTD	Resistance Temperature Detector
SC	Steam to Carbon ratio
SOFC	Solid Oxide Fuel Cells

List of figures

XII

List of tables

Summary

In the last years the depletion of fossil fuels and the increasing of the world energy demand, has foster the interest for renewable energies, including biomass for energy production. The use of biomass as a renewable energy source in industrial applications has increased during the last decade and now it is considered one of the most promising renewable sources.

The large amount of biomass available, that potentially has an energy content that could be usefully exploited, is often disposed of as waste (in some case aggravating environmental problems). It is of primary interest to understand how to exploit its energy content. As it is well known, the thermo-chemical conversion of biomass to energy can be carried out by means of different processes:

- combustion,
- pyrolysis,
- gasification.

The gasification process, on which this project focuses, basically consists of some physical and chemical reactions to obtain the conversion from a primary fuel (liquid or solid) to a new kind of fuel in the gas phase (called syngas). The feedstock is heated in absence of oxygen or in sub-stoichiometric conditions; this turns the biomass into a hydrogen rich gas which can be transported and burned in different locations. The possible gasifying agents are: steam, air (or pure oxygen) or a mix of them. The products emanating from the gasification process mainly comprise a mixture of the permanent gases CO, CO_2, H_2 and CH_4, steam, char, tars and ash.

Recently, gasification of biomass for production of synthesis gas has gained renewed attention. The reason is that the synthesis gas may be utilized in downstream process for production of motor fuels, or in gas turbine and fuel cells for energy production. For example, if the raw synthesis gas is sufficiently cleaned from tars it may be used for production of dimethylether (DME) or Fischer – Trops fuels which may be utilized as fuel in diesel engines (reducing the dependence on fossil energy sources in the motor fuel segment), or if the hydrogen concentration is remarkable it can feed fuel cells. However, as mentioned above, the raw synthesis gas needs to be cleaned from tars before it may be upgraded to other commodities.

At present the research on biomass gasification follows two routes. One focuses on the optimization of the syngas production by means of a proper design of the plant (i.e. fixed or fludized bed, downdraft or up-draft configuration) and the right choices of the parameters values (reaction temperature, type and amount of gasifying agent), the other one focuses on the research of economic and efficient catalysts for tar cracking.

The aim of the present project is to evaluate the potentiality of the steam gasification process for energy production in small scale applications, linking the two research lines. In a first phase a steam gasification plant has been built and tested. Then, thanks to the collaboration with the University of Stockholm, different types of catalysts (dolomite and iron) have been tested. The dolomite has been chosen as the best solution for the steam gasification plant developed in the first part of the project. Thus a cleaning section for the tar cracking has been added to the steam gasifier. Finally the syngas suitability for a fuel cell has been evaluated and some preliminary tests coupling the gasifier with a SOFCs stack have been run.

The present thesis is divided in the following chapters:

- o In *chapter 1* the basic concepts of biomass gasification, gas cleaning and fuel utilization are summarized;
- o In *chapter 2* a literature review on the operative existing plants at pilot, small and lab scale and on the modelling approach at the biomass gasification field is reported. Then the influence of the main gasification parameters has been investigated;
- o *Chapter 3* reports the experimental activity performed in the small scale fixed bed gasifier that has been developed within this project. The final goal is to evaluate the syngas suitability for solid oxide fuel cells stack. During the experimental activity the gasifier has been equipped with a hot gas cleaning system developed in collaboration with the University of Stockholm.
- o In *chapter 4* the comparison between the experimental data and the outputs of a thermodynamic stoichiometric equilibrium model has been reported. In a second moment, a non stoichiometric equilibrium model has been built to be tuned up with the experimental data; a better agreement has been reached between the predicted syngas composition and the measured one.
- o In *chapter 5* the tests run at KTH, Stockholm, in a fluidized bed gasifier to test the efficiency in tar cracking of different types of catalysts have been reported. A comparison between the experimental gas composition and the equilibrium model predictions is also shown.
- o Finally, in *chapter 6* some conclusion and outlooks for the future have been drawn.

Chapter 1

Overview

1.1 Introduction

Until the end of 1800, when in the industrialized countries the fossil fuels era began, biomass was the first supplier of the world's energy demand. From the coming of the era of fossil fuels the biomass as energy source started to be faced out, slowly at first and then more quickly, even if biomass continued to be a major source of energy in most of the developing countries.

After the coming of fossil fuels there were two occasions when the biomass went back to be an important source of energy. One was in the 1970s in the occasion of the First Oil Shock when many governments again considered biomass as a viable, domestic energy resource with the capacity of decreasing the dependence on the fossil fuels and on the countries suppliers. From the First Oil Crisis, a slow but continuous increasing of the percentage of energy produced by biomass was registered. For example in U.S. at the end of 1970s the contribution of biomass to the global energy demand was around 2%, and by 1990 it was increased to 3.2%. The same trend was registered in Canada and for other industrialized countries [Klass, 1998]. The second occasion was during the 1980s when a renewed interest toward biomass was seen. This time the main reason was a global concern for the depletion of fossil fuels that are running out quite quickly. Additionally, since 15 years, an increasing attention of the population for the environment has been seen (greenhouse effect, level of pollutants in the atmosphere, overheating of the earth have become common arguments of discussion). This fact has driven from one side the governments to start policies to support the production of energy from clean and renewable sources and, from the other, has led the research centres and companies to study for improving the efficiency of traditional system (for heat and electricity production) and to look for new technologies for the exploitation of renewable resources.

1.2 Biomass framework

Biomass is a terms that has different tone according to the field of discussion. For ecology and biological application, biomass indicates the total amount of living material in a given habitat, population, or sample. Instead, for the energy and chemical industry, biomass also refers to the organic material on Earth that has stored sunlight in the form of chemical energy. The word "Biomass" includes wood, wood waste, straw, manure, sugar cane, and many other by-products from a variety of agricultural processes. Currently many people advocate the use of biomass for

energy as it is readily available, whereas fossil fuels, such as petroleum, coal, or natural gas, take millions of years to form in the Earth and are finite and subject to depletion as they are consumed.

The biomass is considered a "renewable carbon resource" but this is not completely true. Many reactions, reversible or not, occur in a way that the carbon is stored in different form, including fossil carbon. Which source of carbon can be considered renewable or not is just a matter of time. Fossil fuels could be also a renewable source if the society could wait million of years, unfortunately it cannot. In our society, biomasses are one of the major fixed-carbon containing materials that renew themselves in a time short enough to make them continuously available. In figure 1.1, the main paths of production and transformation of the biomass are schematized.
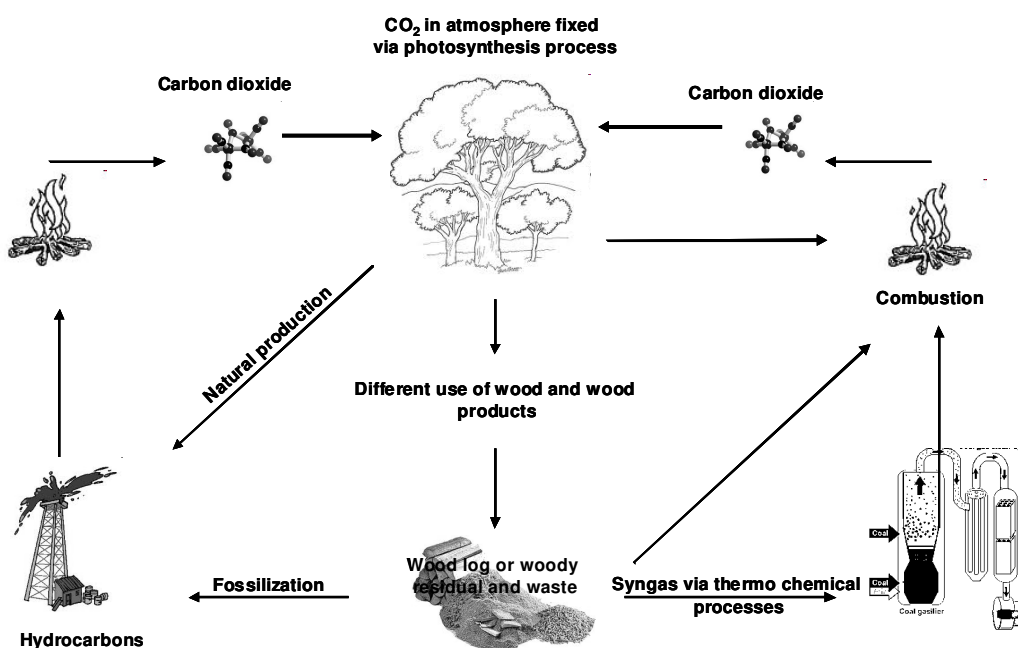
Figure 1.1 Main paths of biomass transformation

1.3 Biomass properties

1.3.1   Chemical properties

The content of certain chemical elements is important for utilization of the biomass itself. The ultimate analyses consist on the measurements of the content of the chemical elements, such as Carbon (C), Hydrogen (H), Oxygen (O), Sulphur (S) and Nitrogen (N),usually expressed in mass % on dry material (wt% dry) or in mass % on dry and ash free material (wt% daf) or in mass % as received material (wt% ar). According to the type of biomass, the elemental composition can be significantly different and the ash content can vary remarkable. On average, the typical values for wood or woody residues are: Carbon 40-50%, Hydrogen 6%, Oxygen below 40%, Nitrogen in most of the case below 1% and Sulphur around 0.5%. In table 1 the composition of common biomasses

are reported. The moisture content is also measured by drying the raw material at 105°C. The ash content, which also varies considerably, is measured by combustion of raw material at 550°C. At chemical level, biomass is mainly composed by cellulose (40-80% in mass), lignin (25-35% in mass) and hemi cellulose (15-30% in mass).

Table 1.1 Ultimate analysis of different biomasses in % dry matter [Hall, 1987]

Residue	Ash	C	H	O	N	S
Black oak	1.34	49.0	6.0	43.5	0.15	0.02
Douglas-fir	0.10	50.6	6.2	43.0	0.06	0.02
Red alder	0.41	49.6	6.1	43.8	0.13	0.07
Cotton gin trash	14.7	42.8	5.1	35.4	1.53	0.55
Grape pomace	4.85	54.9	5.8	32.1	2.09	0.21
Peach pits	0.05	49.1	6.3	43.5	0.48	0.02
Rice hulls	21.0	38.3	4.4	35.5	0.83	0.06
Wheat straw	6.53	48.5	5.5	39.1	0.28	0.05
Rice straw	17.40	41.4	5.1	39.9	0.67	0.13
Sugarcane Bagasse	3.90	47.0	6.1	42.7	0.30	0.10
Coconut shell	1.80	51.1	5.7	41.0	0.35	0.10
Potato Stalks	12.92	42.3	5.2	37.2	1.10	0.21
Lignite	9	70	5.2	22.8	1.99	-
Bituminous Coal	10	80.9	6.1	9.6	1.55	1.88

1.3.2   Proximate analysis

As other solid fuels, biomass can be subjected to a proximate analysis that indicates the water, ash, volatiles and fixed carbon content. The *ash* is usually expressed in weight % on dry bases or in weight % as received material, the *water* in weight % on wet bases and the total amount of *volatile* is expressed in weight % on dry material or as received material or on dry and ash free material. The fixed carbon is calculated as the remaining part according to the formulas reported in table 1.2.

Table 1.2 Fixed carbon calculation [Phyllis]

Dry	Fixed C = 100- ash(dry)- volatiles(dry)
Daf (Dry Ash Free material)	Fixed C = 100-Volatiles (daf)
Ar (As Received)	Fixed C = 100-ash (ar)-water content – volatiles (ar)

A typical plant residue has about 80% of volatiles and 20% of fixed carbon. This means that if the residue is treated by means of a pyrolysis process, about 20% of the initial biomass will result in charcoal, while the 80% will turn in gas and tar. As examples, the proximate analyses performed on different type of biomass are reported in table 1.3.

Table 1.3 Proximate analysis and HHV of some biomass fuels, weight % dry basis [Hall, 1987]

	Volatile matter	Fixed carbon	Ash	Volatile/fixed carbon ratio	HHV (MJkg^{-1})
Duoglas-fir wood	87.3	12.6	0.1	6.9	20.37
Douglas-fir bark	73.6	25.9	0.5	2.8	21.93
Western hemlock wood	87.0	12.7	0.3	6.8	19.89
Western hemlock bark	73.9	24.3	0.8	3.0	21.98
Red alder wood	87.1	12.5	0.4	7.0	19.30
Red alder wood	77.3	19.7	3.0	3.9	19.44
Black oak wood	85.6	13.0	1.4	6.6	18.65
Black oak bark	81.0	16.9	2.1	4.8	17.09
Cotton gin trash	75.4	15.4	9.2	4.9	15.58
Grape pomace	74.4	21.4	4.2	3.5	21.81
Olive pits	80.0	16.9	3.1	4.7	19.37
Peach pits	79.1	19.8	1.1	4.0	19.42
Rice hulls	63.6	15.8	20.6	4.0	14.89
Walnut shell	81.2	17.4	1.4	4.7	19.51
Pensylvania bitumionous coal	6.2	79.4	11.9	0.08	34.9
Wyoming subbituminous coal	40.7	54.4	4.9	0.75	23.3

1.3.3   Combustion characteristics

The heating value of a substance is the heat released during the combustion of 1kg of it, assuming that the combustion products are cooled down to the initial temperature. This value is called High Heating Value (HHV) and it is measured directly in a calorific bomb. The HHV is corrected with the analysis of the water content of the combustible gases and this new value is called Low Heating Value (LHV). On average, the heating value of biomasses ranges from 14 to 19 MJ Nm^{-3}. Several formulas to estimate the heating value knowing the ultimate analyses have been proposed by different authors, since 1924. Here a correlation (1.1) to estimate the heating value for solid liquid and gaseous fuels is reported [Channiwala, 2002]. When the ultimate analysis is not available, the heating value can be estimated with good accuracy starting from proximate analysis (1.2) [Parik, 2005].

$$HHV\,(MJ\,/\,kg) = -1.3675 + 0.3137 \cdot C + 0.7009 \cdot H + 0.03180 \cdot O \;\; R^2 = 0.834 \qquad (1.1)$$

$$HHV\,(MJ\,/\,kg) = 0.3536FC + 0.1559VM - 0.0078\,Ash\,(MJ\,/\,kg)\;\; R^2 = 0.617 \qquad (1.2)$$

Where C, H, O are the % of Carbon, Hydrogen and Oxygen content in weight % on dry material (wt% dry) , FC is the fixed carbon, VM is the volatile matter.

The diagram proposed by [Van Krevelen, 1993] that relates together the LHV, the H/C and O/C ratio, is reported in figure 1.2. As can be noticed from the values listed in table 1.1, the composition of the woody biomass is approximately the same. There is a remarkable difference is between biomass and coal. The low values of H/C and O/C in coal assure a high heating value. Biomass has a lower C concentration and consequently lower heating value respect to coal, but from the other side has a high reactivity. This aspect, together with the wide availability of the biomass in the world, makes the biomass suitable for thermal treatment such as pyrolysis or gasification.
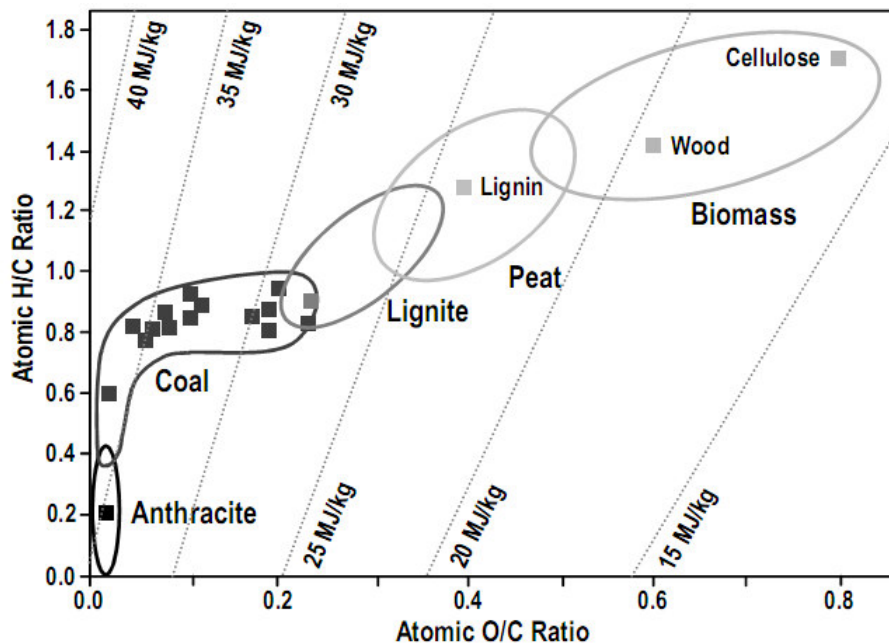
Figure 1.2 Van Krevelen diagram for different dry solid fuel [Van Krevelen, 1993]

1.4 Gasification

1.4.1 Biomass conversion processes

The conversion process to extract energy from the biomass has to be chosen considering the characteristic and the amount of the available biomass. Additionally the subsequent energy-converting device and its requirements have to be considered. The conversion processes can be divided in three main groups:

➢ Physical process such as drying and dewatering;

➢ Thermal processes such as combustion, pyrolysis, liquefaction and gasification;

➢ Biochemical conversion processes such as microbial conversion, biochemical liquefaction.

In figure 1.3 an overview of the conversion processes and possible applications to different energy conversion device is drawn.
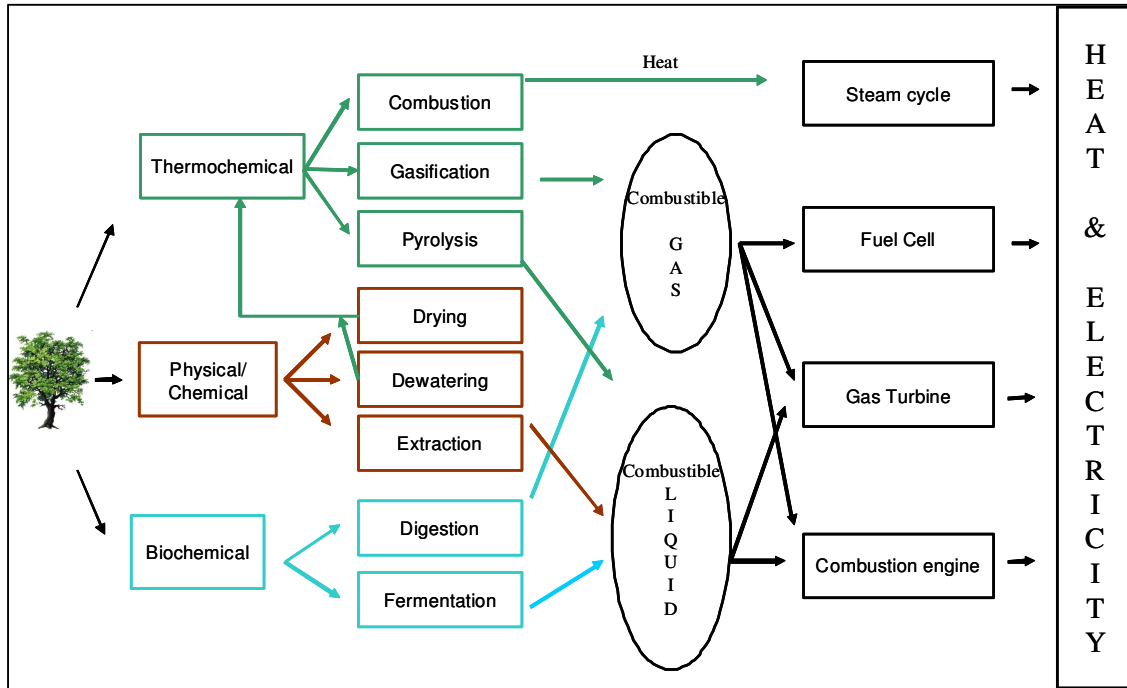
Figure 1.3 Biomass conversion technologies and possible end-use applications

1.4.2   Thermochemical conversion

The main thermochemical processes are combustion, pyrolysis and gasification. The products of all those processes are divided in volatile fraction, consisting of gases, vapours and tar components, and a solid residue rich in carbon. The main differences among the processes are the quantity of oxidant used (if any) and the amount of the different sub products produced.

Combustion is the first process discovered by mankind to produce heat and it is still the most used process to extract the energy stored in the chemical bounds of biomass. Theoretically it consist on the complete oxidation of the considered fuel, it is an exothermal process and it can be applied to every sort of biomass, even if the process efficiency drastically decreases when the moisture content is above 50%. The combustion process can be applied at both small scale (i.e. for domestic application) and at large scale (i.e. incineration and power plant, up to 3000 MW). Direct combustion for simple heating is a very low efficient process even if higher efficiency can be

reached when the combustion runs in large-scale plant or systems for heat recovery are adopted. The net conversion efficiency of traditional power plant ranges between 20 and 40%, according to the plant design and the biomass type. Mixture of coal and biomass are particularly attractive because a higher efficiency can be reached [Mckendry, 2002]. According to [Demirbas, 2009], 4 billions m^3 of wood are annually combusted by the world's population to meet daily energy needs for heating and cooking. Even if various technologies for thermo-chemical conversion of biomass (i.e gasification, pyrolysis) have been developed during the last years, direct combustion is still responsible for over 97% of the world's energy production from biomass. The parameter that characterizes the combustion is the "excess of air", which is the value of the ratio between the air added during the process and the air required for stoichiometric combustion (always greater then one). During the combustion, the sub-processes such as Drying, Devolatilization, Reduction and Oxidation occur simultaneously. The chemical energy is entirely converted in sensible heat of exhaust gases consisting of steam, carbon dioxide and nitrogen. The produced heat can be converted to mechanical work via, for example, steam cycle or Stirling engines.

It is not known exactly when pyrolysis process was discovered and started to be applied, but it was the beginning of a new period for the biomass utilization. Pyrolysis process consists on thermal degradation of the biomass in inert atmosphere. The temperature usually can vary between 200°C and 700°C. The products are a mixture of combustible gas, liquid and solid. The percentage of each sub-product, as well as their composition depends on the process parameters chosen: temperature, pressure, fuel size and composition. The pyrolysis of biomass includes endothermic and exothermic reactions. It is usually an endothermic process for temperature below 450°C and exothermic above. Anyway, the heat required for the process is generally provided by the oxidation of undesired products.

Gasification is defined a partial oxidation of the chosen fuel, since the oxidizing agent is added in substoichiometric condition. The resulting gas mixture, called syngas, is itself a fuel since it is composed, besides of carbon dioxide and nitrogen, by combustible gases. The advantage of gasification is the conversion of a solid fuel in a new fuel in gas phase that can be used in second use apparatus. This process is potentially more efficiency than direct combustion and many types of biomass can be treated and upgraded in this way.

It is important to remind that gasification process is known since the end of 18th century. At that time coal and peat were used to power gasification plant. The first "Gazogene" was built in the town of Sarre-Union (Alsace, France) with the purpose of converting solid fuel (such as wood, coal or peat) into gas to supply internal combustion engines initially fed with gasoline [McKendry, 2002]. The coal gasification process was mainly used to produce coke (70% of the coal treated) but the combustible gas yield during the process (30% of the initial coal), became famous as "town gas", because was sold to municipalities and consumers for lighting and cooking purpose. During the XIX century the town gas was replaced by electricity and natural gas but, since 1878, gasifiers

were successfully coupled with engine for power generation. From 1900 to 1920 many gasifier-engine systems were sold for power and electricity generation and in 1930 began the development of small gasifier for automotive and portable purposes. For example, in 1940, in Sweden, 90% of the vehicles had been converted to producer gas drive and the fuel used was wood and residual charcoal. Following World War II the interest in the gasification process gradually disappeared due to the gasoline and diesel available at cheap cost. Gasification became of interest again during the oil crisis of the 1970s, while over the past 25 years not much effort has been put in developing this process, because of the competition with natural gas and oil derivatives [Turare,1996 ; Srivastava,1993].

Figure 1.4 Cars powered by internal combustion engine with wood gasifier. From the left, Alfa Romeo 1750, Fiat 1100 modified by Baldini in 1946, bus used for public transport in Milan during 1930-40s.

The subject of this project is the biomass gasification process. Up to know we have briefly seen that coal gasification was widely practiced 100 years ago, even if the process has not been studied from the scientific point of view (reactions involved, characteristic parameters and so on), a remarkable experience was acquired during the XIX century in gasifier construction and operation. The scientific approach of the gasification process has started recently thanks to the renewed attention to this process which represents a promising technology to extract energy from the biomass. The chemistry involved in the biomass gasification process is very similar to the coal one that was considering as a starting point to study the process. However, biomass is more reactive than most coals, since it contains more volatile matter (70 to 90% for wood compared to 30 to 45% for typical coals) and thus, gasification can occur under less severe operating conditions. In the next paragraphs the gasification process and technologies available will be briefly summarized.

1.4.3 Gasification process outline

Gasification turns low or null value feedstock in a new and marketable fuel. From the chemical side the gasification process is, as said before, a partial oxidation of the fuel. The whole process can be divided in four sub-processes:

- ➢ Pyrolysis or devolatilization step: the fuel is thermally degraded in gas, condensable compounds and char;

- ➢ The gas and tar yield are themselves subjected to thermal degradation;

- ➢ Char is gasified by carbon dioxide or steam;

- ➢ The sub products (gas, tars and char) are partially oxidized.

In Figure 1.5 the entire process is schematize. The final step is the combustion of the gasification products with the complete oxidation of the gas, tar and char in carbon dioxide and water.
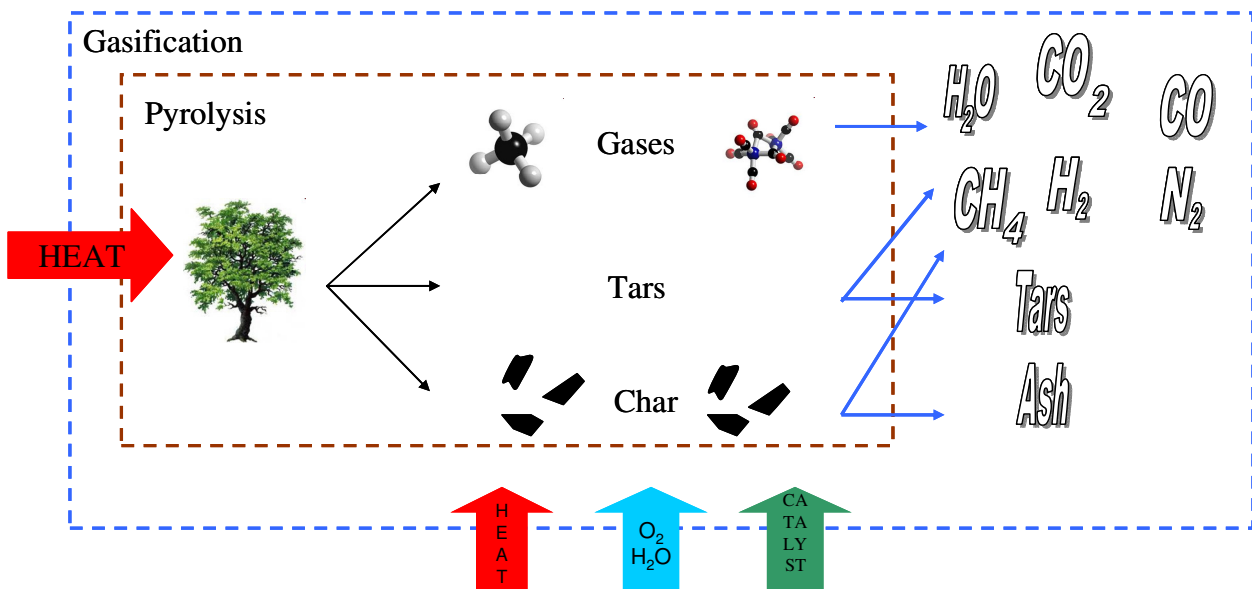
Figure 1.5 Schematic presentation of the gasification process

The pyrolysis step is slightly endothermic and the mass percentage of the initial feedstock, which turns in gaseous or volatiles compounds, can vary between 75 to 90% according to the temperature reached in this stage. The gas and tar composition depend on the gasification temperature and on the amount of oxidizing media fed.

The reactor, due to the endothermic characteristic of the process, need to be heated up. This can be done in several ways such as burning part of the combustible gas or char produced in situ or separately or combusting some of the feed material.

To understand the final syngas composition the main reactions involved in the gasification process are summarized below. The oxidation zone is characterized by the heterogeneous chemical reactions of combustion (1.3) and partial oxidation (1.4).

$$C + O_2 \rightarrow CO_2 \qquad\qquad \Delta H_f^0 = -393.5 \ kJ \ mol^{-1} \tag{1.3}$$

$$C + 1/2O_2 \rightarrow CO \qquad\qquad \Delta H_f^0 = -110.5 \ kJ \ mol^{-1} \tag{1.4}$$
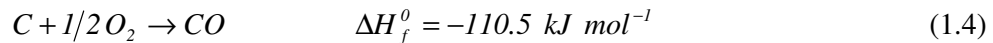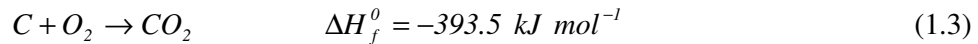
These two reactions are exothermic and can provide the heat necessary for the endothermic reactions occurring in the drying, pyrolysis and reduction zones (i.e. autothermal process).

The water steam can be produced during the drying and pyrolysis of the feedstock or introduced as a gasifying agent or even generated by the reacts with the solid carbon, according to the following reversible water gas reactions (1.5 and 1.6). These two equations together with the Boudouard equation (1.7) are the main endothermic reduction reactions involved in the process. These reactions increase the concentration of carbon monoxide and hydrogen in the produced gas, especially at higher temperatures and lower pressures.

$$C + H_2O \rightarrow CO + H_2 \qquad\qquad \Delta H^0 = 131.3 \ kJ \ mol^{-1} \tag{1.5}$$

$$C + 2H_2O \rightarrow CO_2 + H_2 \qquad\qquad \Delta H^0 = 90.2 \ kJ \ mol^{-1} \tag{1.6}$$

$$C + CO_2 \rightarrow 2CO \qquad\qquad \Delta H^0 = 172.4 \ kJ \ mol^{-1} \tag{1.7}$$
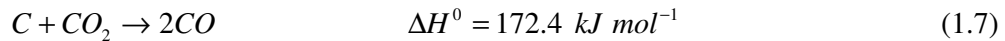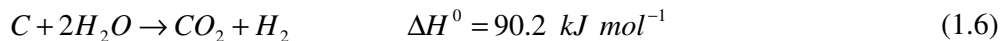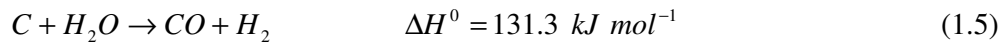
Several other reduction mechanisms occur during the gasification process; some of the most important reactions are listed below. In particular it is worth to underline the importance of the water gas shift equation (1.8) and the reactions for methane production (1.9 - 1.12)

$$CO + H_2O \rightarrow CO_2 + H_2 \qquad\qquad \Delta H^0 = -41.1 \ kJ \ mol^{-1} \tag{1.8}$$

$$2CO + 2H_2 \rightarrow CH_4 + CO_2 \qquad\qquad \Delta H^0 = -247.3 \ kJ \ mol^{-1} \tag{1.9}$$

$$CO + 3H_2 \rightarrow CH_4 + H_2O \qquad\qquad \Delta H^0 = -206.1 \ kJ \ mol^{-1} \tag{1.10}$$

$$CO_2 + 4H_2 \rightarrow CH_4 + 2H_2O \qquad\qquad \Delta H^0 = -165.0.1 \ kJ \ mol^{-1} \tag{1.11}$$

$$C + 2H_2 \rightarrow CH_4 \qquad\qquad \Delta H_f^0 = -74.8 \ kJ \ mol^{-1} \tag{1.12}$$
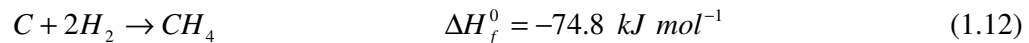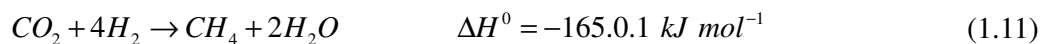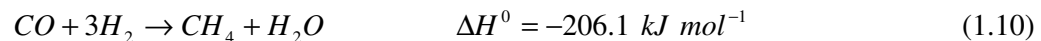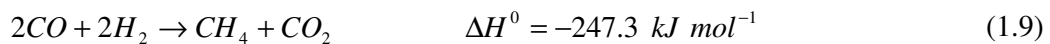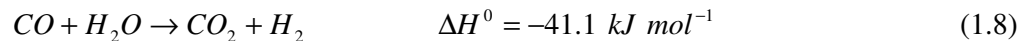
Even if the process runs in substoichiometric conditions a fraction of carbon monoxide and of hydrogen can be completely oxidize in carbon dioxide and water respectively (equation 1.13 and 1.14).

$$H_2 + 1/2 O_2 \rightarrow H_2O \qquad \Delta H_f^0 = -285.9 \ kJ \ mol^1 \qquad (1.13)$$

$$CO + 1/2 O_2 \rightarrow CO_2 \qquad \Delta H^0 = -283.9 \ kJ \ mol^1 \qquad (1.14)$$
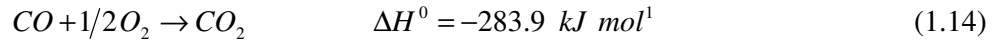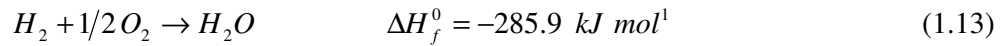
These reactions are usually not desired, because from one side they generate thermal energy which gives a contribution in sustaining the conversion process but from the other side they cause a reduction in the syngas heating value.

The water gas and water gas shift reactions are the ones which determine to a large extent the final gas composition. The equilibrium of these (and also others) reactions is strongly influenced by the temperature, as can be clearly seen in figure 1.6.
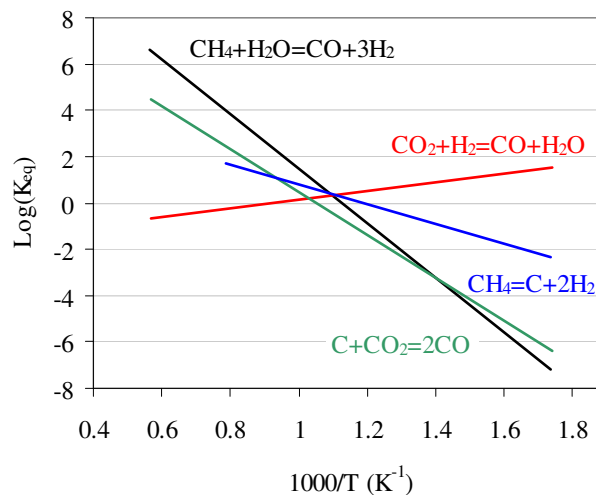
Figure 1.6 The equilibrium constant of reaction (1.7), (1.8), (1.10), (1.12) is reported [Klass, 1998]

Although it is possible to list the most important reactions that occur during a gasification process, in practice the different sub-phases of the process run almost simultaneously and is not possible to control the process with good accuracy. Anyway it is possible to estimate the final gas composition, considering the values of the characteristic parameters of the process and under the hypothesis that the reaction time is long enough to reach almost the equilibrium condition. The characteristic parameters are:

➢ Fuel consumption, moisture and composition;

➢ Temperature and pressure;

➢ Type and quantity of gasifying agent fed;

> ➤ Superficial velocity and heart load;

> ➤ Gas heating value;

> ➤ Gas flow rate and gas production;

> ➤ Efficiency.

It is worth to brief describe the most important parameters among the ones listed aboveThe reaction *temperature* is one of the most important parameter for the overall gasification efficiency. It acts on the carbon monoxide and hydrogen fractions since higher temperatures favour the endothermic reactions. Furthermore if the temperature is above 1100°C the tar conversion is achieved by thermal cracking, even if the typical gasification temperature ranges between 700°C and 900°C. Higher temperatures are possible but difficult to reach operatively. From several experimental results, it can be seen that the temperature influences the gas composition until 1100°C. Above this value the different gas fractions reach stable level as can be seen in many experimental works, i.e. [Li, 2004], [Luo, 2009], [Franco, 2003]. As an example, some experimental results are reported in figure 1.7. The pressure has a minor role on the syngas composition unless going at higher pressure values [Valin, 2010], [van Diepen & Moulijn, 1998].
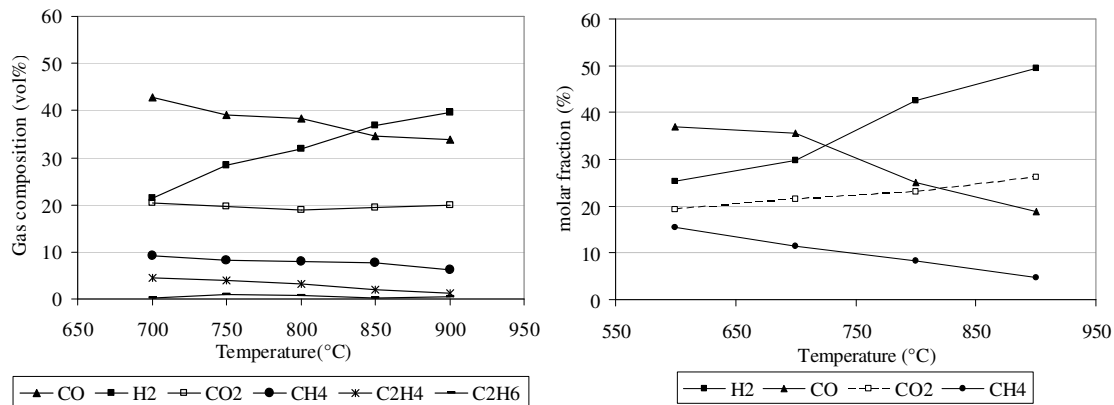
Figure 1.7 Biomass gasification process: Gas composition versus different temperature at feeding rate of 0.44kg h^{-1}, air 0.5Nm^3 h^{-1} and steam rate 2.2kg h^{-1} (left) [Franco,2003] and feeding rate of 0.3kg h^{-1}and steam to carbon 1.43 (right) [Luo,2009]

The amount and the *type of gasifying agent* are also very important. Air, steam or pure oxygen can be used for this purpose. Air is the cheapest and most used gasifying agent, but the heating value of the produced gas is quite low because of the high nitrogen content. Oxygen is the one with the highest reactivity but is less employed due to the high cost and safety problems. Steam is a good compromise even if the heat needed for the steam generation has to be provided in someway. The gasifying agent is usually quantified defining its mass ratio versus the stoichiometric amount or versus the fuel (biomass). The most common parameters used are: *Equivalent Ratio (ER)* for partial oxidation and *Steam to Carbon ratio (SC)* for steam gasification. The ER parameter is defined as

the ratio between the oxygen fed to the gasifier and the stoichiometric quantity of oxygen needed for the complete oxidation of the feedstock. The Steam to Carbon ratio (*SC*) quantifies the ratio between the supplied steam and the carbon fraction present in the feedstock. Typical ER values for biomass range between 0.2-0.3, while for steam gasification SC vary between 1 and 3. The ER and SC values are chosen according to the desired syngas composition. For example, increasing ER value, the CO_2 and H_2O content obviously raise, the syngas heating value decreases, as well as tar amount. In figure 1.8, the influence of ER and SC is shown.

The *residence time* is an important parameter that acts on the final gas quality and composition. In addition, tar conversion improves increasing the reaction time. The minimum residence time to reach a conversion over 98% has been found of 0.02 kg h Nm^{-3}.

The *gas heating value* of the produced gas is defined as the heat released during a complete combustion process. It is measured in units of energy per amount of gas, and it is usually referred to the normal gas volume (at 0°C, and 1bar) and therefore, expressed in J Nm^{-3}.
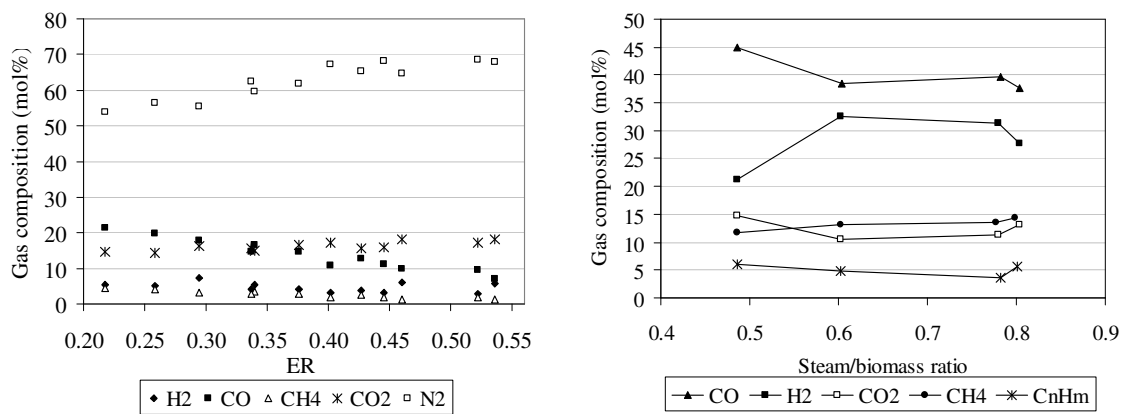
Figure 1.8 Characterization of the syngas as a function of the air ratio (ER) on the left [Li, 2004]; and as function of S/B (Steam to biomass) on the right (gasification temperature 1073 K) [Franco, 2003].

Usually the heating value can be expressed in two different ways:

➢ HHV (Higher Heating Value) which is the maximum energy released during complete oxidation of the fuel, including the thermal energy that can be recovered by condensing and cooling the products down to the initial temperature (before starting the combustion).

➢ LHV (Lower Heating Value): the net energy released during complete oxidation of the fuel, without the energy recovery, due to product condensation (i.e. latent heat).

The syngas heating value together with the produced gas flow rate represent the thermal power at the gasifier outlet and are significant in determining the gasifier efficiency.

The *efficiency* of a gasification reactor is defined as the energy content of the syngas divided by the energy content of the feedstock; typical attainable efficiency values are in the range of 70-80%. Is

obviously important to know the fuel consumption for the overall process efficiency. This quantity, measured directly, or by a mass balance, is usually expressed as unit mass per time ($kg_{biomass}\ h^{-1}$), or per generated energy ($kg_{biomass}\ kW^{-1}$).

1.4.3   Gasification technologies overview

The primary aim of the gasification technology is the efficient conversion of the energy stored in the biomass into the produced syngas. The gas composition and the impurity level depend on the gasification agent and the process conditions, which are influenced by the reactor design.

The design and building of gasification reactor is practice since the 1800s, thus a considerable experience has been developed in more than 150 years. As result, several reactors design is available at small and large scale. The gasifiers can be classified according to their design in:

> ➢ fixed bed;
>
> ➢ fluidized bed;
>
> ➢ Entrained flow;
>
> ➢ Twin bed.

the main difference is the gas/solid flow pattern which determines the sequence of the sub-processes of gasification.

The *Fixed bed rectors* have been widely used for coal gasification since more than 150 years ago. The main advantage of the fixed bed reactors is the simplicity and the high operative temperature, usually around 1000°C, but at the same time the high temperature can cause several corrosion problems and the produced gas has high tar content and low heating value. The operative fixed bed gasifiers, at commercial scale, are very few. The main problem is the high tar concentration, which is caused by the non uniform temperature profile in the gasification zone. A considerable cleaning section has to be foreseen if this reactor is adopted. The fixed bed gasifiers can be classified in Updraft, Downdraft or Cross Flow according to the direction of the airflow.

In the *Updraft gasifier* the feedstock is introduced at the top of the gasifier and the gasifying agent, at the bottom through a grate. The biomass moves downwards running through drying, devolatilization, reduction and finally oxidation. During this process, volatiles compounds are realized: partly condense on the biomass and partly leaves the gasifier with the gas. The gasification process occurs in the lower part of the reactor and the gas produced leaves the reactor in the upper part. In this way the hot gas are cooled down passing through the biomass that is contemporary dried. The syngas leaves the gasifier at 200-300°C and, due to the low temperature, the gasifier efficiency is high but the tar production is also considerable (between 10 and 150 g Nm^{-3} [Hasler,1999]). The particulate matter is usually low due to the filtration effect of the wood material

bed thorough which the producer gas passes on its way to the exit. Commonly air is used in the updraft reactor, thus the gas heating value is around 5-6 MJ Nm^{-3}.

In the *downdraft gasifier* the feed and the gasifying media move in the same direction. The biomass is introduced at the top of the reactor; instead, the air enters just above the heart of the gasifier. The produced gas leaves the system after passing through the "hot zone" and this lead to lower tar concentration because the tar produced during the pyrolysis and gasification processes is thermal cracked. On the contrary, the overall energy efficiency is low since the gas exits at about 800°C and the particulate concentration is higher then in the updraft gasifier.

In figure 1.9 the scheme of an updraft and a downdraft fixed bed gasifiers with their typical vertical temperature profiles have been reported.
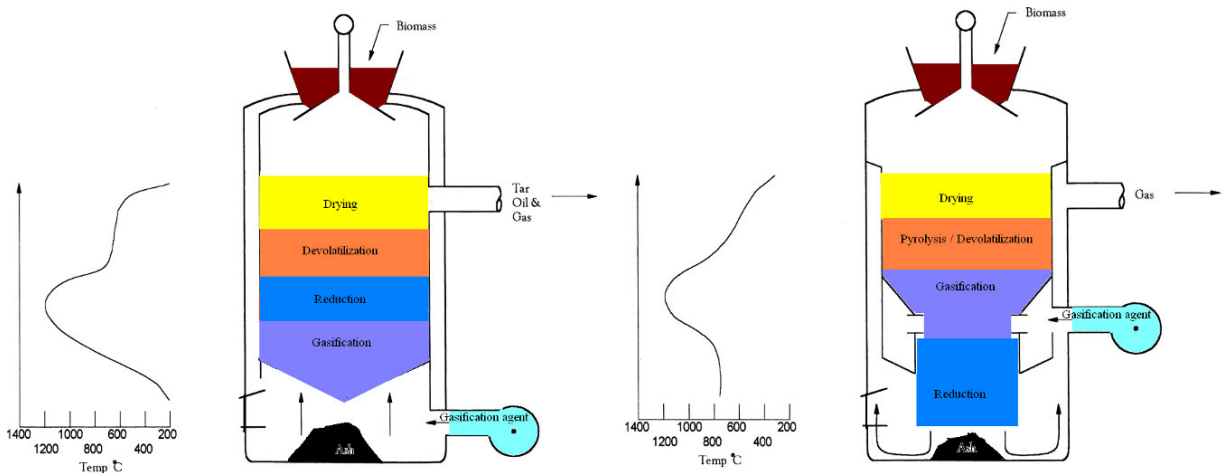
Figure 1.9 Updraft and downdraft gasifiers. Adapted from [McKendry, 2002]

In the *cross-flow gasifiers* the feed moves downwards while the air is introduced from one side. The advantage of this system is that it can work at small scale (under 10kW$_{el}$), but has a very low tar conversion. In this system the feed moves downwards while the air is introduced from one side and from the other the gas leaves the reactor at the same level. In this way the hot combustion/gasification zone is located around the entrance of the air where the temperature reaches also 1500°C, while the drying and pyrolysis zone are located higher up in the reactor. The gas leaves the vessel at 900°C, thus the energy efficiency is quite low.

Fluidized bed gasifier was originally developed for large scale coal gasification, and its main advantage is the uniform temperature in the gasification zone. This is achieved preparing the feedstock in small and uniform particle size and adding to the bed an inert material to improve the heat exchanges. The bed is fluidized with air or oxygen ensuring, in this way, intimate mixing of the biomass with the hot produced gas. The result is the production of a syngas with higher heating value and less tar content, respect to the fixed bed system. This can be also due to the frequent

addition of a catalyst together with the inert bed material. The fluidized bed gasifiers have two main configurations: *circulating fluidized bed* (CFB) or *bubbling bed* (BFB) (see figure 1.10). Both can work either at atmospheric pressure or pressurized.

The *BFB gasifier* is a well established technology. The reactor is divided in two parts: the fluidized bed is located in the lower part, and the upper part is called freeboard. The flow velocity of the gasifying agent is adjusted to avoid that the particles bed is transported out of the reactor. For this reason the ash particles are mainly blown out of the fluidized bed. A cyclone is placed after the reactor to clean the raw gas from particulate material. The outgoing gas has a temperature of 850-900°C, which allows a cold gas efficiency of 70-85%. [Hasler, 1999]). If air is used as gasifying agent the gas heating value is between 3.6-5.9 MJ Nm^{-3}. The BFB is sensible towards the size and the geometry of the wood particles since these properties determine the fluid dynamic behavior of the feed.
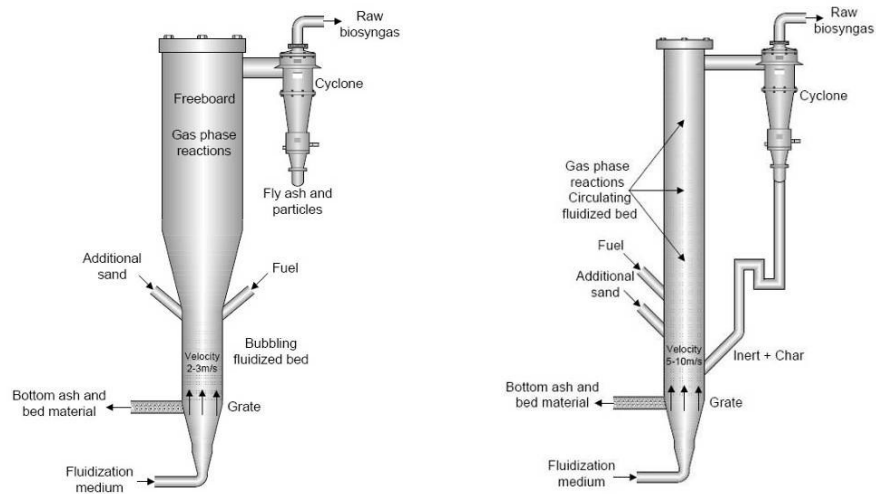
Figure 1.10 Fluidized bed gasifiers: bubbling fluidized bed (on the left) and circulating fluidized bed (on the right) [Olofsson, 2005].

The *CFB* has no clear separation between the fluidized bed and the freeboard. The flow velocity is considerable higher then in BFB. As a consequence, the mixing of bed material and biomass particles reach fully isothermal conditions, but a higher percentage of particulate matter and inert material is blown out of the gasifier.

To solve the problem the solid material collected in the cyclone is re-circulate in the gasifier. With this system a higher char conversion can be achieved. The syngas produced using CFB gasifier has lower tar content and higher heating value.

Two other types of fluidized bed gasifier can be worth to describe briefly. The *Double fluidized bed* which basically couple two CFB in series. In the first reactor the pyrolysis process occur, and in the second one air or steam is added for the gasification process. The first gasifier is heated by means of hot sand circulating from the second reactor. The *entrained flow gasifier (EF)* is commonly used for

coal. This reactor has no inert material; it operates at high temperature (1000-1200°C) and high pressure (25-60bar) and it is used at big scale (>100MW$_{th}$). The feedstock has to be prepared in small fuel particles and it is fed directly in the gasification chamber. Air or pure oxygen is used as oxidizing agent and, due to the high temperature, very low tar is present in the produced gas. The conversion is close to 100%. However the experience in using this gasifier for biomass instead of coal is poor. In table 1.4 and 1.5 some general consideration on the different plants and on the typical composition of the syngas produced are summarized.

Table 1.4 Operating conditions of fluidized and entrained flow gasifier [Knoef, 2005]

	Downdraft	Updraft	BFB	CFB	EF
Gasification temperature (°C)	700-1200	700-900	<900	<900	1450
Tars	Poor	High	Medium	Medium	Very poor
Control	☺	☺ ☺	☺	☺	☹
Suitable scale (MW$_{th}$)	<5	<20	10-100	20-100	>100
Feedstock preparation	Very critical	Critical	Less critical	Less critical	Only fines particles

Table 1.5 Characteristics of the syngas produced by different gasifiers [Hasler, 1999], [Beenackers, 1999]

Process	Gas composition					LHV (MJ Nm^{-3})	Tar (g Nm^{-3})	Particles (g Nm^{-3})
	H$_2$	CO	CO$_2$	CH$_4$	N$_2$			
Fixed bed Updraft	15-21	10-22	11-13	1-5	37-63	4-5.6	0.01-6	0.1-8
Fixe bed Downdraft	10-14	15-20	8-10	2-3	53-65	3.7-5.1	10-150	0.1-3
BFB	15-22	13-15	13-15	2-4	44-57	3.6-5.9	2-30	8-100
CFB	17-36	36-51	7-15	0.1-1	0-39	114-18	1-20	8-100
EF	29-40	39-45	18-20	0.1-1	0.1-9	8.8-9.3	-	-

1.5 Gas cleaning

The term gas processing comprises the combination of gas cleaning and conditioning. Gas cleaning includes the required steps for tar removal, while gas conditioning includes the processes involved in the preparation of the syngas yield into a fuel suitable for the subsequent energy generation apparatus.

The produced gas derived from biomass gasification of solid fuels normally contains CO$_2$, H$_2$, CO, CH$_4$, H$_2$O, N$_2$ and in addition to the main components organic and inorganic impurities as well as solid matter. In details, besides the permanent gases, can be found:

> ➢ Sulphide compounds (mainly H$_2$S and COS, if the fuel used includes sulphur);

> ➢ Nitrogen compounds (NH$_3$ HCN,NO$_x$, generated from the N contained in the fuel);

> ➢ Tar;

> ➢ Halogen compounds (ex. HCl);

> ➢ Particulate matter;

> ➢ Alkali and metallic compounds.

According to the final use of the gas produced, it can be necessary to clean it from any or all these impurities. Thus, the gas cleaning session is usually thought and built for the specific requirement of the subsequent energy production system. In short, the most common technologies for the abatement of the different impurities are summarized below.

1.5.1 Tar removal

"Tar" has been operationally defined in gasification field as the material in the product stream that is condensable at a temperature below 450°C, in the gasifier or in downstream processing steps or conversion devices; more precisely, in a recent EU/IEA/DOE meeting, Tar has been defined as "organic compounds with molecular weight higher than benzene". Several studies have interested the tar formation, composition and degradation. Besides the gasifying agent concentration which acts on the quantity of tar produced, a clear relationship also exists between the process temperature and the tar composition [Elliot, 1998]. In table 1.6 the tar compounds generated at different temperature are listed.

Table 1.6 Chemical compounds in biomass tar

Conventional Flash Pyrolysis (450-500°C)	High-Temperature Flash Pyrolysis (600-650°C)	Conventional Steam Gasification (700-800°C)	High Temperature Steam Gasification (900-1000°C)
Acids	Benzenes	Naphthalenes	Naphthalene
Aldehydes	Phenols	Acenaphthylenes	Acenaphthylene
Ketones	Catechols	Fluorens	Phenanthrene
Furans	Naphthalenes	Phenanthrenes	Flouranthene
Alcohols	Biphenyls	Phenols	Pyrene
Complex Oxygenates	Phenanthrenes	Naphthofurans	Acephenanthrylene
Phenols	Benzofuranes	Benzanthracenes	Benzanthracenes
Guiacols	Benzaldehydes		Benzopyrenes
Syringols			226 MW PAHs
Complex Phenols			276 MW PAHs

Evens and Milne [Evens,1997] suggested the use of a classification of pyrolysis products as primary, secondary and tertiary according to the formation temperature. Four major classes were identified as a result of gas-phases thermal cracking reactions:

> ➢ Primary products: characterized by cellulose-derived products such as levoglucosan, hydroxyacetaldehyde and furfurals; analogous hemicellulose-derived products; and lignin-derived methoxyphenols;

➢ Secondary products: characterized by phenolic and olefins;

➢ Alkali tertiary products: includes methyl derivatives of aromatics, such as methyl acenaphthylene, methylnaphtahlene, toluene and indene;

➢ Condensed tertiary products: includes the PAH series without substituents: benzene, naphthalene, acenaphthylene, anthracene/phenanthrene, pyrene.

As shown in figure 1.11 the primary and tertiary products are mutually exclusive; the primary products are destroyed before the tertiary products appear [Toman, 2001]. Usually the gasification process runs between 700°C and 900°C; nevertheless the tertiary compounds are predominant, especially benzene, naphthalene, phenantrene and pyrene.
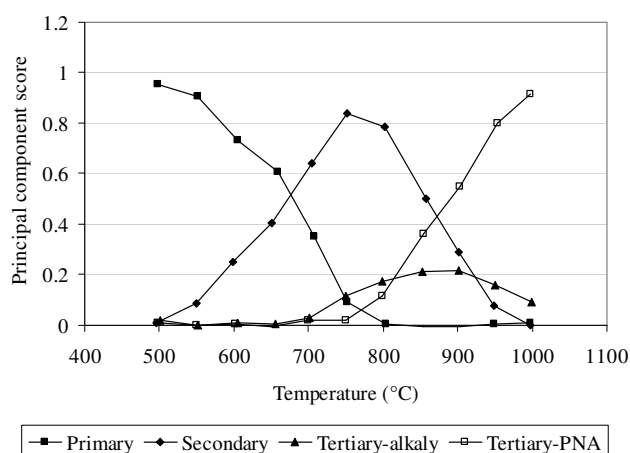
Figure 1.11 Classification of tar compounds according to the formation temperature

The technologies available for tars removal are based on different principles. The most diffused technology is based on *physical tar removal* by means of wet scrubbers (water or oil based) or electrostatic precipitators. The first ones works below 65°C, while the second can receive gas at temperature up to 150°C. With these systems, the tar load in the cleaned gas can range from 10 mgNm^{-3} (with oil based wet scrubber) to 40 mgNm^{-3}. The main disadvantage is the heat loss due to the low operative temperature of these technologies.

Thermal tar decomposition requires high temperature, from 900 to 1200°C according to the species present in the tar. This temperature can be reached heating electrically special surfaces up to 1200°C, or through the partial oxidation of the gas, using oxygen. In the second case, very low oxygen to fuel ratio is necessary for tar conversion, thus a few of the gas energy content is lost, but the oxygen is expensive. The disadvantages of thermal processes are the incomplete tar decomposition and the energy losses, even if the energy content of the tar is preserved in the producer gas in form of sensible heat or heating value of the tar decomposition products.

Finally, the catalytic tars removal, allow the tar degradation at temperatures between 800-900°C. The catalyst can be placed inside the reactor, mixed with the inert bed, or in an external vessel. The

main advantage of the "in situ decomposition" is the possibility of tar decomposition while the gasification process runs, In fixed bed reactors, the contact between gas and catalyst is not enough to reach a good tar conversion, instead in fluidized bed, the catalyst shows fast deactivation, due to the attrition with the solid material. The best solution is to remove tars in a separate reactor, even if this required a separate heating system and higher costs. The catalysts active in tar decomposition are many and with different costs. Dolomite, olivine, calcites and zeolites are cheap and show a good efficiency in tar cracking. Metallic catalysts, such as Mo, Ni, Co, Pt, allow a most complete decomposition of tar and ammonia but they are quite expensive and the long-term efficiency has not been well demonstrated yet.

1.5.2 Particles removal

The particulate matter in the gas can cause erosion and blocking in the downstream equipment of the gasifier. Additionally, particles are subjected to emission limits. Therefore, the particles removal section is almost compulsory in every cleaning system for gas yield from biomass gasification. The most common technologies for particulate removal are: *wet scrubber*s which have a maximum operative temperature below 100°C and for which gas cooling is compulsory. *Electrostatic precipitators*, classified in wet or dry according to their removal system. The wet precipitators have a maximum operative temperature of 65°C, instead the dry ones can tolerate a gas temperature up to 500°C. *Cyclones,* which are quite simple system, have an operative temperature limited only by the construction material and remove large quantities of large particles. Usually the fluidized beds are equipped with a cyclone due to the high quantity of particles that is blown out of the gasifier. The last systems are *barrier filters*; the gas pass through a special barrier and the particulate matter stops on it. These system need to be periodically cleaned according to the particles concentration in the treated gas. The barrier filters are chosen according to the type of particulate matters and the gas temperature (bag filters, packed bed filters or rigid barrier filters).

1.5.3   Alkali and impurities removal

Alkali metals are usually removed cooling the gas below 600°C, and then the solid particles generated are removed by means of particle filtration. A recent research has shown that bauxite has a good efficiency at temperature between 650 and 750°C as alkali absorber [Cummer, 2002].

The removal of impurities in trace such as N, S, Cl is also required for most of the end-uses applications. The *Chlorine* in the biomass is usually converted in HCl during the gasification process, and its concentration in the gas depends on the Cl concentration in the feedstock. The HCl removal is typically achieved with web scrubbers or adsorption on active material such as CaO/MgO [McKendry, 2002]. The *nitrogen* concentration in the biomass is converted mainly in NH_3. If air is used as gasifying agent, the N_2 content is considered as inert and it has no contribution on the ammonia formation. If the syngas is combusted in gas engines or turbine the ammonia is converted in NO_x during the combustion at high temperature. NO_x emissions are subjected to restrictive limits, thus it is important to remove NH_3 to avoid their formation. Ammonia can be removed by wet scrubber or by catalytic decomposition. The first technology is well known, but the

gas has to be cooled down to 50°C. The latter technology is more recent and still not used commercially. It has been seen that the catalyst used for tar removal have also a good efficiency in ammonia removal (99% at 900°C for dolomite, nickel or iron-based catalyst). On the contrary, a recent research has shown that, if the syngas is produced to be fed in high temperature Fuel Cell, the ammonia removal is not necessary, since it is well converted inside the fuel cell with a very low NO_x emission [Wojcik, 2003].

1.5.4   Sulphur abetment

The *sulphur* content in the feedstock is usually below 0.01%. During the combustion of the syngas the sulphurous compounds are oxides in SO_x which can be easily removed to respect the emission limit. If the gas is produced to be burned in gas engines or turbines the prior sulphur removal is uncommon. Actually, the most advanced research on gasification process is trying to feed a fuel cells with syngas produced from biomass. Fuel cells are very sensible to H_2S which remarkable reduce the fuel cell efficiency and can also cause permanent damage. Wet scrubbers are efficient in sulphur removal but the process is quite complex and requires the gas cooling. For hot gas cleaning adsorption on zinc oxides (maximum temperature 350-450°C) shows good efficiency. Recently, the sulphurous compounds adsorption on metal-oxides (i.e. magnesium, lantanium, iron) has been tested and promising results have been achieved up to 500°C. Active carbon can also be used for sulphur removal even if the high steam content in the gas may decrease the efficiency [Cal, 2000].

1.6   Syngas utilization

The gas produced via gasification process can be used in several applications for power generation, for heat and/or combined heat and power applications and for the generation of liquid fuels and chemicals products. Several progresses have been done in the last 20 years in this field, but the efficiency and the tar removal are still a problem for most of the applications.

One of the most common applications is *co-firing* coal and gas from gasification of biomass in existing coal power plants. The plants can tolerate up to 10% of gas without any modification of the coal boiler; indeed, the critical problem in co-firing is the effect of the biomass ash on the quality of the boiler flying and bottom ash. The application of the flying and bottom ash in construction and cement production often sets the specifications for the amount and type of biomass that can be co-fired. Examples of biomass co-firing plants are the AMER 85MWth circulating fluidized bed (CFB) gasifier in the Essent power plant in Geertruidenberg (The Netherlands) and the foster Wheeler CFB gasifier in Lahti (Finland) and Ruien (Electrabel power plant,Belgium).

The syngas produced is also used for power generation in *combined cycle of heat and power (CHP)* production. In these systems the gas yield is burned on a gas engine. Opportunely modified gas engine can works without troubles with gas of different quality, even those with calorific values around 5-6 MJ Nm^{-3}. The output energy is one-third electric energy and two-third heat energy. The most important aspect to improve the performance of CHP plants is the removal of tar from the product gas. Higher is the tar and aerosol concentration in the gas more frequently revision and

repairs have to be done to the system; this leads to a decrease of revenues and to higher investments, as some equipment will be installed double to avoid the standstills. Furthermore, removal of tar components can become very expensive as some tar components show poisoning behavior in biologic wastewater treatment systems. The few successful systems are the ones in Gussing (Austria) and Harboore (Denmark) and they are neither cheap nor simple.

To produce electricity on larger scale the *IGCC* (integrated gasification combined cycles) are preferred instead of CHP; in the IGCC the gas is fired on a gas turbine. Gas turbines requires a pressurized feed gas, thus the syngas has to be pressurized or it should be carried out from the gasification equipment at the pressure of the turbine (5-20 bar). The second solution is preferred as in that case only dedusting of the gas and cooling to the turbine inside temperature (400-500°C) is required, while in the other route the gas has to be completely cooled and cleaned to allow the compression. By the way, the major drawback for pressurized gasification is the cost related to the electricity consumption to pressurize the inert gas.

Fuel Cells can achieve, potentially, higher electrical efficiency than the simple combustion systems or gas engines; a fuel cell downstream a gasifier functioning as the combustion room for a micro gas turbine, is a combination with high electric efficiency; in a simpler system, the fuel cell is connected to a gasifier to both have a high electric efficiency and a high overall efficiency. Anyway the application of gas yield from biomass gasification to fuel cells is still in its early development. A fuel cell burns H_2, but also CO and CH_4 according to the type of cells, and produces electricity directly through electrochemical reactions. The use of methane as fuel provides effective cooling of the fuel cell (due to the endothermicity of the reforming reaction) which should otherwise be done in a way that increases the costs and decreases the overall efficiency.

The acceptable levels for the concentrations of impurities and the required main gas composition could vary according to the final utilization of the gas (summarized in table 1.7).

Table 1.7 Syngas required for different applications

Second use system	Required gas
Power-Combined cycle	Product gas
Power-CHP gas engine	Product gas, low tar content
Power-CHP fuel cell	Product gas, low hydrocarbon & organic content
SNG	Product gas, nitrogen free, high methane content
Liquid Fuel synthesis	Product gas, nitrogen-free
Chemical synthesis	Product gas, nitrogen-free
Hydrogen production	Product gas, nitrogen free
Ammonia production	Product gas, containing nitrogen

1.6.1 Fuel cells

Since the main goal of this project is to verify the syngas suitability from biomass gasification for SOFC fuel cells, a brief description of the main characteristics of these systems is here done.

Fuel cells are electrochemical power generation systems that convert the chemical energy stored in a fuel into an electric current. The electricity is generated inside the cells through reactions between a fuel and an oxidant, stroked by an electrolyte. All the fuel cell types consist of two electrodes (of porous material) separated by an electrolyte. The electrodes act as catalytic environments for the cell reactions, while the electrolyte transports the produced ions from two generic reactions, closing the electric circuit in the cell. Fuel cells differ from conventional electrochemical cell batteries because the reactants flow continuously into the cell from an external source (thermodynamically is an open system). Instead the traditional batteries have the chemical energy stored in the battery itself (closed system). Fuel cells can operate continuously as long as the necessary reactant and oxidant flows are maintained. The occurring electrochemical reactions are exothermic and, for that reason, a cooling system is usually needed to keep the operation temperature in a desired range. Here the main fuel cells types are presented, classified according to the function of the utilized electrolyte and characterized by their operation parameters (table 3.1).

Table 1.8 Main fuel cells type and operative parameters

Fuel cell type	Temperature	Pressure	Cell	Power
AFC (Alkaline Fuel Cells)	< 80 °C	4 bar	60-70%	10-100 kW
PEM FC (Proton Exchange Membrane Fuel	50-220 °C	atmospheric	50-70%	100W-
PAFC (Phosphoric Acid Fuel Cells)	150-200°C	8bar	55%	< 10 MW
MCFC (Molten Carbonate Fuel Cells)	600-700°C	3.5bar	55%	100 MW
SOFC (Solid Oxide Fuel Cells)	800-1000°C	atmospheric	60-65%	< 100 MW
DMFC (Direct Methanol Fuel Cells)	90-120°C	atmospheric	20-30%	100mW-1kW
RMFC (Reformed Methanol Fuel Cells)	250-300°C	atmospheric	50-60%	5W- 100kW

The use of synthesis gas (in particular from coal gasification) in fuel cells has been investigated since the 1960s [Shoko, 2006]. Among the different types of fuel cells the *SOFC* and the *MCFC* are particularly attractive for the use of synthesis gas from biomass conversion, since they can directly utilize both hydrogen and carbon monoxide and can accept higher levels of contaminant (NH_3, H_2S, HCl, particulates, tar).

The molten-carbonate fuel cells (MCFCs) are high temperature fuel cells (working temperature above 600°C) characterized by an electrolyte composed of a molten carbonate salt mixture suspended on a porous, chemically inert ceramic matrix of beta-alumina solid electrolyte. Because of the high working temperature, non-precious metal can be used as catalysts, reducing costs. Molten carbonate fuel cells do not required an external reformer to convert more fuels in hydrogen because the fuel is converted to hydrogen within the fuel cell by internal reforming; additionally

they are not prone to poisoning by CO or CO_2 —they can even use carbon oxides as fuel— making them more attractive for fuelling with gases made from coal. The carbon monoxide is internal oxidizes through the water gas shift reaction producing hydrogen and increasing the overall efficiency. The global efficiency is around 45%, even if, theoretically, efficiencies of 65 % can be reached.

The MCFC electrochemical reactions are:

Anode: $H_2 + CO_3^{-2} \rightarrow H_2O + CO_2 + 2e^-$ (1.1)

Cathode: $CO_2 + \frac{1}{2}O_2 + 2e^- \rightarrow CO_3^{-2}$ (1.2)

Total: $H_2 + \frac{1}{2}O_2 \rightarrow H_2O + Energy$ (1.3)

It is possible to notice the presence of carbon dioxide among the reacting species. Due to the CO_2 concentrations required at the cathode, usually it is necessary to circulate the anodic exhaust (that is a CO_2 rich effluent) to the cathode. The reformed hydrocarbons or the biomass and coal synthesis gases contain significant concentrations of carbon dioxide and this make the synthesis gas particularly suitable for feeding such fuel cells.

MCFC typical performances are: current intensity of 160 A/cm^2, cell voltages of 0.75 V, pressure 3.5 bar and temperature 650°C. Given the high temperatures and pressures of the outlet streams, it seems reasonable to foresee an integration of the system with a micro gas turbine, capable to recover the inlet gas compression work and to generate an electric power by means of a coupled alternator. The primary disadvantage of current MCFC technology is durability. The high temperatures at which these cells operate and the corrosive electrolyte used accelerate component breakdown and corrosion, decreasing cell life. Typical applications are plants for stationary power generation, between 0.1-10MW sizes.

A solid oxid fuel cell (SOFC) works at high temperature(800-1100°) and, as for MCFC cells, the noble catalyst can be eliminated. The advantages of this type of fuel cells are the high efficiency, the long-term stability and the fuel flexibility. The main disadvantage is the high operative temperature which results in a long start up time and in the compulsory heating of the fuel entering in the cell. The SOFC cell is characterized by a solid oxide or ceramic electrolyte, often stabilized by means of zirconium. The electrodes (usually nickel and zirconium as anode, and lanthanum manganate as cathode) are manufactured by means of thin films deposition on a base support and act as catalysts. The cell reactions are:

Anode: $H_2 + O^{-2} \rightarrow H_2O + 2e^-$ (1.4)

Cathode: $\frac{1}{2}O_2 + 2e^- \rightarrow O^{-2}$ (1.5)

Total: $H_2 + \frac{1}{2}O_2 \rightarrow H_2O + Energy$ (1.6)
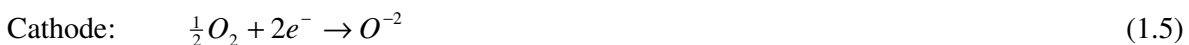
The main advantages of these cells are the high flexibility to different fuels. They can work with both H_2 and CO which are converted in the anode side. The SOFCs are not vulnerable to carbon monoxide that is reformed inside the cell. Because of the high operative temperatures, light

hydrocarbon fuels, such as methane, propane and butane can be also internally reformed within the anode. SOFCs can also be fueled by externally reforming heavier hydrocarbons, such as gasoline, diesel or biofuels. Such reformates are mixtures of hydrogen, carbon monoxide, carbon dioxide, steam and methane, formed by reacting the hydrocarbon fuels with air or steam in a device upstream of the SOFC anode. SOFC power systems can increase efficiency by using the heat given off by the exothermic electrochemical oxidation within the fuel cell for endothermic steam reforming process. However, they are very sensible to sulphur poisoning, so the sulphur must be removed before entering the cell using adsorbent beds or other means.

SOFC proposed configurations are tubular, planar and monolithic. Typical tubular stack performances are 300 mA cm^{-2} of current intensity and cell voltage of 0.6 V at atmospheric pressure and 1000°C temperature.

Nowadays there are pilot scale plants of 100 e 200 kW size. The advantages of this technology are the possibility of CHP production (thermal recovery option), the wide range of usable fuel and interesting global conversion efficiency (greater than 45%, for some authors can reach 70%). The main drawbacks are related from one side to the costs of the materials and of the manufacturing technologies and from the other to the low stability of the components mainly stressed by the high temperatures.

Chapter 2

Biomass gasification: state of the art

2.1 Experimental activity in Europe

The development and installation of gasification plants has remarkable grown during the last 15 years. Gasification for heat production is a competitive technology and hundred of gasifiers are installed in many developing countries but also in Europe and USA for heat production. These plants are fixed bed reactors, downdraft or updraft, which can work with several types of feedstock (i.e. rice husks, rice straw, bark, sawdust, olive waste). The feedstock is pyrolysed or gasified with air and the produced gas is burned in a second chamber for heat production. The gas yield is characterized by low heating value and high tar content.

The idea of power generation from the gasifier plants was born few years after the development of Otto and Diesel engines. Several plants for power generation have been built at demonstrative scale and even if now the technology seems to be ready for commercialization, the number of plants that successfully works is small, compared to the numbers of plant built. Moreover the size of the plant is often above 1MW. Absolutely, it is possible to say that there is a number of operative gasification plants that have demonstrate that the gasification technology can be really used for heat and electricity production at large scale, but it is still difficult to find successful experience of plants at small scale (200-400 kW). This is the future direction of the gasification field: small plant that can be used in remote or rural area for heat and energy production.

In the first part of this chapter a review of the operative plants at small and large scale is done. In the second part an overview of the gasifier at lab or pilot scale is also reported.

2.2   Operative gasification plant at large scale

The plants shown in figure 2.1(and briefly describe below) are considered as successfully experience since they are operative under commercial conditions and, at least, for more then 6000 hours (or for 2000 hours per year) [Knoef, 2005]. The size of the considered plants is between 1 and 20 MW_e.

Gussing, Austria: this plant is a CHP plant at demonstrative scale, in operation since 2002. It is a twin fluidized bed reactor with steam as gasifying agent. The gas yield is cooled and cleaned and then burned in a gas engine. Thanks to this plant, the whole city is supplied with green electricity and heat from biomass [Hofbauer, 2007].

26

Figure 2.1 Successfully operative gasification plants in Europe

Grevè di Chianti, Italy: the plant was designed to be fed with RDF (Refuse derived fuel) in pellets form. The system consists of a TPS-designed gasifier, fluidized with air at atmospheric pressure, the power production stage and the cleaning section to respect the emission limits required. The boiler/combustor is built to accept the raw gas from the gasifier. The electric power output is up to 6.7 MW [Granatstein, 2003].

Enemora, Spain: the gasification plant (developed by Energia Natural de Mora and EQTEC Iberia s.r.l) located in Spain it is a fluidized bed gasifier. Air is used as gasifying agent and almond shell as feedstock. Two engines are fuelled with a mixture of diesel and gas produced via gasification process. The plant was planed to produce from 250 to 750KW$_{el}$. The global efficiency is reported to be 22%.

Lahti, Finland: A CFB co-firing gasification plant has been built by Foster Wheeler Energia in 1998. Air is used as fluidizing and gasifying agent. The operative temperature is between 800-1000°C and the syngas produced is burned in a boiler mixed with coal or natural gas. Different feedstocks are suitable for the plant: (i.e. wood, plastic, RDF, paper) and moisture content up to 50% can be accepted. The stability of the boiler steam cycle is also good.

Rudersdorf, Germany: A CFB has been incorporated into a cement production process to provide energy for the cement production process. The CFB built is composed by a reactor, an integral

recycle cyclone and a seal pot. The gasifying agent is air and it is fed in two points as primary air to fluidize the bed and secondary air above the feed point. The gasification process takes place at temperature between 800-950°C, the bed material is distributed almost uniform in the reactor and this allows a high carbon conversion rate. Up to four different biomasses can be fed at the same time through four hoppers, but the fuel has to be prepared in size of 25-50 mm.

Varnamo, Sweden: in 1990 a pressurized CFB gasification plant was built by Sydkraft. It was mothballed in 2000 when the demonstration program was over. In 2004 it was bought by VVBGC (Vaxio Varnamo biomass gasification center) and upgraded and restarted in 2007. The first gasifier was air-blow, but after the rebuilt it can work also with steam or oxygen as gasifying media. The syngas produced is partially burned in a gas turbine to generate electricity, and the heat recovered from the hot flue gas of the gas turbine is used for steam generation. Then the super-heated steam is supplied to a steam turbine and more electricity is produced [VVBGC, 2010].

Freiberg, Germany: The CHOREN Company developed, since 1997-98, the so called Carbo-V process. In The Carbo-V gasifier the process is divided in three steps: low temperature gasification, high temperature gasification and endothermic entrained flow gasification. In the first the biomass is predried with process energy (waste heat) to a moisture content of 15 - 20 %. It is then carbonized in the LTP section (low-temperature pyrolysis) through partial oxidation with a gasification agent (air and/or oxygen) at temperatures between 400 °C and 500 °C. In the second stage the carbonized gas is post-oxidized in the high-temperature gasifier's combustion chamber using air and/or oxygen. The heat released by oxidation heats the carbonization gas to temperatures higher than the fusion temperature of the input fuels' ash. In the last step the char is blown into the hot combustion gases in the lower section of the endothermic entrained flow gasifier. The carbon reacts with the carbon dioxide and steam to form CO and H_2. Because of these endothermic reactions, the gas temperature is instantly reduced to approx. 900°C. This "chemical quenching" allows highly efficient production of a tar-free raw gas. The syngas yield is used for heat and power generation, for methanol production and for BtL (Biomass to Liquid) generation through Fischer-Tropsch process [Choren, 2010].

DTU, Denmark: The technical university of Denmark is studying biomass gasification since the late 80'.During 20 years, several fixed bed gasifier have been tested. In 2002 DTU decided to build a continuous running gasifier for heat and power production. The reactor is a co-current - two stage fixed bed. The gas produced is cooled and fuelled to a gas engine. The heat released from the hot gas during the cooling is utilized for drying and pyrolysis of the biomass and for pre-heating the air fed as oxidizing agent in the gasifier [Hemriksen, 2006].

Harboore, Denmark: since 1996 more than 8000 hours of operation have been registered for the plant in Harboore. The gasifier provides district heat for the municipality of this city. It is an updraft wood-chips gasifier and the gas is burned in a gas-fired boiler. Since 2002 the gas cleaning system

has reached an adequate level to be used as fuel in a gas-engine (two engines of 750 kW_e have been added)

Graested Denmark: The Biosynenergi has built and operates a small demonstration plant for heat and power generation that has been in operation for more than 4000 hours. The plant it is a continuous downdraft fixed bed gasifier (open core), with two points for air input (primary and secondary). The plant supplies 175kW_{th} of heat in the district heating of the local community and 75kW_e.

For some of the plants described above has been possible to find data on the typical gas composition produced and they have been reported in table 2.1.

Table 2.1 Main characteristics of the gasifier described above

Location	Fuel	Gasifying agent	CO	CO_2	H_2	CH_4	N_2	Power output
Grevè di Chianti, Italy	RDF	Air	8.8	15.7	8.6	6.5	45.9	6.7MW_e 15MW_{th}
Gussing, Austria	Wood chips	Steam	20-30	15-25	35-45	8-12	3-5	2MW_e 4.5MW_{th}
Enemora, Spain	Almond shall	Air	-	-	-	-	-	750kW_e
Lahti, Finland	RDF, wood paper	Air	-	-	-	-	-	20MW_e 70MW_{th}
Rudersdorf, Germany	Biomass and raw materials	Air	5.4	-	-	2.5	-	-
Varnamo,Sweden	Wood chips, pellets, RDF	Air,steam oxygen	16-19	15-18	9.5-12	6-7.5	50	6MW_e 9Mw_{th}
Freiberg, Germany	Wood chips, waste wood,	Steam oxygen	32	25	14	0.2	-	150 kW_e BioDiesel
DTU, Denmark	Wood chips	Air	19.6	15.4	30.5	1.2	33.3	17.5kW_{el}
Harboore, Denmark	Wood chips	Steam air	22.8	11.9	19.0	5.3	40.7	1.4MW_e 3.4MW_{th}
Graested,Denmark	Wood chips	Air	-	-	-	-	-	75kW_e 175KW_{th}
Skyve, Denmark	Wood chips	Air	22	11	20	5	40	5.4MW_e 11.5MW_{th}
Kokemaki,Finland	Wood fuel	Air	-	-	-	-	-	1.8MW_e 3.3MW_{th}

Several other gasification plants exist in Europe and are already operative or under investigation even if they have not been included in the group above because they have less then 2000 hours of operation. However, it is worth to mention some of them. The scale of the plant goes also below 1MW. The smaller gasifier reported is of 70kW_e.

Kokemaki, Finland: Condens Oy with VVT has developed a new Novel gasification process that seems to be an economical attractive solution for power generation. The system has an innovative fuel feed system, based on forced fuel flow (suitable light and fine fuel such as REF), a fixed bed reactor and an advanced cleaning system for tar removal. It can work with different fuel with moisture content up to 50%. The outgoing gas is used in turbo-charged gas engines. [Hannuala, 2007]

Skyve, Denmark: In Skyve a bubbling fluidized bed (BFB) gasifier is used to produce gas from wood-based biomass. This gas is then used in of reciprocating engines in a combined heat and power (CHP) application. The fuel is fed through two lock hopper systems by feeding screws into the lower section of the gasifier's fluidized bed. The gasifier can operate at a maximum of 2 bars over pressure and 850 ° C temperatures. Air is used as the gasification medium and dolomite is used as the fluidized bed material [Salo, 2009].

Gjol, Denmark: T/K Energi A/S has developed, built and tested a three-stage gasifier with dry cleaning. In this design the three sub processes of pyrolysis, oxidation and reduction are separated. This enables to optimize each step and the raw gas produced show a low tar content. Steam is injected as heat transfer medium in the pyrolyser which is not externally heated. The gas cleaning session is very simple, since the gas is almost free of tar.

The notable gasification plant developed in Europe at demonstration or commercial scale are listed in table 2.2 [Shures, 2006]. At every plant a number is associated, thus it is possible to see the location of the plant in figure 2.2.

Table 2.2 Gasification plant active in Europe

Country	Location (n°)	Plant description	MW$_{th}$
Austria	Gussing(1)	FICFB BMG CHP at demonstrative scale	8
	Neustadt (2)	Down draft BMG CHP demonstrative scale	2
Denmark	Harbore (3)	Updraft CHP demonstrative scale	5
	Gjol (4)	3-stage gasification process at demonstrative scale (TKEnergi)	3
	Graested (5)	Continuous open core gasifier Biosynegeri	0.17
	Lyngby(6)	3-stage gasification plant for heat and power generation (Viking)	0.07
	Skive (7)	Carbona Renugas fluidized bed CHP at demonstrative scale	30
Finland	-	8 updraft gasifier by Bioneer	5
	Kokemaki (8)	Novel updraft gasifier at demonstration scale	7
	Lahti (9)	CFB co-firing plant by Foster Wheeler	50/86
	Varkaus (10)	Fluidized bed metal recovery gasifier	40
Germany	Schwarze (11)	Plant for waste to methanol conversion at commercial scale	130
	Rudersdorf (12)	Lurgi CFB gasifier firing cement kiln	100
	Oberhausen (13)	Fraunhofer Umsicht CFB at pilot scale	0.5
	Freiberg (14)	CHOREN Carbo-V two stage entrained pilot plant	1.0
	Freiberg (15)	Future energy pyrolyser/entrained flow GSP gasifier	3-5

Germany	Pfalzfeld (32)	A new fully automatic wood gasifier developed from Mothermik® which is available for commercial market.	0.25
Italy	Chianti (16)	TPS CFB RDF plant at Greve in Chianti	15
	Trisaia (17)	ENEA CFBG pilot plant	0.5
Netherlands	Geertruidenberg(18)	AMER/Essent/Lurgi CFB gasification co-firing plant	85
	Willem-Alexander (19)	Biomass co-gasification Shell entrained coal gasifier (35 MW$_e$ from biomass)	250
	Tzum (20)	CFBG plant	3
	Petten (21)	Several pilot plants at ECN	
Spain	Enemora (32)	Fluidized bed gasifier for almond shell	0.75
Sweden	Karlsborg (22)	Foster wheeler Energy CFBG using paper mill	30
	Norrsundet (23)	Foster wheeler Energy CFBG using paper mill	20
	Sodracell (24)	Gotaverken CFBG at Sodracell for paper mill	30
	Varnamo (25)	Bioflow foster wheeler Energy CHP at demonstration scale	18
Switzerland	Spiez (26)	Pyroforce downdraft BMG system	0.2
UK	North-Ireland (27)	Rural generation downdraft BMG system	0.1
	North- Ireland (28)	Biomass Engineering Ltd, down draft BMG CHP system	0.25
	North Ireland (29)	Exus Energy down draft BMG CHP systems	0.3
	Gloucestershire (30)	Charlton energy rotary kiln waste gasification plant	-
	Bristol (31)	Compact power two stage waste gasification	-
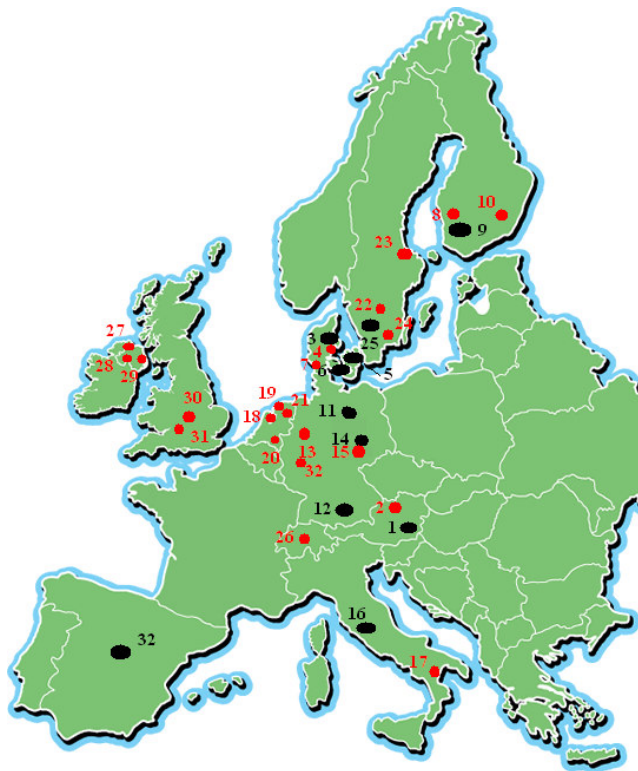
Figure 2.2 Gasification plant built and operative in Europe (data in table 2.2). In black, the so called "successful experience" and, in red, others remarkable plants.

31

2.3 Operative gasification plant at lab, small and pilot scale

A similar research has been done on gasification plant at smaller size. Indeed, plants at large scale are in operation since several years. The future step is the development of the gasification technology at small scale to serve remote areas, a few number of houses or a single unit. The gasification systems between 1 and 100 kW are very interesting and represent a remarkable opportunity for developing countries, mountains areas and solitary residence/houses. Anyway the technology at small scale is still not commercially available.

By means of a literature review over the last 10 years, more than 30 papers have been gathered on biomass gasification experiments run in different plants, often with different feedstock. The gasifiers analyzed have been divided in three categories according to their size: laboratory scale (maximum high 1meter, power up to 1kW), small scale (maximum high 2 m, power up to 10kW) and pilot scale (maximum high 5-6m, power up to 100kW). In figure 2.3 and table 2.3 the plants considered are shown and listed. It can be seen that the plants at small scale are the less numerous.

Table 2.3 Gasifiers at lab-small and pilot scale

Laboratory Scale	Number on the maps	bed	Gasification agent
Ibaraki, Japan (1) [Toshiaki, 2005]	1	Fixed	air-steam
Newcastle, UK (2) [Midilli, 2001]	2	Fixed	air
Paris, France (3) [Nagel, 2005]	3	Fixed	air
Aquila, Italy (4) [Rapagnà, 2000]	4	Fluidized	steam
Zaragoza, Spain [Manya, 2006]	5	Fluidized	air
Lisboa, Portugal [Pinto, 2002],[Franco,2003]	6	Fluidized	air/steam
Hawaii, USA [Turn, 1998]	7	Fluidized	air-steam
Extremadura, Spain [Gonzalez, 2008]	8	Fixed	air-steam
Zaragoza,Spain [Gil, 1999]	9	Fluidized	air
Marylend, US [Ahmed, 2009]	10	Fixed	steam
Trento, Italy [Baggio, 2009]	11	Fixed	Inert/air
Nykoping, Sweden [Zevenhoven-Onderwater, 2001]	12	Fluidized	Oxygen
Small scale			
Stockholm, Sweden [Zanzi, 2005],[Baratieri,2010]	13	Fixed	air
Londra,UK [Pindoria, 1998]	14	Fixed	air
Pelten, Netherlands [Van Kasteren, 2006]	15	Fluidized	air-steam
Eindhoven, Netherlands[Kersten,2003]	16	Fluidized	air
Guangzhou, China [Lv, 2004]	17	Fluidized	air-steam
Ibaraki, Japan [Wu, 2006]	18	Fluidized	air-steam
Zaragoza, Spain [Herguido, 1997]	19	Fluidized	steam
Guangzhou, China [Pengmei,2007]	20	Fixed	air/oxygen-steam
Trento, Italy [Pieratti, 2010]	35	Fixed	steam

Pilot scale

Penang, Malysia [Zainal,2002]	21	Fixed	air
Sevilla, Spain [Campoy,2009]	22	Fluidized	Air/oxygen/steam
Melle-Gontrode, Belgium [Vervaeke, 2006]	23	Fixed	air
Newcastle, UK [Dogru, 2002], [Dogru, 2008]	24	Fixed	air
Madrid, Spain [García-Ibañez,2004]	25	Fluidized	air
Vancuver, Canada [Li, 2004]	26	Fluidized	air
Delft, Netherlands [Chen, 2004]	27	Fluidized	air-steam
Lisboa, Spain [García-García, 2003]	28	Fluidized	air-steam
Medellin, Colombia [Ocampo, 2003]	29	Fluidized	air
Vienna, Austria [Kramreiter, 2008]	30	Fixed	air
Gujarat, India [Pathak, 2008]	31	Fixed	air
Zaragoza, Spain [Gil, 1997]	32	Fluidized	air-steam
Coimbra, Portugal [Kikuchi, 2005]	33	Fixed	oxygen
Catalonia,Spain [Mitta,2006]	34	Fluidized	Air-steam
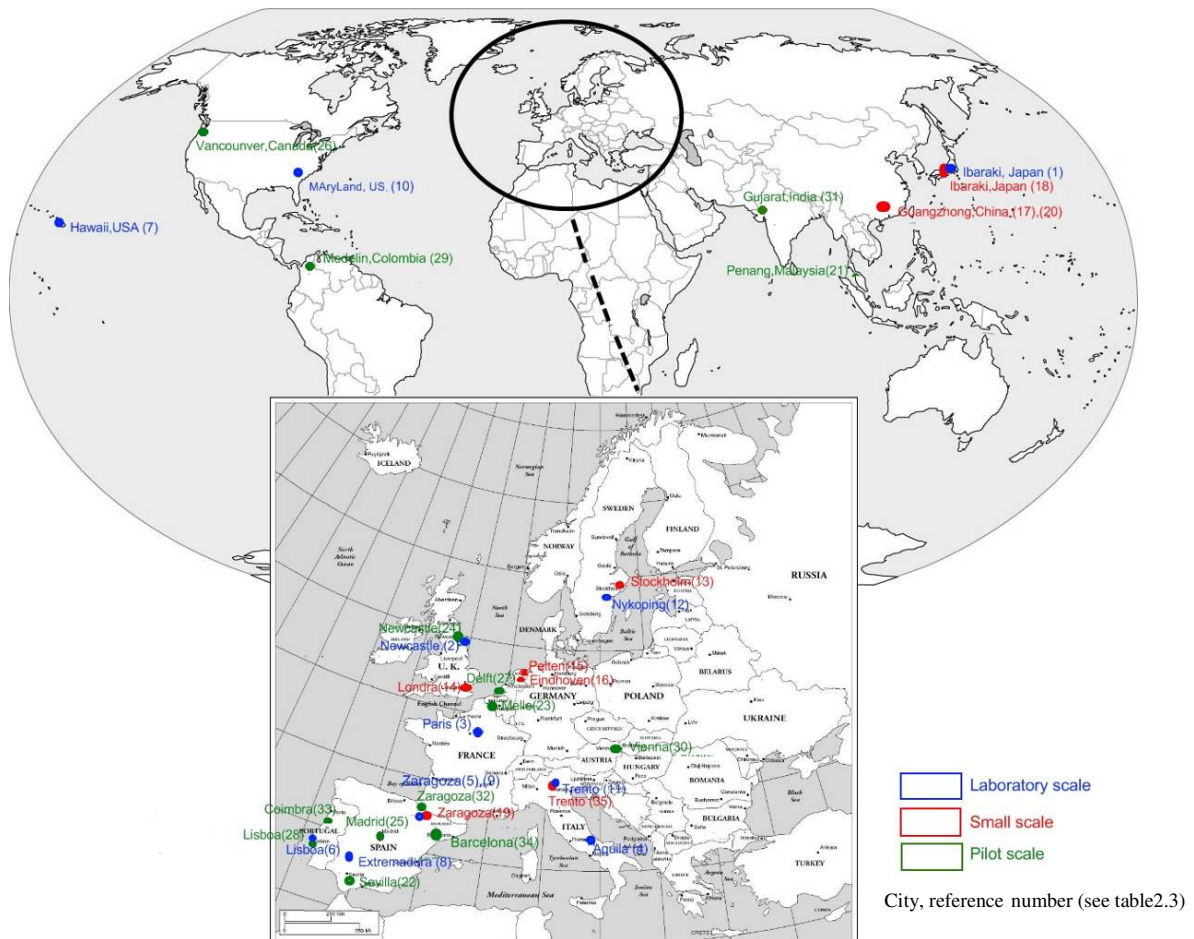
Figure 2.3 Gasifiers at lab-small and pilot scale (references in table 2.3)

The data reported on every paper have been analyzed and compared [Pieratti, 2008]. In each of the three categories investigated there is a slight tendency to adopt a fluidized bed configuration (55% on the total number of plants considered). The gasifying agent mainly adopted is air or a mixture of air and steam. Air is the primary choice since it is free and no further equipments are required to generate it as actually steam does. The less used is pure oxygen, even if it produces a gas with higher heating value. The use of oxygen implies its purchase, a safe storage place and safety measures to handle it. Figure 2.4 shows the gasification media adopted at different scales.
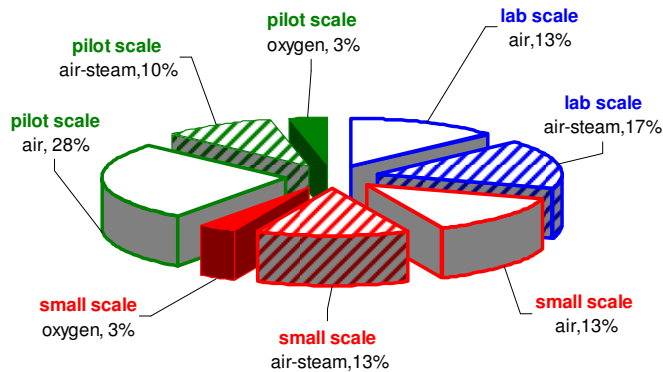
Figure 2.4 Gasifying media adopted at different plant scale

To achieve a comparison among the different experiences, the parameters equivalent ratio (ER), steam to carbon (SC), gasifying ratio (GC) low heating value (LHV) for biomass and gas produced, process efficiency and carbon conversion have been considered. Sometimes these information were directly available in the papers, otherwise they have been calculated, starting from other information, such as, for example, the type of feedstock or its proximate analysis, the final gas composition, the feeding rate, the gas production rate, the amount of oxygen, air or steam fed for kilogram of biomass. However, it has not been possible to collect the same information for all the gasifiers considered, hence some data are missing.

Since the gasification tests, especially at lab and small scale, are usually performed to investigate the influence of different parameters on the whole process, the data collected have often a wide range of variation. Therefore a rectangular representation has been adopted to compare the results. Close to each rectangle the bibliographic reference has been reported, and in some case, also the gasifying agent adopted (a=air, s=steam; a-s=air-steam; ox=oxygen).

Some calculations have been performed to use a unique measuring unit; where possible, the biomass heating value, expressed in different ways (on wet basis, as received (ar), on dry basis or on dry ash free) has been converted to $LHV_{(dry\ basis)}$. Instead when only the proximate analysis was available, the HHV (High heating value) has been computed according to the Milne's formula.

In the papers where the gas composition rather then the gas heating value was recorded, the LHV$_{(dry\ basis)}$ has been computed as the weight average of the low heating values of the main gases, reported by [Waldheim,2001].

The characteristic parameters of the gasification processes have been compared in different way to find out functional relations among them. The process efficiency (ε), where not indicated, has been calculated if the gas flow rate was known.

2.3.1 Temperature versus gas heating value

In figure 2.5 the gas heating value has been plotted versus the gasification temperature (on the left) and versus the biomass heating value (on the right). Theoretically, with a constant ER, it is expected an increasing of the heating value with the temperature up to 600-700°C, and then an almost constant LHV is reached. This tendency is not seen in the chart below, since different ER have been used in the experimental experiences compared, and the gasification temperature starts from 700°C. Viceversa, increasing ER the gas heating value decreases.

Figure 2.5 Gas heating value versus temperature and biomass LHV. For the associated number see table 2.3

Actually the syngas heating value depends on the gasifying agent, on the type of feedstock used and on the plant configuration. This explains why the heating value of the gas can varies in a wide range even at the same gasification temperature. It has been seen that the operative gasification temperature ranges between 700-900°C; Among 900 and 1000°C few experiences have been found, and always in fixed bed plants.

In table 2.4 the values of ER and the correspondent heating value (HV) of the gas produced are listed.

Table 2.4 Gasifiers at lab-small and pilot scale

Bib. ref.	Gasifying media	Equivalent ratio	HV (MJ Nm^{-3})	
[Turn, 1998]	air/steam	0.00-0.37	9-11.5	LHV$_{dry}$
[Lv, 2004]	air/steam	0.19-0.27	6.7-9.2	LHV$_{ar}$
[Ocampo, 2003]	air	0.21-0.27	2.7-3.3	HHV$_{ar}$
[Li, 2004]	air	0.22-0.54	2.4-6.1	LHV$_{dry}$
[Gil, 1997]	air	0.18-0.45	3.7-8.4	LHV$_{dry}$
[Chen, 2004]	air/steam	0.3	3.46	LHV$_{ar}$
[Van Kasteren, 2006]	air/steam	0.1-0.4	11.2-20.1	LHV$_{dry}$
[Toshiaki, 2005]	air/steam	0.2-0.4	8.9-13.1	LHV$_{dry}$
[Zainal,2002]	air	0.27-0.43	4.6-5.6	HHV$_{ar}$
[García-Ibañez,2004]	air	0.41-0.73	2.9-3.8b	LHV$_{dry}$
[Wu, 2006]	air/steam	0.2	16-20	LHV$_{dry}$
[Manya, 2006]	air	0.25-0.35	3.9-4.1	LHV$_{dry}$
[Pindoria, 1998]	air	0.2-0.55	4.5-8	LHV$_{dry}$
[Kersten,2003]	air	0.0-0.19	12.8	LHV$_{dry}$
[Kramreiter, 2008]	air	0.28-0.36	5.6-6.3	LHV$_{dry}$
[Kramreiter, 2008]	air	0.22-0.26	4.7-5.7	LHV$_{dry}$
[Kramreiter, 2008]	oxygen- steam	0.22-0.26	9-11.1	LHV$_{dry}$
[Gil, 1997]	oxygen- steam	0.24-0.51	10.3-13.5	LHV$_{dry}$
[Herguido, 1997]	steam	0.0	12.2-13.8	LHV$_{dry}$

It can be pointed out as the higher HVs are registered for ER lower or equal to 0.25; when the ER raises the gas energy content decreases because of the greater availability of gasifying agent which increases the percentage of oxidized species. On the contrary, when steam is added, the HV reaches higher values since the gas is enriched in hydrogen. Furthermore it has been noticed that ER values for pilot plants are sensibly higher than the one adopted in laboratory or small scale apparatus; this is due to the need of supporting a stage of combustion in order to obtain a self-sustained process; as a consequence, the gas yield by pilot plants has lower calorific value then the ones produced by the others.

2.3.2 Temperature versus efficiency and carbon conversion

The data related to the process efficiency have been charted in Figure 2.6 versus temperature. It clearly appears that, the highest efficiencies are reached with a mixture of air and pure oxygen (filled rectangular) even at lower temperatures respect to other experiences where only air was used. Theoretically, the carbon conversion is linked to the temperature even if, from the data collected,

this relation has not been observed. Here, except for [García-García, 2003] where the goal was to maximize the char production, the conversion percentages reached are always higher than 50%.
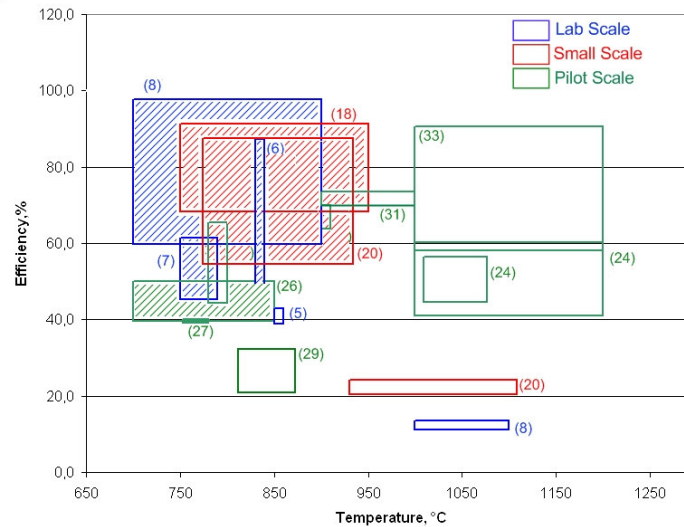
Figure 2.6 Process efficiency versus temperature. The filled rectangular are the tests performed with a mixture of air-steam as gasifying agent (for the number-reference see table 2.5).

Table 2.5 Gasification temperature and carbon conversion of some experiences

Rif. Bib	Temp [°C]	Temp [°C]	CC [%]
[Lv, 2004] (17)	air-steam	700-900	68.7-92.6
[Ocampo, 2003] (29)	air	812-872	47-70
[Li, 2004] (26)	air-steam	700-850	81.6-100
[Pinto, 2002] (6)	air-steam	730-900	50-98
[García-Ibañez,2004] (25)	air	780-800	81-87
[Manya, 2006] (5)	air	850	57-60
[Pindoria, 1998] (14)	air	700-950	75-90
[García-Garcia,2003] (28)	steam	800-850	10-23

2.3.3 ER versus efficiency and carbon conversion

Finally the equivalent ratio has been charted against carbon conversion; it is expected an increasing in carbon conversion with the ER value; the few data deduced prove this tendency as shown in figure 2.7. Globally, the process performance floats between 40% and 60%, except for one experience [Ocampo, 2003, (29)]. The data show that this parameter tends to increase with the equivalent ratio. Both carbon conversion and process efficiency seem to have a similar trend regarding the ER; an opposite behavior characterizes the relation between ER and gas heating value. High carbon conversion values increase the global process performance, and it result in higher outgoing gas flow rates. However, the efficiency depends also on the gas calorific value, as

shown by ([Li, 2004], [Manya, 2006]); the former shows smaller efficiency even with higher carbon conversion due to a lower gas heating value.

Rif. Bib*	ER	Efficiency,%
(7) a-s	0-0.37	45-62
(29) a	0.21-0.27	21-32
(26) a	0.22-0.54	39-50
(27) a-s	0.3	39
(25) a	0.41-0.73	44-65
(5) a	0.25-0.35	39-43
(20) a	0.22-0.26	20-24
(20) a-s	0.22-0.26	55-88

* For the connection number-reference see table 2.5
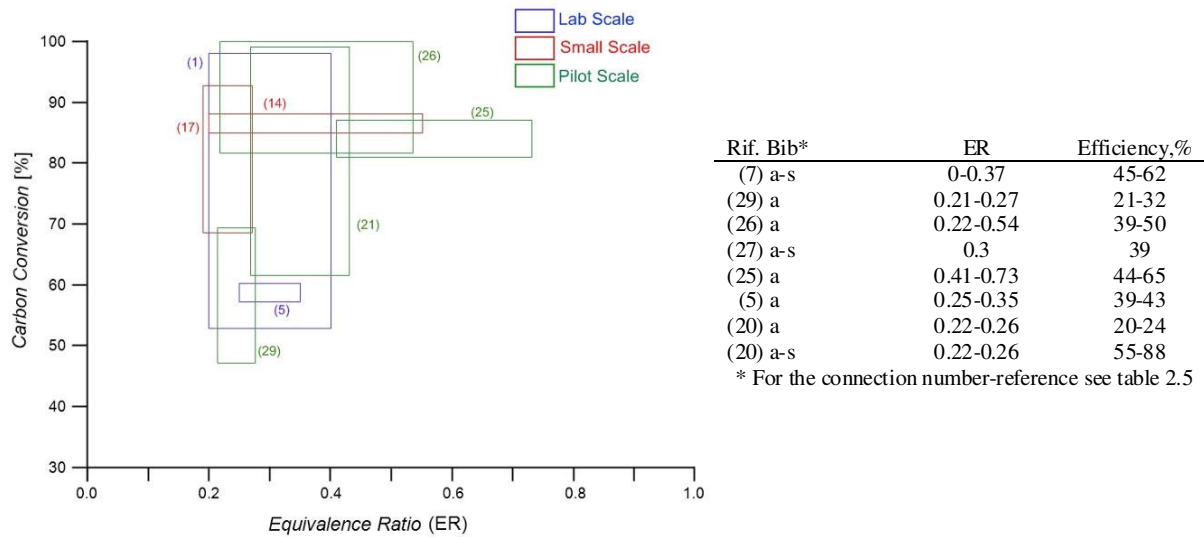
Figure 2.7 Equivalent ratio versus carbon conversion

Globally it can be concluded that the equivalent ratio is one of the most significant parameter since for ER reduced values, high heating value of the syngas and lower conversion efficiency of the process have been observed. The temperature plays an important role on the final gas quality, although it is of secondary importance if compared with the equivalent ratio. The carbon conversion is generally above 50% unless the goal is to maximize char production. The energy efficiency is linked to the gas heating value and to the conversion percentage; comparable energy efficiencies can be obtained both by means of high gas heating value and low carbon conversion (which usually occur in pyrolysis processes) and by means of low gas heating value and high carbon conversion (as in gasification processes). The analysis performed can be used as a starting point to plan future thermochemical biomass experimental facilities or industrial plants.

2.4 Modelling activity: equilibrium and kinetic models

The gasification process includes different sub processes: fast pyrolysis, partial oxidation of pyrolysis products, gasification of the remaining char and tar conversion in other. A high number of complex reactions occur during these sub processes and influence the process efficiency. The gas produced is also influenced by all these sub processes and by the rate of heating and the residence time in the reactor.

The gasification process has been studied by the theoretical point of view, and different mathematical models have been built to try to simulate the thermochemical processes and to evaluate the influence of the main parameters such us temperature, moisture content, air/fuel ratio,

steam/fuel ratio, gas composition and its heating value. Some models only look for the final gas composition at chemical equilibrium, while others try to reproduce the different sub processes along the reactor.

The models can be divided in three groups: equilibrium models (stoichiometric and non stoichiometric), kinetic models and neural network models. Models where both equilibrium and kinetic aspects are linked have been also developed.

2.4.1 Kinetic models

The so called "kinetic models" are based on the description of the reactions mechanism of the process under the kinetic point of view. It is very important in designing, evaluating and improving gasifiers to have a realistic description and prediction of the gasification process. These models can be very accurate but heavy in calculations. Several models have been developed in these years based on the kinetic approach, i.e. [Wang, 1993], [Di Blasi, 2000], [Fiaschi, 2001], [Giltrap, 2003], [Yang, 2003], [Jayah,2003], [Roshmi, 2004], [Dennis, 2005], [Babu, 2006], [Gobel, 2007], [Sharma, 2008], [Fernoso, 2010], [Gordilla, 2010].

Wang and Kinoshita developed a model based on the mechanism of surface reactions at a fixed residence time and reaction temperature. By minimizing the difference between experimental data and theoretical results, the apparent rate constants were determined for different temperatures and residence times. The kinetic rate expressions found by [Wang, 1993] were used by Giltrap et al. to develop a model of the reduction zone in a downdraft biomass gasifier to predict the gas composition in steady-state conditions. The authors introduced the char reactivity fraction (CFR), which represents the reactivity of the char and is an important variable in the simulation, which was kept constant through the reduction region. The limit of this model is the difficulty in founding data to set the initial condition at the top of the reduction zone; indeed the pyrolysis and cracking reactions are usually not considered in the models, since the great number of reactions would make the model very complex.
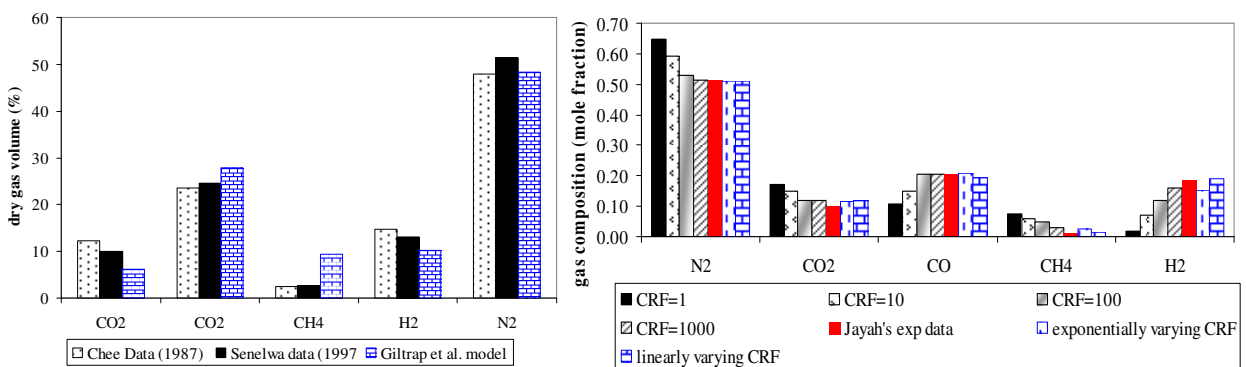
Figure 2.8 Gas composition foreseen by Giltrap model (left) and gas composition of Babu's model changing the CRF value (right)

The model works under the hypothesis that the oxygen from the air inlet is totally consumed by combustion reactions with char while the N_2 remains inert, that the pyrolysis products are completely cracked and that the solid carbon, in the form of char, is presents throughout the reduction zone.

The model outputs were compared with experimental data and a good agreement was found. The only problem is the over prediction of methane respect to the experimental data. The authors try to correct the model considering that the oxygen in the air reacts with CH_4 produced from the cracking of pyrolysis products but the predicted methane was still higher than the values observed in the test (figure 2.8 a).

This model was drawn on by Babu who suggested of modifying the Char residual fraction (CRF) considering an exponential variation in order to better predict the temperature profile along the reactor. The model was implemented with a finite difference method. Several simulation were run changing the CRF value from 1 to 1000 but constant throughout the reduction zone, and then it was increased both linearly and exponentially along the reduction bed with values from 1 to 10000. The authors pointed out that a changing of the CRF value during the process leads to a better agreement with the experimental data considered, as shown in figure 2.8 (right).

Di Blasi developed a one-dimensional unsteady model for a downdraft gasifier (stratified). Moisture evaporation, biomass pyrolysis, char combustion and gasification, gas-phase combustion, heat and mass transfer across the bed have been considered. The model has allowed the investigation of the influence of several gasification parameters, i.e. the biomass feeding rate and air to fuel ratio, on the produced gas quality and on the process efficiency.

Jayah et al. built a model based on a previous one developed by Chen in 1987. The model is divided in three parts: in the first one the amount of oxygen needed is calculated on the basis of the fuel fed and the operating condition (ER value); in the second step the drying, pyrolysis and combustion processes are considered together and the air to fuel ratio calculated previously is used as input. The outputs of this second step are the concentrations and the temperatures of the solid and gaseous phases. These values are inputs for the third section which predicts the temperature profile along the axis of the gasification zone, as well as the gas composition and the conversion efficiency. Jayah changed the model introducing the Millingan's Daming flaming pyrolysis sub-model to solve the over-prediction of the gas exit temperature. The model consists on two sub model, the Daming pyrolysis and the gasification zone. The first sub model is used to determine the maximum temperature and the product concentration of the gas leaving the zone. In the gasification zone the physical and chemical processes, the conservation flow equations, the transport phenomena and conservation principles are described, under the assumption that a single char particle moves vertically along the axis of the gasifier.

Sharma has recently developed a thermodynamic and a kinetic model for the char reduction zone in a downdraft gasifier. Both the models have been coupled with mass and energy balance to predict the gas composition, the heating value, the conversion efficiency and the status of un-converted

char. The model predictions have been compared with experimental data, as shown in figure 2.9 (left). The influence of the char bed length in the reduction zone has been also evaluated.

Gordillo and Belghit have built a two phase biomass char steam gasification kinetic model for a bubbling fluidized bed with a nuclear heat as source of energy. The model can predict the gases concentration and temperature profiles. The model has been used to simulate three different gasifiers to see the effect of varying the height-to-diameter (H/D) ratio. Hydrogen has been found to be the principal product of the steam only gasification, as can be found in literature data. In figure 2.9 (right) the hydrogen and carbon monoxide production for three different gasifiers is reported (G1: H/D=32, G2: H/D=12.67, G3: H/D= 5). The effect of the gas input superficial velocity effect, which is defined as the ratio between the steam input superficial velocity and the minimum fluidization velocity, has been investigated. The steam temperature is 800°C.
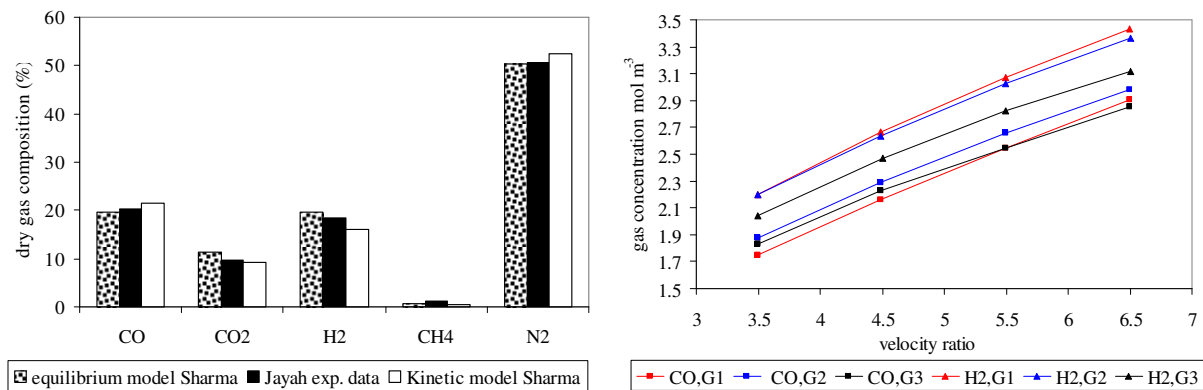
Figure 2.9 Ccomparison of the equilibrium and kinetic model predictions for dry gas composition with experimental data(left), H_2 and CO production foreseen by Gordillo's model versus velocity ratio (right)

Gobel developed a mathematical model for a fixed bed reactor based on: the mass and energy conservation in a simple one-dimensional flow, the chemical equilibrium in the gas phase, and the Langmuir-Hinshewood correlation to describe the char reaction kinetics. The results from the model have been compared with experimental data gathered from tests performed on a 100kW gasification plant at Denmark Technology University. The comparison is reported in figure 2.10 (left). To test the dynamic response of the model a study was carried out changing the operation condition from full load to half load. The model was able to predict satisfactorily the change in bed as function of time as well as the variation of temperature in time and gas concentration.

Fiaschi and Michelini developed a mathematical model for bubbling fluidized beds starting from a previous one-dimensional model. The model is able to predict temperature and gas concentration along the reactor and take into account two phases: bubble and dense phase. The model is in agreement with the results of other kinetic models and gives a good correspondence with experimental results.

Kaushal et al. have also recently built a two-phase one dimension kinetic model. Several sub-models to simulate pyrolysis, gasification, bed hydrodynamics and material property calculations compose the model. The model can deal with different biomasses and gasifying media and is able to predict temperature and gas concentrations along the reactor. The comparison with different experimental experiences has shown a satisfactory agreement (figure 2.10, right)

[Gomez, 2010] has recently given an extensive survey of models for biomass gasification in fluidized bed.
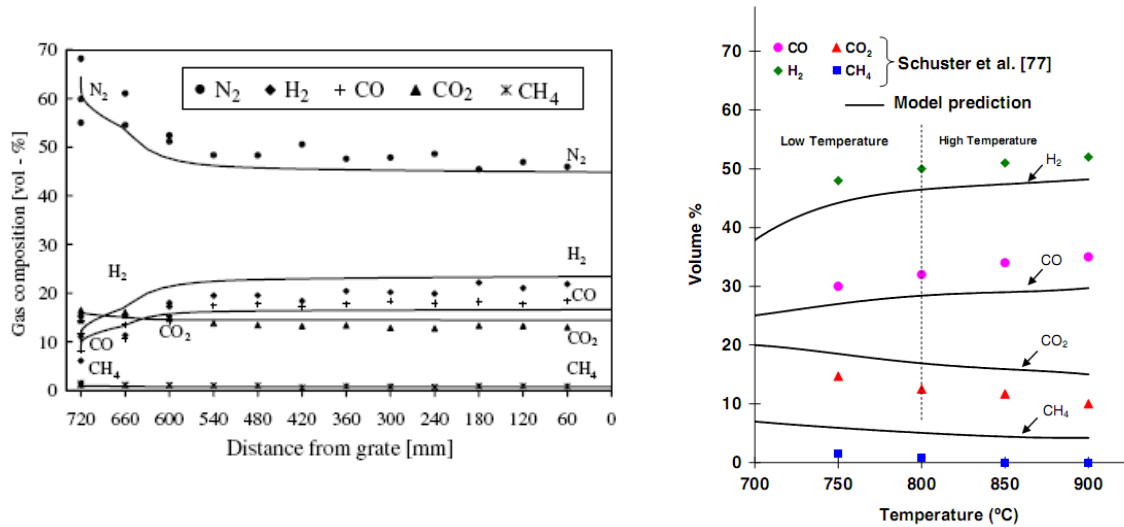
Figure 2.10 Comparison between the measured gas composition (points) and the measured gas composition (lines) (left) comparison of model prediction for steam as gasifying agent (right)

2.4.2 Equilibrium models

The weakness of the kinetic model is that their simulations cannot be generalized. They are strictly linked to a specific gasifier configuration and shape. The thermodynamic equilibrium models are more general because they are not influenced by the gasifier design. These models can help in study the influence of the main gasification parameters.

The composition of a mixture at equilibrium can be studied using different approach. One of the main approaches is the so-called "Gibbs energy minimization method". It consists in evaluating the concentrations of the species present that minimize the total Gibbs energy of the products, in accordance with the constraints imposed by the principle of conservation of mass and of the stoichiometry (elements conservation). Indeed the Gibbs energy reaches a minimum value at thermodynamic equilibrium. For a closed system at uniform temperature and pressure, (not necessarily constant) with a certain number of species in several phases, evolving from a non equilibrium to an equilibrium state the following expression can be written:

$$dU^t + PdV^t - TdS^t \leq 0 \qquad\qquad (2.1)$$

This expression is valid both for irreversible path (inequality) and for reversible path (equality). If the closed system is kept at constant temperature and pressure during the evolution, the equation can be simplified in:

$$d\left(G^t\right)_{T,P} \leq 0, \text{ where } G = U + PV - TS \qquad (2.2)$$

All irreversible process, at constant T and P, evolve in the direction that causes a decrease of the Gibbs energy. Indeed, the equilibrium state of a closed system, is the one for which the total Gibbs energy reaches a minimum with respect to all possible changes at the given T and P.

The Gibbs energy minimization method, then, consists in writing an expression for (G^t) as a function of the number of moles of the species present in the several phases and then finding the set of values for the mole number that minimizes this function, subject to the constraints of mass conservation and stoichiometry (i.e. elements conservation).

For open system, with mass exchange with the surroundings, an expression for the Gibbs function can be also written, considering that the number of moles of the species can vary because of the mass exchange. In this case it is necessary to introduce a chemical potential μ_i, that is a function of the n_i moles of the different compounds.

$$dG^t = -SdT + VdP + \sum_{i=1}^{S}\mu_i dn_i \qquad (2.3)$$

Two approaches can be used to solve a minimization problem: stoichiometric and non-stoichiometric. Several authors have demonstrated that the two processes are essentially the same [Smith, 1982].

The main hypothesis on which these models works are:

The gasifier is considered zero-dimensional;

➢ The heat losses are neglected because the reactor is considered perfectly insulated;

➢ The reactor is considered perfectly mixed and with uniform temperature;

➢ The residence time inside the reactor is assumed to be long enough to reach the equilibrium condition;

➢ Tars are not modelled;

➢ No information on the sub-processes or intermediate products is provided.

2.4.2.1 Applications of equilibrium models

Several authors have built and tested stoichiometric and non-stoichiometric equilibrium models [Ruggiero, 1999], [Zainal, 2001], [Li, 2001], [Kersten, 2002], [Altafini, 2003], [Li, 2004], [Melgar, 2006], [Jarungthammachote, 2007], [Sharma, 2008], [Jarungthammachote, 2008], [Loha, 2011]. Often the equilibrium models have been modified in order to better predict the gas composition.

The authors who have worked on equilibrium models have pointed out that these models are a very useful tool even if they cannot always reach high accuracy. However, they are independent from the reactions mechanism and allow the prediction of the thermodynamic limits of the gasification process. Equilibrium approach is particularly suitable for downdraft fixed bed gasifier, characterized by a long residence time, and entrained flow gasifier. To simulate updraft fixed bed and fluidized-bed gasifiers with good accuracy, modified equilibrium model are usually needed. Some of the experiences found in literature are briefly summarized below.

Ruggiero et al. developed a black box non-stoichiometric equilibrium model to predict the gas heating value and composition produced by a biomass gasification process. The model considers well-stirred reactor, adiabatic conditions and perfect gas behaviour for reactants and products (so the pyrolysis phase can not be modelled). The conservation of chemical species is described by a set of equations plus the equations needed to take into account the thermal equilibrium. Ninteen compounds were considered in the model.

Zainal et al. modelled a downdraft gasifier by means of a stoichiometric equilibrium model. The model was used to investigate the influence in the gas composition of different biomasses and different moisture contents. The gas heating value predicted by the model was in reasonable agreement with the experimental one.

Jarungthammachote et al. built an equilibrium model based on the equilibrium constant to foreseen the gas composition coming from a downdraft gasifier. Comparing the model's output and the experimental results of other researchers, they found out some coefficients to correct the equilibrium constant of the water-gas shift reaction. The predicted results showed a good agreement with experimental values. The same authors, in 2008, developed a non-stoichiometric equilibrium model and applied the model to three different gasifiers: a central jet spouted bed, a spout-fluid bed and a circular split spouted bed. The model showed a significant deviation respect to experimental values especially in CO and CO_2 concentrations. The model was modified to take into account the carbon conversion, which is a very important factor. In this way, the agreement between the experimental and modelled data increased, even if high accuracy was not reached. The gas heating value (which is the measure of the energy that can be gained burning the produced gas) was overestimated due to the over-prediction of the carbon monoxide content in the gas. In table 2.6 the model versus experimental data of [Jarungthammachote, 2008] are reported. Loha et al used the same approach.

Li et al developed in 2001 a non-stoichiometric equilibrium model to predict the gas yield from a circulating coal gasifier. Later, in 2004, the model was used to foreseen the gas composition from a circulating fluidised bed biomass gasifier. The agreement between experimental and modelling data was not satisfactory, thus the model was modified taking into account the non-equilibrium factors. Indeed, using the data from a pilot plant on the residual carbon and methane concentration in the syngas, the correspondent carbon and hydrogen fractions were withdrawn from the initial input data on the biomass composition. This method shows very good agreement between modelled and real

data both in coal and biomass gasification case, as shown in figure 2.11 for the biomass gasification case.

Sharma proposed a full stoichiometric equilibrium model to predict the gas composition, the reaction temperature, and the solid residual fraction of a downdraft biomass gasifier. The model describes the char-gas and gas-gas reactions in the char reduction zone. The model results are in reasonable agreement with experimental data collected from various source. The author has investigated the influence of moisture content in the feedstock, pressure, temperature and equivalent ratio. The best conditions for an efficient gasification process are: moisture content between 10-20%, equivalent ration 0.3-0.4, and gasification temperature around 950°C.

Table 2.6 Comparison between experimental results, original model (O-Model) and modified model (M-Model) from [Jarungthammachote, 2008]

	$H_2(\%_{vol})$	$CO_2(\%_{vol})$	$CO(\%_{vol})$	$CH_4(\%_{vol})$	$N_2(\%_{vol})$	$O_2(\%_{vol})$	HHV	RMS_{error}
			Central jet spouted bed at 1323 K					
Exp	12.56	14.56	14.97	0.7	54.96	2.27	3.90	
O-Model	11.08	2.6	30.36	0	55.96	-	5.44	8.020
M-Model	13.55	8.73	19.18	0	58.53	-	4.302	3.319
			Circular split spouted bed at 1388.3 K					
Exp	10.98	13.7	16.41	0.88	57.47	0.55	3.961	
O-Model	10.26	3.17	29.23	0	57.34	-	5.183	6.807
M-Model	12.45	9.16	18.15	0	60.22	-	4.022	2.385
			Spout-fluid bed ER=0.35 at 1148.7 K					
Exp	8.43	14.95	11.61	2.52	61.55	-	3.891	
O-Model	14.99	10.42	20.68	0	53.9	-	4.688	5.935
M-Model	16.07	14.42	13.71	0	55.8	-	3.917	4.133
			Spout-fluid bed ER=0.30 at 1127.65 K					
Exp	11.86	14.48	13.03	2.95	56.87	-	4.01	
O-Model	15.45	10.43	21.08	0	53.3	-	4.801	4.400
M-Model	16.72	14.5	13.76	0	55.02	-	4.01	2.459

Altafini et al. and Melgar et al. have reported similar conclusions about the influence of the air to fuel parameter and the biomass moisture on the gasification temperature, the gas composition and system efficiency.

The modification of the equilibrium model by means of some coefficients coming from the experimental results is not the only way; another solution to improve the agreement between the model and the real data is the Quasi Equilibrium Temperature (QTE) approach. Usually the reaction temperature considered is the bed average temperature for the fluidized bed and the outlet temperature at the throat exit for downdraft gasifier. The idea is to use, in the equilibrium models, a lower reaction temperature instead of the real one, a so called "Quasi Equilibrium Temperature". In this way a better accuracy between the model predictions and the real data has been observed. For example, Li et al. [Li, 2001] found that the kinetic carbon conversion in a pressurized gasifier of

coal at a temperature between 747-877°C is comparable to equilibrium predictions for a temperature of 250°C lower. Kersten et al. showed that for operating temperature between 740-910°C the reactions equilibrium temperature for reaction 2.9, 2.10 and 2.11 should be assumed lower then the gasification temperature (583 ±25°C, 535 ±25 °C and 454 ±29°C respectively).
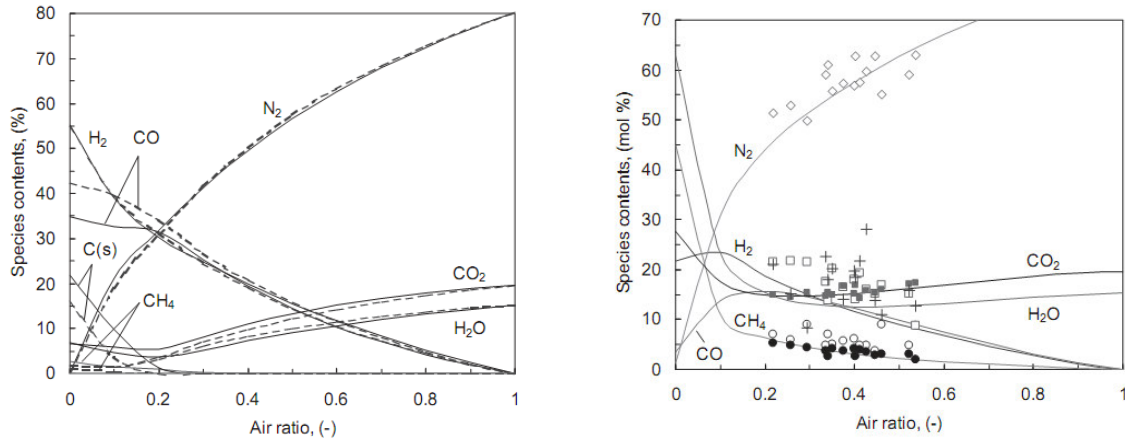
Figure 2.11 Gas composition foreseen by the equilibrium model for different Air ratio values (left), comparison between the outputs of the modified models and experimental data (right) Legends $H_2 \rightarrow$: $\circ$, $CH_4 \rightarrow \bullet$, $CO \rightarrow \square$, $CO_2 \rightarrow \blacksquare$, $H_2O \rightarrow +$, $N_2 \rightarrow \diamond$ [Li, 2004]

2.4.3 Neural network models

Some researchers have applied the neural network approach to biomass gasification field. Artificial neural networks (ANN) are widely used in the field of pattern recognition, signal processing, process simulation and function approximation. ANNs are made up by interconnected layers of simple nodes which can be called "neuronlike". The neurons act as nonlinear process elements within the network. The peculiar property of the ANN is that they are able to characterize non linear functional relationship. Additionally, little prior knowledge of the process technology is necessary to determine the structure of the resulting neural network based process model. Often a hybrid neural network (HNN) model is created for process modelling. This approach usually includes a part of the model where the first-principles of the analyzed process describes some characteristics of the process itself, and the neural network part which is used to estimate the unmeasured process parameters that are difficult to estimate from first principles. Frequently a multilayer feedforward neural network (MFNN) is adopted, which is a universal function approximator that is able to approximate any continuous function to an arbitrary precision even without a previous knowledge of the structure of the function to be approximate [Hornik, 1991].

Wills et al. [Wills, 1991] tried to apply the ANN model to provide estimations of biomass concentration in fermentation processes. Experimental measurements were used as secondary variables in the process. Promising results were obtained considering that was one of the first steps in the application of neural networks to biomass field. This topic was investigated also by Guo et al.

[Guo, 1997],[Guo,2001] who started performing a series of tests of coal gasification in a fixed bed reactor. Then they developed a HNN model combining a first-principles model with neural network parameter estimation. The model was tested with the data collected during the experimental activity. By means of the NN model, a parameter called "active char ratio" (ACR) was identified, as a function of gasification temperature and time, which shows a strong dependency with the type of coal. Afterwards they developed a HNN model to simulate the steam biomass gasification process in a fluidized bed gasifier. As before, a series of tests were performed in a fluidized bed gasifier investigating different biomasses, then the model was built to investigate the gasification profile of the biomass types. The model suggests that gasification behaviour of arboreal species is different from herbaceous ones. More recently Brown et al. [Brown, 2007] developed a model combining the equilibrium model and the neural network approach. The advantage of this approach is, from one side to improve the accuracy of the equilibrium model, and from the other to reduce the experimental data required avoiding the need of the NN model to take into account the mass and energy balances. The complete stoichiometry is formulated and the correspondent "reaction temperature difference" parameters are computed under constrain of non-equilibrium distribution of gasification products determined by mass balance data reconciliations. Temperature differences, fuel composition and gasifier operating conditions are related by the NN regressions. The model has been tested using data from an atmospheric fluidized bed gasifier. The first application of this new approach has given a useful insight for equilibrium modelling even if a further calibration of the NN model with more data is recommended.

Chapter 3

Steam gasification: syngas suitability for Solid Oxide Fuel Cells

3.1   Introduction

The aim of the present project is to couple a small-scale gasifier with a SOFC stack. The fuel cells show high efficiency and little long term degradation when fed with hydrogen, but they successfully work also with methane, propane, carbon monoxide or a mixture of them. Considering the characteristics of the fuel requested by the SOFCs, the idea is to produce a syngas as rich as possible in hydrogen. For this reason, the gasification process has been studied to choose the proper gasifier, the gasifying agent and the operative temperature.

3.1.1   Integrated biomass gasifier and fuel cell systems

The performances of integrated biomass gasifiers and SOFCs systems have been investigated from the theoretical point of view by several authors, i.e. [Alderucci, 1994], [Omosun, 2004], [Cordiner, 2007], [Bang- Moller, 2010], [Nagel, 2009], [Nagel, 2011], [Athanasiou, 2007], [Panopoulos, 2006].

Omosun et al. have developed a steady state model to investigate the performances of the integration of a Solid Oxide Fuel Cell with a biomass gasifier. The model was used to study the system efficiency and the costs considering two different options: a cold process for gas cleaning at a reduced temperature and a hot process involving gas cleaning at high temperature. The simulations showed an overall system efficiency of 60% for the hot process and 34% for the cold one.
Cordiner et al. simulated a 14 kW energy generation system where a SOFC stack is supplied by a biomass gasifier. The gasifier is integrated with a system for heat recovery by SOFC off gas combustion, to realize high efficiency concept. An equilibrium model has been used (zero-dimensional) for the gasifier and 3D CFD for the SOFC. The overall system efficiency found was 45%.
Nagel et al. have published a couple of works on the technical and on the cost analysis of a biomass integrated gasification (B-IGFC) fuel cell system. The work published in 2011 shows the experimental results collected from a series of tests performed in a B-IGFC demonstration unit composed by gasifier, gas cleaning session (with catalyst) and fuel cell stack. The gasifier and the

catalytic unit could work without problems; the SOFC unit feed with syngas produced approximately 40% less current compared to methane operation. Ash deposition was the major obstacle for a smooth SOFC system operation.

3.2   Steam gasification for hydrogen production

The syngas produced from a gasification process can have different composition depending on process temperature, type and amount of gasifying agent and feedstock. In the preliminary part of this project a two phases, thermodynamic equilibrium model has been developed by Baratieri et al. [Baratieri, 2008] to compare different gasification processes, from a thermodynamic point of view. Data from different experimental experiences were used to test the model and a good agreement was found. The idea was to find out the best configuration and the parameters values to maximize the hydrogen content in the syngas. In the following paragraphs a brief description of the model and the simulations outputs is given, since it has been the starting point of the reactor design.

3.2.1   Structure of the thermodynamic equilibrium model

As described in Chapter 2, the equilibrium composition of a mixture can be estimated with different approaches. In this model the so called *Gibbs energy minimization method* has been chosen; it consists in looking for the composition of the species which minimize the Gibbs energy of the products, respecting the constraints imposed by the mass and stoichiometry conservation. The main advantage of this method is that it does not require the selection of a number of "representative" chemical reactions allowing the formation of (equilibrium) products; it is nevertheless necessary to establish the chemical species expected in the product mixture.

The code uses the Cantera software library tool (a collection of object-oriented software tools for problems involving chemical kinetics, thermodynamics, and transport processes [Goodwin, 2005]). The solver implemented in Cantera is a version of the Villars-Cruise-Smith (VCS) algorithm (a well suited method to handle multiphase problems), that finds the composition minimizing the total Gibbs free energy of an ideal mixture [Smith & Missen, 1982]. The NASA [McBride et al., 1993] and the GRI-MECH [Smith et al., 2000] databases have been used to evaluate the thermodynamic properties of the chemical species considered in the model. The VCS algorithm applied the stoichiometric formulation to solve the problem. In details, the constraints of the closed system are treated by means of the independent stoichiometric equations and the result is a problem of unconstrained minimization.

$$\vec{n} = \vec{n}^{0} + \sum_{j=1}^{R} v_j \xi_j \qquad (3.1)$$

where:

$\vec{n}^{0}$ initial composition vector

v_j stoichiometric coefficients vector

ξ_j extents of the reaction

The minimization procedure applied to the G function implies the computation of its partial derivatives with respect to the ξ_j extents of the reactions (3.5) and gives the equilibrium condition (3.6).

$$\left(\frac{\partial G}{\partial \xi_j}\right)_{T,P,\xi_{k\neq j}} = \sum_{i=1}^{N}\left(\frac{\partial G}{\partial n_i}\right)_{T,P,n_{k\neq j}}\left(\frac{\partial n_i}{\partial \xi_j}\right)_{\xi_{k\neq j}} \tag{3.2}$$

$$\sum_i \nu_{ij}\mu_i = 0 \tag{3.3}$$

The VCS algorithm utilizes this procedure, that may be the more efficient when there are only a few independent stoichiometric equations. Stoichiometric algorithms search among a set of states that all satisfy the element constraints for the one state that satisfies the conditions of chemical equilibrium. The model considers 63 chemical species, 60 for the gaseous phase and 3 for the solid one (shown in table 3.1). The information required in input are the elemental biomass composition, the process temperature and pressure and the amount of gasifying agent fed to the process.

Table 3.1 Chemical species considered in the model

Phase	Group	Compounds
Gas phase	Inorganic carbon compounds	$C(g)$ CO CO_2
	Hydrogen compounds	H H_2 O O_2 OH H_2O HO_2 H_2O_2 HCO
	Nitrogen compounds	N N_2 NH NH_2 NH_3 NNH NO NO_2 N_2O HNO CN HCN H_2CN $HCNN$ $HCNO$ $HOCN$ $HNCO$ NCO
	Sulfur compounds	S SO_2 SO_3 H_2S COS CS_2
	Hydrocarbons	CH CH_2 CH_3 CH_4 C_2H C_2H_2 C_2H_3 C_2H_4 C_2H_5 C_2H_6 C_3H_7 C_3H_8 C_6H_6 $C_{10}H_8$ $C_{12}H_{10}$
	Other organic compounds	CH_2O CH_2OH CH_3O CH_3OH $HCCO$ CH_2CO $HCCOH$ CH_2CHO CH_3CHO
Solid phase	Carbon	$C(s)$
	Ash	CaO SiO_2

3.2.2   Model outputs

The model simulations show that the gas yield is mainly composed by six of the 63 chemical species considered: carbon dioxide, carbon monoxide, hydrogen, methane, water and residual solid carbon. Nitrogen is present only if air is used as gasifying medium. Several simulations were performed considering different biomasses, different operation temperature and gasifying agent (steam or air).

The hydrogen concentration is greater if steam is used as gasifying agent. Investigation on the effect of different Steam to Carbon values (SC= ratio between the moles of H_2O fed and the moles of carbon in the biomass) have also be done. In figure 3.1 and 3.2 the results of the model simulations are reported [Baratieri, 2008].
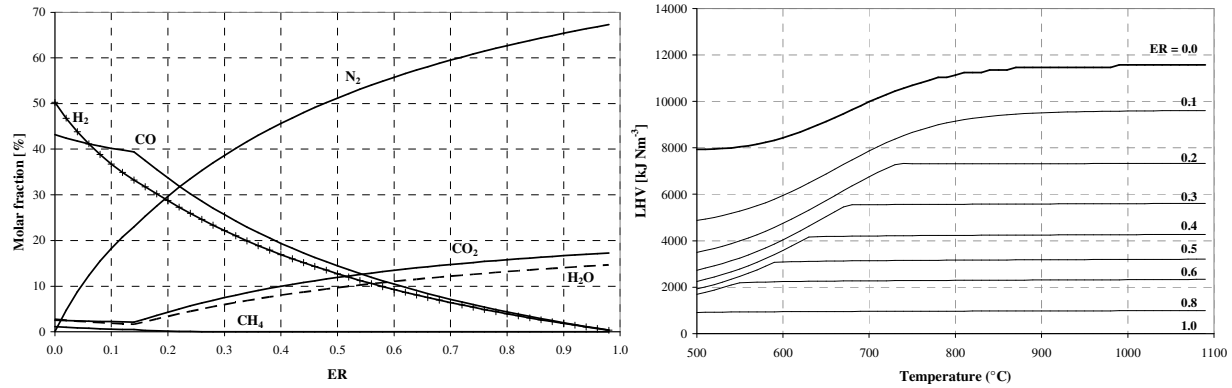
Figure 3.1 Simulation output for air gasification process: gas composition (left) and LHV (right) for different Equivalent ratio values (ER= ratio between moles of O_2 fed and moles of O_2 needed for complete oxidation) [Baratieri, 2008]
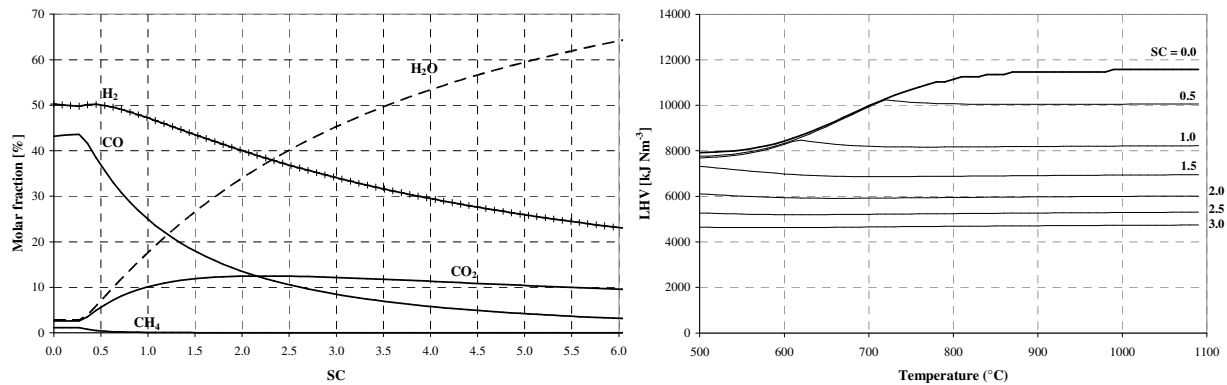
Figure 3.2 Simulation output for steam gasification process: gas composition (left) and LHV (right) for different SC values

Thanks to the model outputs, the steam gasification process has been chosen as the most suitable for the purpose of the present project. In Figure 3.3 only the hydrogen concentration (%, dry composition) is reported for different temperature and SC values. These values have been chosen to reduce the residual solid carbon. Indeed the 2-phase model has estimated that for SC greater than 1.5 no solid char is formed (figure 3.4). Thus, considering SC=2 and SC=3, the highest hydrogen production is theoretically reached for gasification temperature above 650°C, as shown in figure 3.4.

The reactor has been designed to work at a maximum temperature of 1000°C, even if this value has never been tested. The experimental activity has been performed at temperature between 700 and 800°C. Lower gasification temperature are not recommended because more tars are produced and the temperature of the outgoing syngas is not enough high to be fed in the SOFCs. On the other

side, too high temperatures reduce the tars concentration but increase the energy required to heat the system up and can decrease the life of the materials due to thermal stresses.
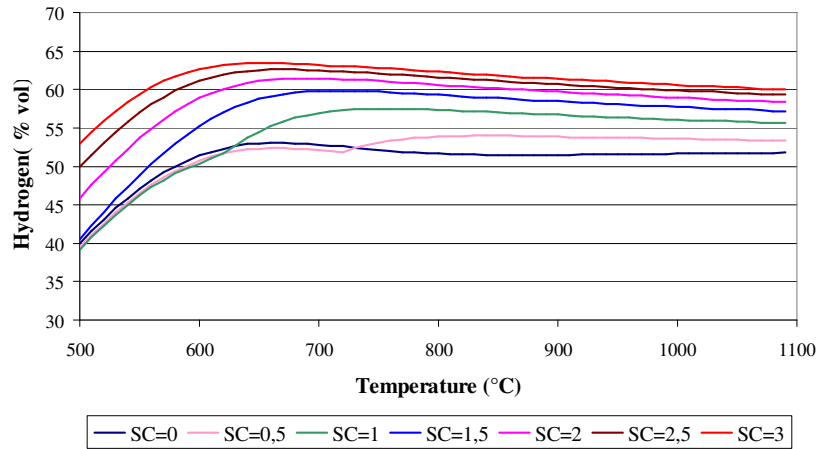
Figure 3.3 Hydrogen concentration for different SC values from 0 to 3
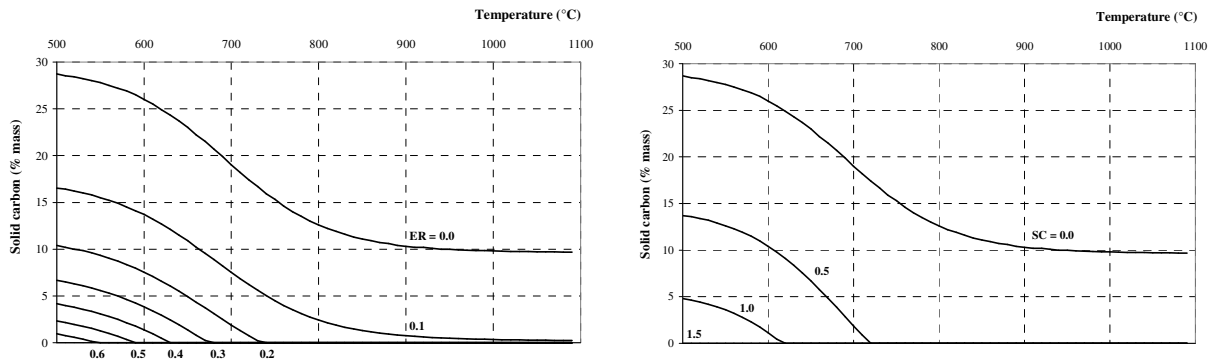
Figure 3.4 Solid carbons residual for different ER (left) and SC (right) values

3.3   Fixed bed gasifier and experimental facilities

Since the modelling part has pointed out that the use of steam as gasifying agent allows a higher hydrogen concentration in the syngas, the experimental activity has started designing and building up a co-current gasifier for steam gasification.

The main parts of the gasifier realized are:

> ➢ the reactor;
> ➢ the ash collector;
> ➢ the feeding system;
> ➢ the steam generator;
> ➢ the cleaning stage;
> ➢ the measurements tools.

During the development of the present work, the gasifier has been modified and improved several times. The experimental activity has been divided in two phases: the first performed with a semi-continuous fixed bed gasifier and the second with a continuous fixed bed gasifier. The difference between the two configurations consists in the system of char discharging that has been changed in the middle of the project. As it will be seen from the experimental results, this change has had a strong influence on the system.

3.3.1 Fixed bed gasifier: description

The *reactor* consists of two coaxial cylinders shaped vessels, having external diameter of 102 mm, height 480mm, and net volume available of 0.0037 m^3. A scheme of the reactor is reported in figure 3.5 (Section C-C).
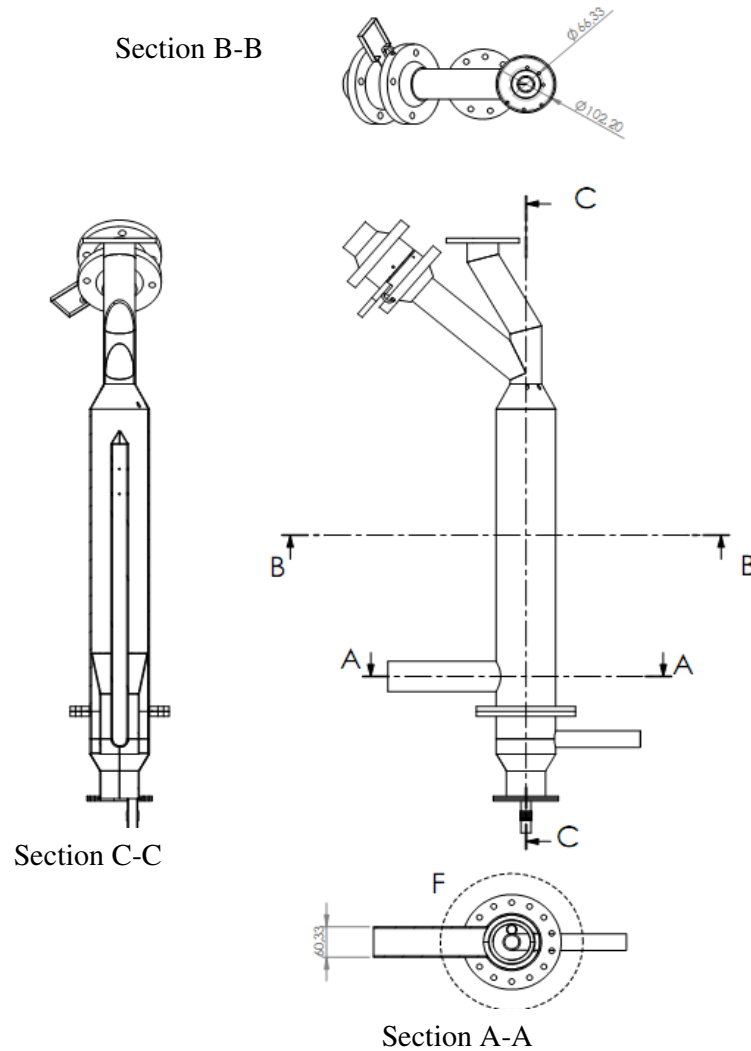
Figure 3.5 Scheme of the reactor: the two coaxial cylinders are visible in section C-C.

The gasification reactions occur in the external cylinder: the biomass is fed from the top and the steam is fed through the internal cylinder. Indeed the steam, externally generated, flows first in the internal cylinder from the bottom to the top; at the top a series of holes allow the passage of the steam from the internal to the external tube.

Since both the biomass and the steam are fed from the top of the rector, the gasifier has a co-current configuration. The reactor is externally heated by means of four electric ovens placed around the reactor (maximum power 1.5kW each). The reactor is realized in Inconel® (1300 K, 2 barg design) and it has a maximum power input between 11-13 kW. The nominal load is 2.5kg h^{-1} of biomass.

In the upper part of the gasifier, two compressed air-driven valves are placed. The aims of these valves are:

  ➢ to divide the reactor (the hot zone) from the biomass feeding system avoiding that air comes in the reaction chamber by means of the feeding tube;

  ➢ to avoid that the hot syngas yield exits from the gasifier through the feeding box.

To reach these goals the valves are open alternatively during the feeding of the system.

The *ash-collector* is a small box placed at the bottom of the reactor, below a grate, which divides the reaction chamber from the ash collector. It is of small size, since from the simulation performed, the residual solid fraction for SC=2 or SC=3 should be close to zero. The ash and the fraction of solid carbon produced during the process remain on the grate until when the operator manually moves the grate discharging the char in the downstream collector. This operation can be done at variable interval of times according to the amount of solid carbon produced (function of the feeding rate, the gasification temperature and the SC value).

The original *feeding system* consisted of an open container, funnel-shaped, connected with the reactor through a vertical tube. As said above, two compressed air-driven valves, located along the vertical tube, divide the hot zone from the feeding system. The biomass is manually loaded in the container before the heating up of the system. Different type of feedstock can be used, as long as cut in small pieces (length: 10-20 mm, width 5-10 mm).
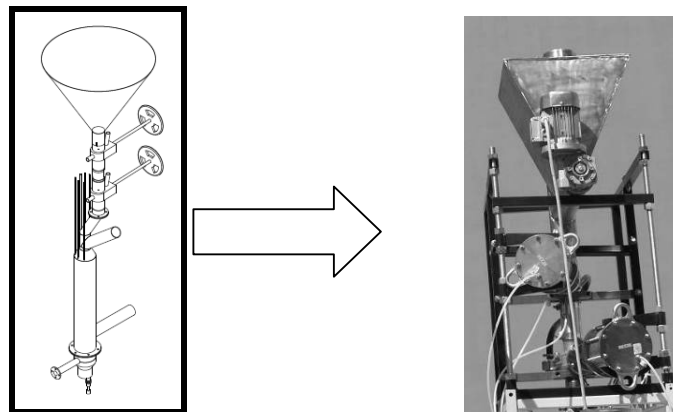
Figure 3.6 The original feeding system (left) and the modified one (right)

The feeding system has been modified after few preliminaries tests because, due to the heat conduction phenomena, the temperature reached by the vertical tube during the heating phase is high enough to cause the sticking of the biomass pieces in a single block that cause the closing of the tube. In spite of the two valves that divide the feeding box by the hot zone, two times happened that the feeding pipe was blocked due to the pellets sinterization in a single block. This is probably due to the glue used in the pellets preparation. Anyway, the funnel-shaped container was changed with a closed hopper and a horizontal Archimedean screw which transports the biomass to the vertical tube only when the operative temperature has been reached and the test can start. The Archimedean screw is moved from an engine connected to an inverter. The feeding rate depends on the rpm (rounds per minute) which can be manually set on the inverter. To know the amount of the biomass fed according to the screw running time a series of tests have been done. The characteristic parameter considered is the "exit frequency" of the screw which can be manually set on the inverter. The tests results are reported in table 3.2.

Table 3.2 Feeding rate according to the frequency exit of the Archimedean screw

"Frequency exit"	Running time (s)	Biomass fed (g)	Feeding rate (g/s)
	10	738	73.83
70	20	1463	73.15
	30	2160	72.02
	10	424	42.4
50	20	1050	52.5
	30	1605	53.5
	10	315	31.5
30	20	618	30.9
	30	924	30.8
10	10	100	10
	17	170	10

The tests have been pointed out that for values of the frequency exit below 10, the Archimedean screw has not enough energy to crash the pellets which cause the stop of the screw rotation. Thus, at least for this type of biomass (pellets), the minimum feeding rate is 10g /s.

For the gasification tests the frequency exit has been kept fixed to 50, changing the running time according to desired feeding rate (i.e. to feed 1 kg of pellets 20 seconds are needed, for 1.5 kg 30 seconds are needed).

A known flow of nitrogen has been added from the top of the hopper and let flows through the entire system; thanks to the closed hopper and the nitrogen flow, the compressed air-driven valves are not more necessary. The nitrogen keeps the atmosphere inert and, at the same time, avoids the running up of the hot syngas toward the biomass box. A picture of the original and the new feeding system is reported in figure 3.6.

The biomass tested within this project is pellet of pinewood. The pellets have been chosen to guarantee homogeneity in size and composition, avoiding the problems connected with the non-uniformity of the feedstock. The analysis of the elemental composition of the feedstock has been done and the data are reported in table 3.3.

Table 3.3 Elemental composition of the biomass employed

Elemental composition (% mass, dry sample)				
Pinewood pellets				
C: 47.03	H: 6.12	O: 46.83	N: 0.01	S< 0.01
Moisture (% mass a.r.)				7.0
Ash (%mass a.r.)				0.2
Density (kg m^{-3})				1250
LHV (MJ kg^{-1})				18.5
Lenght (mm)				10-20

An external company (Hysytech s.r.l) has provided the steam generator. The water is pumped in the steam generator and the flow is regulated by a flow meter. According to the feeding rate and the desired Steam to Carbon value, the water flow is set on the flow meter.

Table 3.4 Amount of water required for different feeding rate and SC value

Feeding rate: 1 kg h^{-1}				*Feeding rate: 1.5 kg h^{-1}*			
SC	kg steam h^{-1}	g H$_2$O h^{-1}	ml min^{-1}	SC	kg steam h^{-1}	g H$_2$O h^{-1}	ml min^{-1}
0	0.0	0	0.0	0	0.0	0	0.0
0.5	0.4	364	6.1	0.5	0.5	546	9.1
1	0.7	728	12.1	1	1.1	1091	18.2
1.5	1.1	1091	18.2	1.5	1.6	1637	27.3
2	1.5	1455	24.3	2	2.2	2183	36.4
2.5	1.8	1819	30.3	2.5	2.7	2728	45.5
3	2.2	2183	36.4	3	3.3	3274	54.6
Feeding rate: 2 kg h^{-1}				*Feeding rate: 2.5 kg h^{-1}*			
SC	kg steam h^{-1}	g H$_2$O/h	ml min^{-1}	SC	kg steam h^{-1}	g H$_2$O h^{-1}	ml min^{-1}
0	0.0	0	0.0	0	0.0	0	0.0
0.5	0.7	728	12.1	0.5	0.9	909	15.2
1	1.5	1455	24.3	1	1.8	1819	30.3
1.5	2.2	2183	36.4	1.5	2.7	2728	45.5
2	2.9	2910	48.5	2	3.6	3638	60.6
2.5	3.6	3638	60.6	2.5	4.5	4547	75.8
3	4.4	4365	72.8	3	5.5	5456	90.9

The steam can be superheated at temperatures up to 600°C. Due to the coaxial structure of the system, the heat exchange between the gasification zone and the inner cylinder where the superheated steam run, is favoured. Te higher is the steam temperature, the lower is the external

energy required to keep the system at the operative temperature (700°C or 800°C). In table 3.4 the amount of water required according to the feeding rate and the SC value is reported.

Figure 3.7 shows the entire system. The red arrow indicates the reactor surrounded by the four electric ovens; the yellow arrow indicates one of the compressed air-driven valves (the biomass hopper is placed just above); the green arrow points the steam generator and the superheater and the blue one shows the ash collector.

The *cleaning unit* that has been used for most of the tests performed consists of three cylindrical containers placed in series, filled with active carbon. In this way, the syngas produced is cooled and cleaned before the exit in the atmosphere. Only in a second phase, a catalytic filter has been added for hot gas cleaning before the fuel cells.
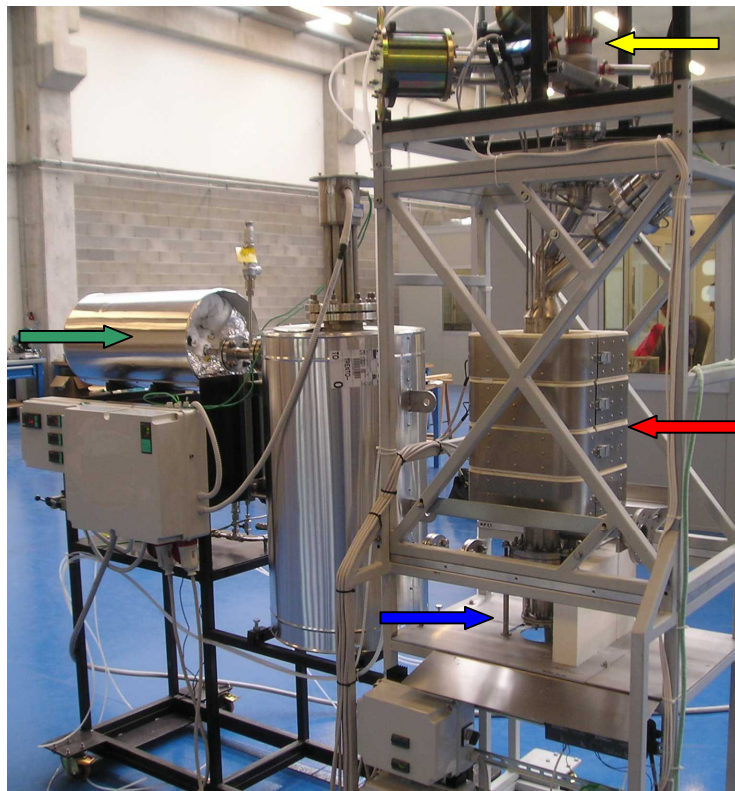
Figure 3.7 Picture of the first version of the reactor realized

3.3.2 Measurements tools

A *portable Hp Agilent 3000 Micro GC* able to measure the concentration of CO_2, O_2, N_2, CH_4, C_2H_2, C_2H_4, C_2H_6, H_2 and CO has been adopted for the gas analysis. Actually, this micro GC is one of the few portable instruments able to measure the hydrogen concentration besides the permanent gases. The system uses solid-gas columns which work at isothermal conditions. The gas is cooled down and cleaned before entering in the GC.

The temperatures inside the reactor have been recorded by means of three *K-thermocouples*

consisting of two wires of Chromel® (Nickel-Chromium – positive lead) and Alumel® (Nickel-Aluminium – negative lead). These sensors have been chosen because of their good performances in corrosive and oxidizing environments and for their wide operation temperature range, between -200°C and 1370°C (accuracy range ±1.1°C to ±2.2°C). The thermocouples have been placed at different heights and radial positions (figure 3.8) to control the heating of the reactor, the influence of the superheated steam on the internal reactor wall, and to characterize the feedstock thermal behaviour (during the tests at least the deepest thermocouple is placed inside the biomass bed).

A high sensitive *flow meter* has been used to control the water flow in the steam generator.

Four *energy meters* allow the measurement of the energy required by the system. One measures the total energy (reactor + steam generator and super-heater) and three measure the energy required by the four electric ovens to heat the reactor at the set point temperature.
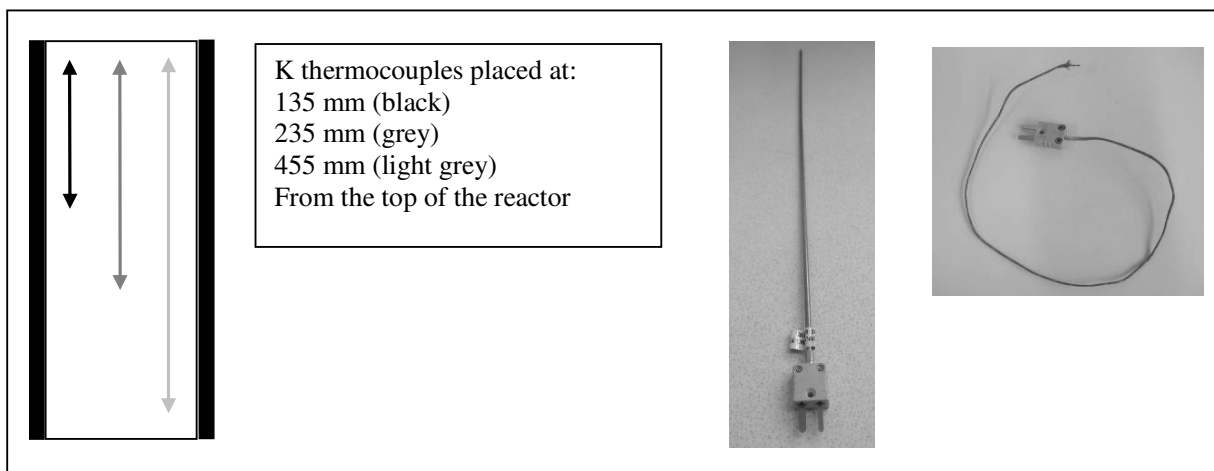
Figure 3.8 Scheme of the thermocouples positions inside the reactor (on the left). Insulated and bare wire thermocouples (on the right).

During the development of the project, several changes have been done to improve the system. At present, the whole system is almost completely controlled via PC (i.e. start and stop of the water pump for the steam generator, start and stop of the feeding system, acquisition data system). The interface PC-gasifier has been built in LabView environment.

A *Thermo Camera* (ThermoCAM E 300, FLIR System) has been used in some occasions to estimate, qualitatively, the surface temperature of the reactor and to localize the major heat losses.

3.4   Semi-continuous configuration

The aim of the first experimental activity was to investigate the syngas composition at different gasification temperature and Steam to Carbon Value. The series of tests performed is summarized in table 3.5. The steam temperature has been also varied to see if any difference was visible in the temperature profile inside the reactor.

Table 3.5 Experimental tests performed

Test number	1	2	3	4	5	6	7
SC (mol H_2O/mol C)	2	2	3	2	2	3	3
Gasification temperature (°C)	800	800	800	800	800	800	800
Steam temperature (°C)	200	600	400	400	400	400	400
Feeding rate (kg h^{-1})	1	1	1,5	1-1.5	1.5	1-1.5	1-1.5
Test duration (h)	2	4	3	3	3	3	3

3.4.1   Experimental procedure

During the gasification tests the procedure below has been followed:

➢ First of all approximately 5 kg of biomass are loaded in the hopper;

➢ the set point temperature is fixed for both the reactor and the steam generator;

➢ a flux of nitrogen of 2 NL min^{-1} flows through the system during the heating up phase;

➢ when the reactor and the steam generator have reached the desired temperature, the steam and then the biomass are added to the system; the nitrogen flux is rise up to 5 NL min^{-1};

➢ the biomass is loaded every hour (20 or 30 seconds for 1 or 1.5 kg of biomass respectively), while the steam is added continuously;

➢ the syngas produced is measured every 2 minutes by means of the portable GC;

➢ the signal of the thermocouples is registered every 5 seconds during both the heating phase and the gasification test;

➢ the char is manually discharged every hour before the next biomass load;

➢ when the test is considered over the steam is closed and the nitrogen flux is set again on 2NL min^{-1} until the complete cooling down of the system (or at least until the temperature is below 200°C).

As said previously, pellets of pinewood have been used for the experimental activity. The residual solid fraction of the gasified pellets is around 18% of the original biomass weight. Additionally, the gasified pellets maintain the same shape and size of the fresh pellet, even if with a fragile and high porosity structure (figure 3.9). Since the grate placed at the bottom of the gasifier was designed with a close-mesh net to let only the char and ash pass in the ash collector, the char cannot be discharged easily. Only a small fraction of the char is mechanically crushed by the successive loads of fresh biomass and falls down in the char collector.

Figure 3.9 Fresh pellets (left) and gasified pellets (right)

This particular behaviour of the pellets implies that the reactor cannot be emptied after every load, and the char produced remains inside the reactor. Since the char is approximately 18% of the initial biomass weight and it is characterized by high porosity of the gasified pellets the bulk density has been estimated around 450kg m^{-3}. With this value some simulations of the reactor filling according to the feeding rate have been done. The results are reported below.
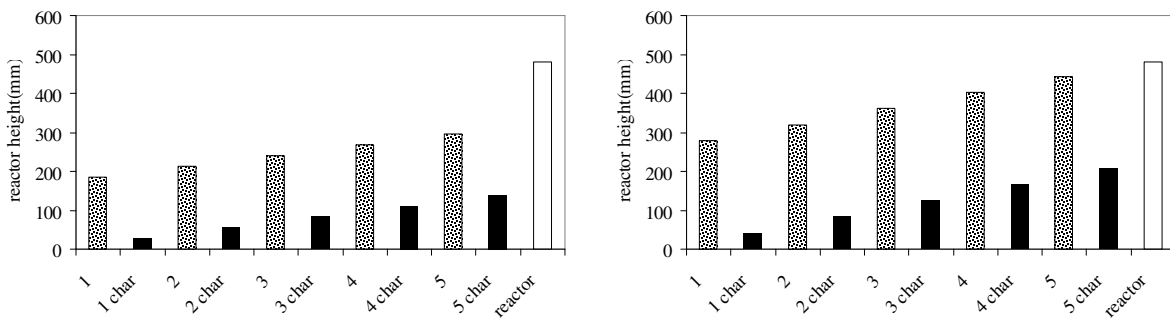
Figure 3.10 Simulation of the reactor filling considering feeding rate of 1 kg h^{-1} (left) and 1.5 kg h^{-1} (right)

Considering the amount of char produced for every biomass load, the number of successive loads according to the feeding rate has been estimated. For 1 kg h^{-1} the system can work for more than five hours, even if the bed height continuously increases; for 1.5 kg h^{-1} the maximum numbers of successive loads are 5. At the 6th load, the biomass would overflow from the reactor. For 2 kg h^{-1} it is possible to arrive at two successive loads, and for the nominal load (2.5 kg h^{-1}), only one load is possible, as shown in figure 3.11.
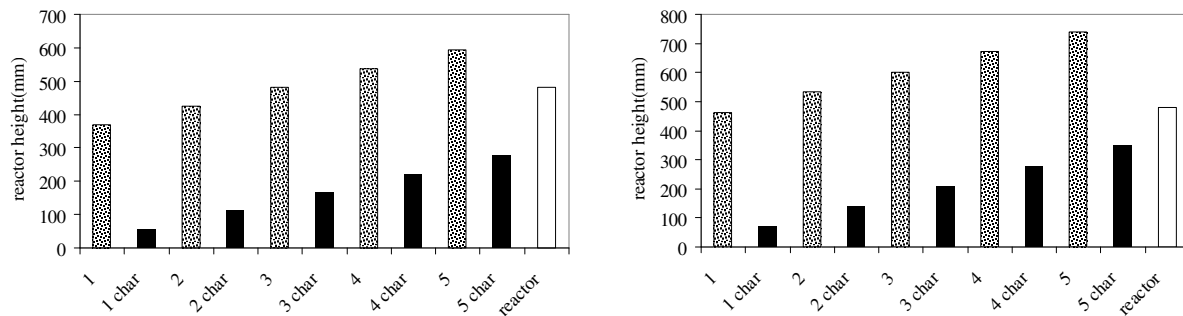
Figure 3.11 Simulation of the reactor filling considering feeding rate of 2 kg h^{-1} (left) and 2.5 kg h^{-1} (right)

Due to this reason, the feeding rates tested in the experimental activity are 1 and 1.5 kg h^{-1}.

In figure 3.12 the PFD of the reactor is drawn. The dashed lines indicate the non-operative parts in the first experimental phase.
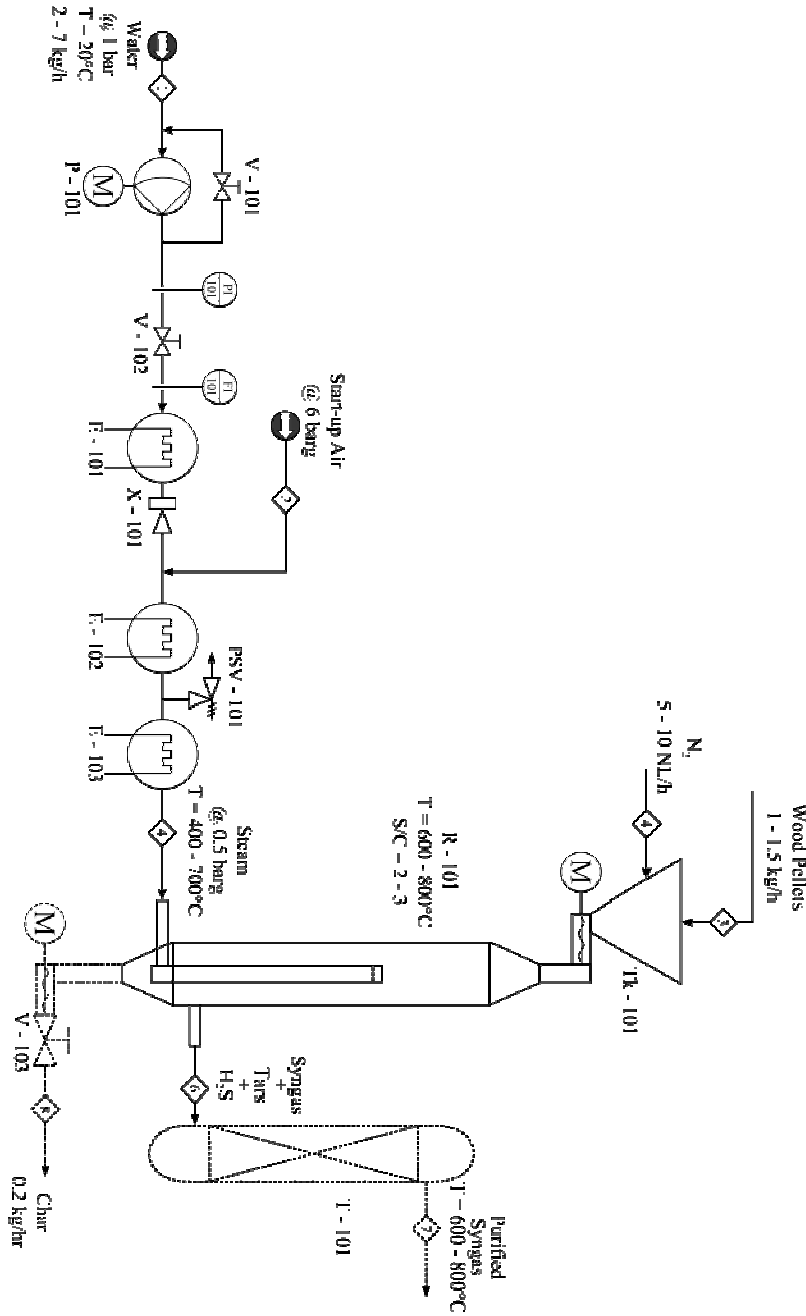
Figure 3.12 PFD of the system

3.4.2   Experimental results

In this paragraph, the results of the 7 most remarkable tests performed in the first part of the experimental activity are listed.

The legends in the charts of the temperature profile are referred to the three thermocouples placed in different positions inside the reactor: thermocouple 1 placed at 125 mm from the top,

thermocouple 2 at 255 mm from the top

thermocouple 3 at 455 mm from the top.

➢   Test number 1

Reaction temperature = 800°C   SC= 2   Steam temperature = 200°C   Feeding rate = 1 kg h^{-1}
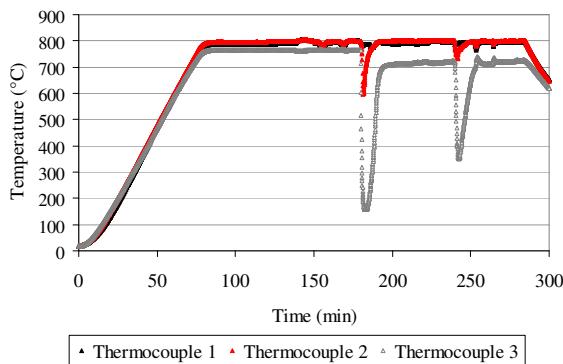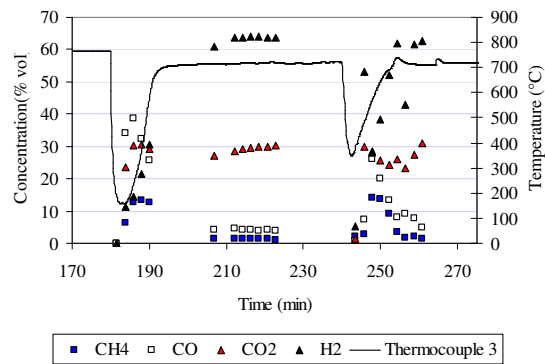
Temperature profile   Evolution of dry gas composition

➢   Test number 2

Reaction temperature = 800°C   SC= 2   Steam temperature = 600°C   Feeding rate = 1 kg h^{-1}
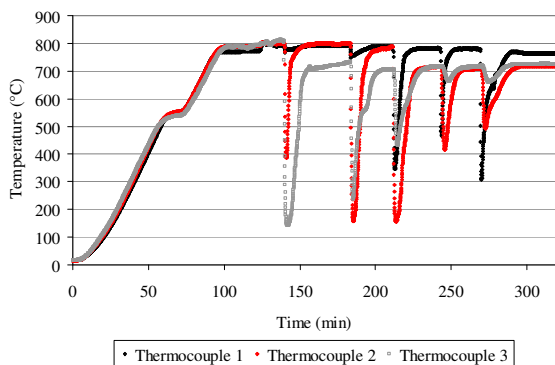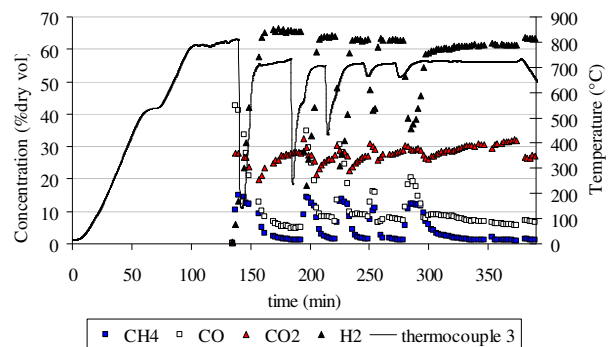
Temperature profile   Evolution of dry gas composition

➢ Test number 3

Reaction temperature = 800°C   SC= 2   Steam temperature = 400°C   Feeding rate =1.5 kg h^{-1}
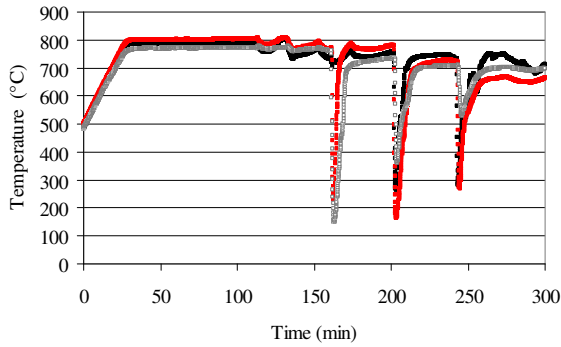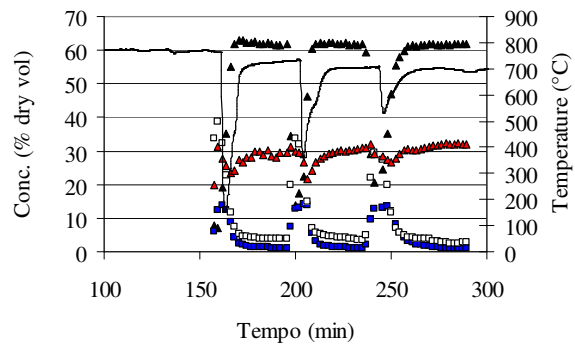
Temperature profile

Evolution of dry gas composition

➢ Test number 4

Reaction temperature = 800°C   SC= 2   Steam temperature = 400°C   Feeding rate =1/1.5 kg h^{-1}
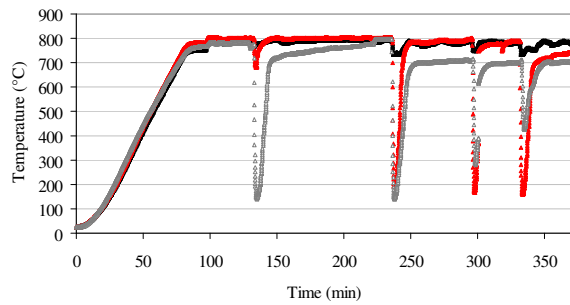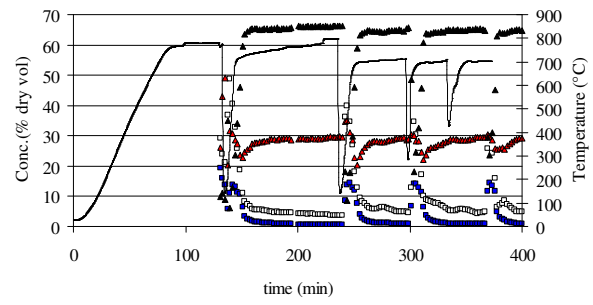
Temperature profile

Evolution of dry gas composition

➤ Test number 5

Reaction temperature = 700°C   SC= 2   Steam temperature = 400°C   Feeding rate =1.5 kg h⁻¹
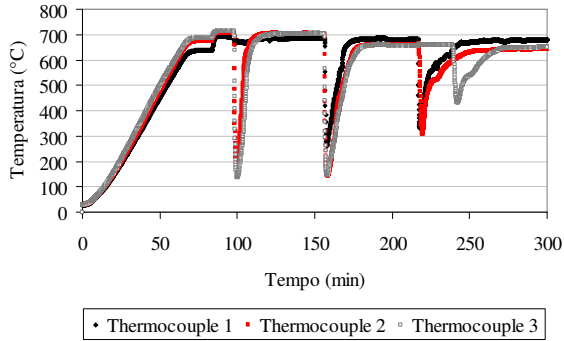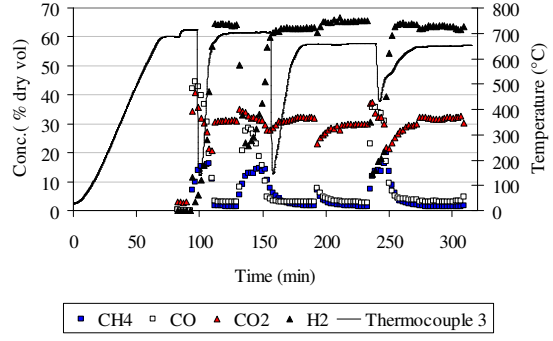
Temperature profile   Evolution of dry gas composition

➤ Test number 6

Reaction temperature = 700°C   SC= 2/3   Steam temperature = 400°C   Feeding rate =1.5 kg h⁻¹
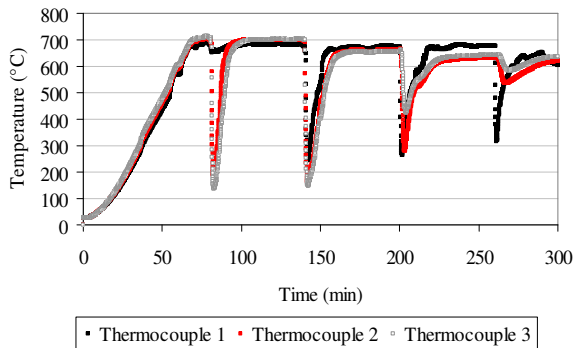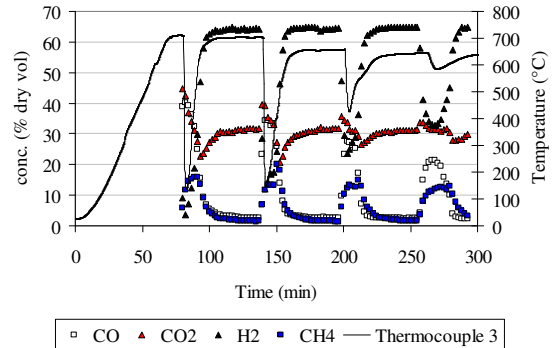
Temperature profile   Evolution of dry gas composition

➢   Test number 7

Reaction temperature = 700°C   SC= 2/3   Steam temperature = 400°C   Feeding rate =1/1.5 kg h^{-1}
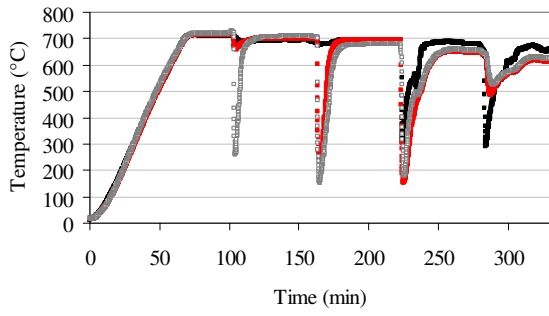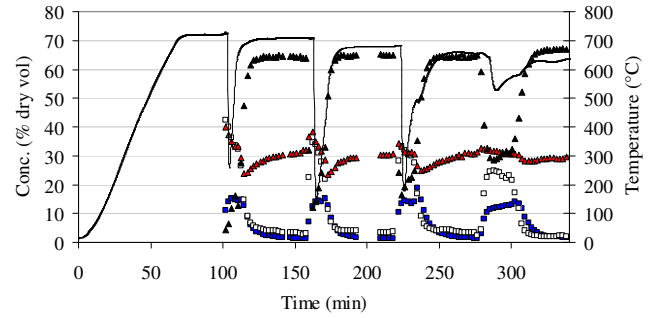
Temperature profile

Evolution of dry gas composition

3.4.3 Data analysis

A first consideration can be done on the temperature profiles of the seven tests reported. As can be seen, the biomass loads, fed at room temperature, are clearly registered by the thermocouples. The first load is registered by the deepest thermocouple, and the next loads stop above the bed of char formed during the gasification process touching the middle and at last the highest thermocouple. Due to the difficulties in char discharging (as described previously), the reactor is gradually filled and, according to the feeding rate (1 or 1.5 kg h^{-1}), the test can be run for 4 or 5 hours. Furthermore it can be noticed that the temperature registered in the bed of biomass/char is 100°C lower then the gasification temperature set for the test.

The syngas production is characterized by an initial transitory phase after the biomass load, that last approximately ten minutes, during which a peak of methane and carbon monoxide is produced. Afterwards a stable phase up to the next biomass load is registered. In the stable phase, methane is almost totally converted due to the high residence time inside the reactor. The average gas composition in the stationary phase has been calculated for each test, and the data are compared in table 3.6. The typical syngas composition is, on dry basis and N_2 free, hydrogen (more than 60%), carbon dioxide (around 30%), methane (1-3%) and carbon monoxide (5-8%).

Table 3.6 Average syngas composition during the stable phase

Test number	C_2H_2 % vol	C_2H_4 % vol	C_2H_6 % vol	CH_4 % vol	CO % vol	CO_2 % vol	H_2 % vol
1	0	0.00	0.00	1.3	4.2	29.2	63.4
2	0	0.00	0.00	1.5	7.0	28.2	63.1
3	0	0.00	0.00	1.4	3.7	30.0	64.9
4	0	0.01	0.01	1.9	6.6	27.2	64.3
5	0	0.03	0.03	2.9	3.6	30.4	63.0
6	0	0.03	0.03	2.9	3.6	30.4	63.0
7	0	0.03	0.03	3.5	4.0	28.4	64.0

In figure 3.13 the concentration of the main gaseous compound comparing different gasification temperature and Steam to Carbon value are reported. A higher SC value produces higher hydrogen concentration even if the effect is not so noticeable. No remarkable differences in the gas composition can be noticed decreasing the gasification temperature from 800 to 700°C or changing the SC values.

Probably the main effect of the decreasing of the gasification temperature is in the Tars amount (the higher is the gasification temperature the lower is the tar production due to the hydrocarbons thermal cracking) [Yu,2009]; unfortunately the Tars concentration has not been measured in these experimental campaign.
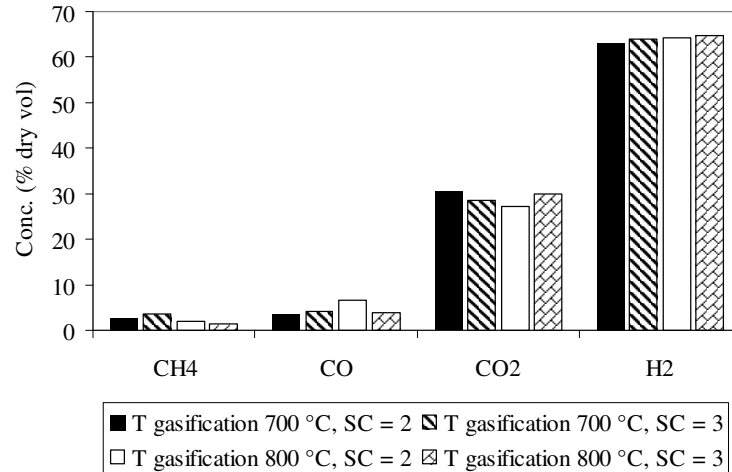
Figure 3.13 Gas composition at different gasification temperature and SC values

To evaluate the process efficiency and the carbon and energy balance, it is necessary to know, in input, the amount of biomass and, in output, the char and gas production. Thanks to a known amount of nitrogen fed from the biomass hopper, it has been possible to estimate the syngas production. In figure 3.14, for instance, the instantaneous syngas production for one of the test performed (number 7) is reported. Similar graphs have been obtained for the others tests. In test number 7 the amount of nitrogen has been varied from 2 to 5 to 10 NLmin^{-1} to investigate if the syngas production (N_2 free) remains constant.
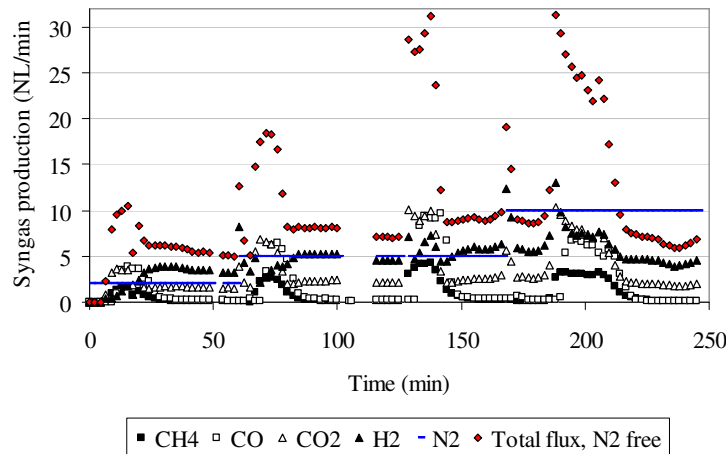
Figure 3.14 Instantaneous syngas production (N_2 free) for test number 7

The syngas production has been calculated knowing the N_2 flow fed to the system and the N_2 concentration in the outgoing syngas. The measure of the gas production is strictly linked to the measure of the nitrogen in the syngas. The peak of syngas production registered immediately after the biomass load has not been considered reliable, since in that period of time, the falling down of the biomass cause a movement of the bed and a mixing of the gases (transitory phase). The gas

production in the stable phase is approximately constant at 8-10 NL min^{-1}. Considering the total syngas production in the whole test a value of 0.65 Nm^3/kg$_{pellets}$ has been calculated. This value is lower than the ones reported from other authors for different biomass type. For example, Lv et al. report a syngas production of 1.5 Nm^3 kg^{-1} for biomass steam gasification at 700°C and 2.2 Nm^3 kg^{-1} at 800°C using pine sawdust as biomass [Lv, 2004]; Gonzalez et al. have measured, in an air-steam gasification process (700-800°C), a production of 1.5-1.8 Nm^3 for kilogram of olive waste [Gonzalez, 2008]. In 2007 Lv et al. have performed a series of gasification tests at 800°C in a downdraft gasifier adopting pine wood blocks as feedstock. The syngas production was around 1.5 Nm^3 kg^{-1} using an air-oxygen mixture as gasifying agent and 0.9 Nm^3 kg^{-1} (N$_2$ free) with air as gasifying agent [Lv, 2007]. Probably pellets, due to their low moisture and high density, have a lower gas production respect to the wood logs or chips. Observing the results for all the tests and excluding the peak of production just after the biomass load (one load every hour), the syngas yield is higher in the first 20-25 minutes. It has been concluded that feeding the system more regularly should lead to a higher and more stable syngas production.

The gas heating value (LHV or HHV) has been also calculated for the gas composition measured during the stable phase of the test. The value is calculated as the weighted average of the heating values of the gaseous species present in the syngas (3.7)

$$\sum_{gas} x_{gas} \cdot LHV_{gas} \tag{3.7}$$

The Low and High Heating value of the syngas are reported in table 3.7. The values are approximately the same for all the tests in spite of the temperature and the SC differences.

Table 3.7 LHV and HHV of the syngas yield

Test num	T reactor (°C)	T steam (°C)	SC	HHV(MJ Nm^{-3})	LHV (MJ Nm^{-3})
1	800	200	2	9.14	7.85
2	800	600	2	9.52	8.22
3	800	400	3	9.29	7.96
4	800	400	2	9.80	8.46
5	700	400	2	9.67	8.35
6	700	400	3	9.65	8.32
7	700	400	3	10.0	8.71

3.4.4 Carbon and energy balance

At the end of each test, the char produced has been collected and weighted during the cleaning phase of the reactor. In table 3.8 the amounts of char measured are reported. On average, the char production is around 18-20% of the total biomass fed. Some problems have occurred during the cleaning phase of the test number 1 and 4 and the data have not been considered. The char produced from 1 kg of gasified pellets has been heated up to 550°C. The unburned residual quantity (ash) after the thermal treatment was about 1-2% of the initial mass of char (globally 0.3% of residual ash for 1kg of pellets). Thus, the char is carbon at almost 99 % with a remarkable heating value and, in the energy balance, is considered as a further energy source. Indeed, changing the system for char discharging, the residual char could be recycled and used to heat the reactor up.

Table 3.8 Residual ash of the 7 tests

Test number	Biomass fed (kg tot)	Total char (g)	g char/kg pellet
1	1	n.a.	n.a.
2	4	700	175
3	4.5	527	117
4	4.5	n.a.	n.a.
5	4.5	800	177
6	5	900	180
7	5	1150	220

To calculate the carbon balance, the input moles of carbon have been deduced knowing the elemental composition of the biomass. From the syngas production, the moles of carbon in the outgoing syngas have been estimated. Finally, the moles of carbon presents in the residual char have been added. A scheme is reported in figure 3.15 and the data related to the total syngas production of test number 6 and 7 are reported in table 3.9. It is important to remember that the measurement of the biomass fed is based on the measure of the operating time of the Archimedean screw (1 kg of pellets in 20 seconds). Since in this first part of the experimental activity the switching on and off of the Archimedean screw is manually controlled, the biomass fed has been estimated considering an approximation of 5-10%. Unfortunately the amount of tars has not been measured and a literature value of 60 g Nm^{-3} [Umeki, 2010] has been considered to close the carbon balance.
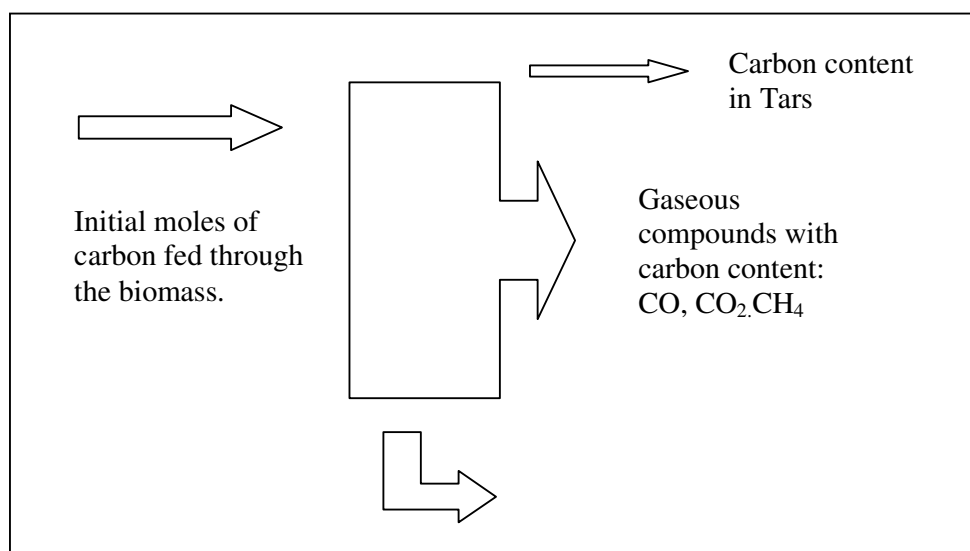
Figure 3.15 Scheme of the carbon balance

Table 3.9 Syngas production and composition of the test number 6 and 7

	CO_2	C_2H_4	C_2H_6	C_2H_2	H_2	O_2	CH_4	CO	N_2
				Test number 6					
Syngas tot. (NL)	875.9	16.9	18.7	0.2	1227.6	0.0	220.4	406.0	1496.85
Molecular Weight	44	28	30	26	2	32	16	28	28
Moles	39.1	0.8	0.8	0.0	54.8	0.0	9.8	18.1	22.1
C Moles	39.1	1.5	1.7	0.0	-	-	9.8	18.1	
				Test number 7					
	CO_2	C_2H_4	C_2H_6	C_2H_2	H_2	O_2	CH_4	CO	N_2
Syngas tot. (NL)	829.2	18.9	18.3	0.4	1190.6	1.2	224.9	427.7	1434.7
Molecular Weight	44	28	30	26	2	32	16	28	28
Moles	37.0	0.8	0.8	0.0	53.2	0.1	10.0	19.1	64.1
C Moles	37.0	1.7	1.6	0.0	-	-	10.0	19.1	

In table 3.10 the carbon balance is summarized for test number 6 and 7. Almost 50% of the initial moles of carbon remain in solid phase (char); the other 50% turns in gas (40%) and condensable compounds (Tars, 10%). The carbon balance is closed with an error of plus or minus 5%.

Table 3.10 Carbon balance for test number 6 and 7.

Test number	6	7
Biomass fed (error 5-10%) (kg)	5	5
Input carbon moles	182	182
Moles of carbon in the syngas	70	69.5
Moles of carbon in char	88	90
Moles of Carbon in Tars	14	14
Total moles of carbon out	172	174
Global balance	95 %	96 %
Percentage of moles in gas	39 %	38 %
Percentage of moles in the solid residual fraction	46 %	50 %

To evaluate the process energy balance all the energy fluxes have to be considered. The input fluxes are the biomass characterized by its heating value, the energy required to keep the reactor at the gasification temperature and the energy needed for the steam generator and the super heater. Thanks to four energy meters (installed for the tests number 4-5-6-7) the electric energy required by the whole system (reactor + steam generator and super heater) has been measured both during the heating up phase and during the gasification tests. The raw data collected for the four tests are reported in table 3.11. The electric consumptions reported are referred to the heat required during the gasification test, excluding the heating up phase.

The 4 measures listed are referred to:

- o M1: consumption of the whole system (reactor + steam generator + super heater);
- o M2: consumption of 2 electric ovens for the reactor heating;
- o M3: consumption of 1 electric oven for the reactor heating;
- o M4: consumption of 1 electric oven for the reactor heating.

Table 3.11 Raw data of the electric consumption as red from the energy meters

	Time [h]	Biomass [kg]	SC [-]	M1 [kWh]	M2 [kWh]	M3 [kWh]	M4 [kWh]	Tot ovens [kWh]	Steam only [kWh]
Test number 4									
Load 1	8.45	1	2	12.23	4.61	1.6	2	8.21	4.02
Load 2	10.30	1.5	2						
Load 3	11.30	1	2	40.18	15.9	3.7	5.9	25.5	14.68
Load 4	12.30	1	2						
End	13.25			51.79	20.6	4.7	7.4	32.7	19.09
Test number 5									
Start	6.44			51.86	20.64	4.7	7.4	32.74	19.12
Load 1	8.15	1.5	2	61.67	24.07	5.6	8.7	38.37	23.3
Load 2	9.10	1.5	2	66.77	26.29	5.8	9.3	41.39	25.38
Load 3	10.11	1.5	2	72.31	28.39	6.2	9.9	44.49	27.82
End	11.46			80.01	31.54	6.6	11	49.14	30.87
Test number 6									
Load 1	8.46	1.5	2	87.56	34.06	7.1	12	53.16	34.4
Load 2	9.46	1.5	3	92.86	36.19	7.4	12.7	56.29	36.57
Load 3	10.46	1	3	98.85	38.14	7.9	13.3	59.34	39.51
Load 4	11.46	1	3						
End	12.26			107.22	41	8.4	14.5	63.9	43.32
Test number 7									
Start	10.00			107.29	41.03	8.4	14.5	63.93	43.36
Load 1	11.32	1	2	116.07	45	8.9	15.9	69.8	46.27
Load 2	12.32	1	2	121.54	47.55	9.2	16.6	73.35	48.19
Load 3	13.32	1.5	3	127	50.11	9.6	17.3	77.01	49.99
Load 4	14.32	1.5	3	132.65	52.54	10	18.1	80.64	52.01
End	15.32			139.3	54.79	10.5	19.1	84.39	54.91

From the values collected, the power required for a single load has been calculated. The data are reported in table 3.12. The test number 7 is double because the SC value has been changed after two

biomass loads. Considering the differences among the four tests, the data on the energetic consumption have been compared in figure 3.16 and 3.17. In figure 3.16 the consumption of the test performed at the same gasification and steam temperatures (700 and 400°C respectively) but at different SC values are reported. As expected, the energetic consumption rises with the SC value and with the increasing of the feeding rate (from 1 to 1.5 kg h^{-1}).

Table 3.12 Power required by the system during the gasification tests number 4-5-6-7.

Test number	T [°C]	SC [-]	Pellets [kg]	M1 [kW]	M2 [kW]	M3 [kW]	M4 [kW]	Tot ovens [kW]	Steam generator [kW]
4	800	2	1	5.81	2.35	0.5	0.75	3.60	2.20
5	700	2	1.5	6.01	2.45	0.3	0.68	3.46	2.54
6	700	3	1	5.99	1.95	0.5	0.6	3.05	2.94
7	700	2	1	5.47	2.55	0.3	0.7	3.55	1.92
7	700	3	1.5	6.65	2.25	0.5	1	3.75	2.9
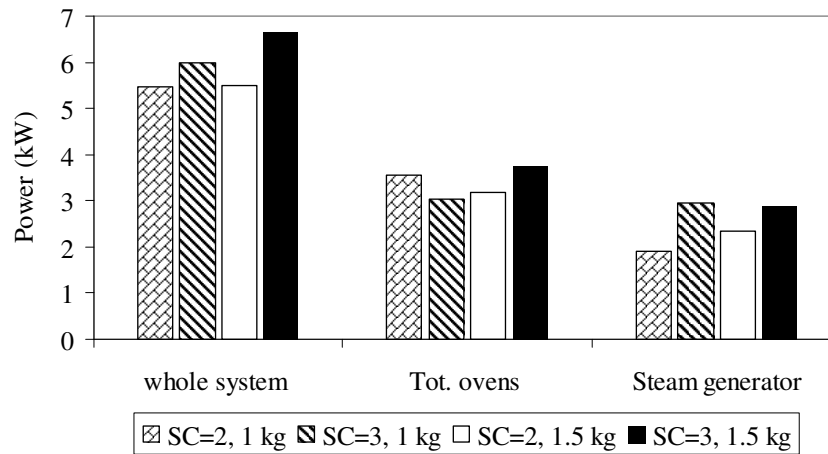
Figure 3.16 Power required for different SC values, gasification temperature = 700°C and steam temperature= 400°C.

In figure 3.17, the comparison of the electric consumption has been done for test run with the same biomass loads (1 kg h^{-1}) steam temperature (400°C) and SC value (SC=2) but with different gasification temperatures (700 and 800°C). There is only a slight difference in the global consumption which is lower for the test run at 700°C.
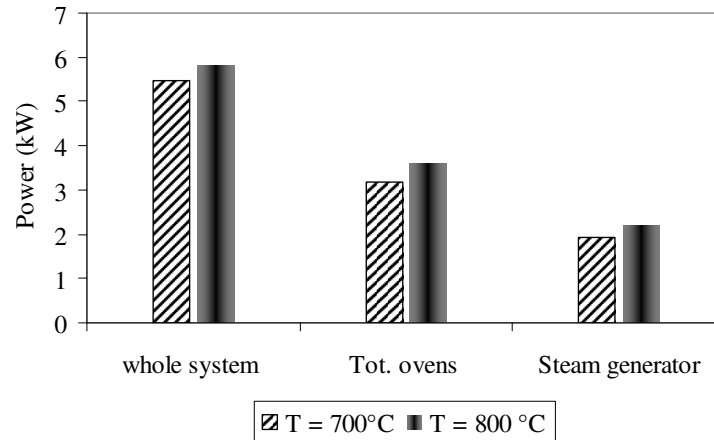
Figure 3.17 Power required for tests at different gasification temperature, with SC=2 and steam temperature = 400°C

3.4.4.1 System efficiency

Thanks to the data provided by the energy meters, the energy required by the entire system and by the single units is known. During the gasification test, the average consumption is 3-3.5 kWh for the ovens, for each single load. The steam generator requires between 2 and 3 kWh according to the SC value chosen. It is possible to estimate the system efficiency, considering the efficiency of the electric oven and the steam generator.

To estimate the energy efficiency of the system the "in and out" energy fluxes have been considered. The input fluxes are:

  ➢ biomass fed: 1-1.5 kg h^{-1};

  ➢ Energy required in input by the system;.

The output fluxes are:

  ➢ The syngas produced (the syngas composition and production are known). The gas leaves the system at 600°C so the enthalpy of the outgoing syngas at high temperature has been calculated;

  ➢ Residual solid carbon with a LHV of 32 MJ kg^{-1}.

The calculations of the energy balance of the test number 6 and 7 are reported in table 3.13.

Characteristics of test number 6:

1kg h^{-1}, SC=3, Gasification temperature =700 °C, Steam temperature = 400 °C.

And test number 7:

1 kg h^{-1}, SC=2, Gasification temperature =700 °C, Steam temperature = 400 °C;

1.5 kg h^{-1}, SC=3, Gasification temperature =700 °C, Steam temperature = 400 °C.

Table 3.13 Energy balance for test number 6 and 7

Test number	6	7	7
SC	3	2	3
Feeding rate (kg h^{-1})	1	1	1.5
Biomass Low Heating Value (MJ kg^{-1})	18.5	18.5	18.5
Biomass input energy (kWh)	5.14	5.14	7.71
Energy required by the ovens (kWh)	3.05	3.55	3.75
Energia required by the steam generator (kWh)	2.94	1.92	2.9
Ovens efficiencies (%)	70	70	70
Efficiency of the steam generator (%)	75	75	75
Energy required by the whole system (kWh)	4.34	3.93	4.80
Total input Energy (kWh)	**9.48**	**9.06**	**12.51**
Syngas produced (Nm^3/kg)	0.7	0.7	0.7
Syngas LHV (MJ Nm^{-3})	8.3	8.70	8.7
Syngas entalphy at 873 K (MJ Nm^{-3})	9.3	9.5	9.50
Syngas Energy content (MJ/kg pellets)	6.5	6.68	6.68
Char produced (kg/kg pellets)	0.2	0.2	0.20
Char production during the test (kg h^{-1})	0.2	0.2	0.30
Recoverable Energy from burning char (kWh)	1.78	1.78	2.67
Output energy (kWh)	**3.6**	**3.63**	**5.45**
System efficiency	38%	40%	44%

The global Energy efficiency is around 40%. This is an experimental apparatus and the heat losses through the envelope are remarkable. No great attention has been paid to the system insulation since the main goal was to study the gasification process. The temperature on the external surface is around 200°C. By means of a thermal infrared camera (ThermoCAM E 300, FLIR System) is possible to see, qualitatively, where the main heat losses are located. The pictures made with the thermocam are reported in figure 3.18. From the pictures, it can be seen that the hottest areas are the conjunctions between the electric ovens (clearly visible from the picture) and the upper (partially visible) and bottom part of the reactor (not visible in the picture) which are not completely insulated. The system has not been well insulated to be faster in the cleaning operations; indeed, after every test the system must be completely disassembled to be cleaned.
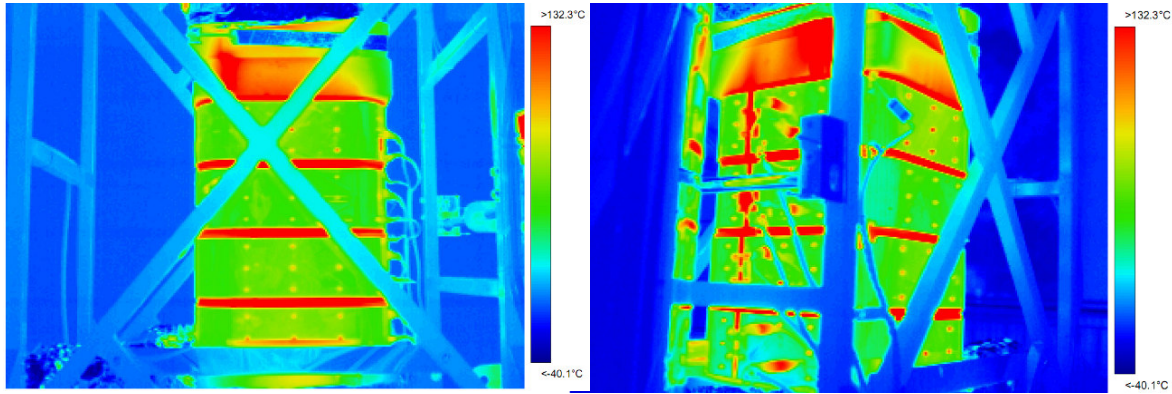
Figure 3.18 Pictures of the reactor done with a ThermoCam

The "Cold gas efficiency" (E) has been calculated and it is around 38%. It is defined as:

$$E = \frac{HHV_g \cdot v_g}{HHV_{biomassa}} \qquad (3.8)$$

where v_g is the syngas production per kg of biomass.

If the carbon formed is also considered as an energy source, the 70% of the energy fed with the biomass is given back as in gas phase (35% as syngas) and as char (35%).

In conclusion, this system configuration not allows a constant feeding of the biomass during the test. A remarkable amount of solid carbon is formed during the process, which remains inside the reactor due to the discharge problems previously describe. In spite of this, the system works and the syngas seems to be suitable to fed a SOFC fuel cell due to the high hydrogen content.

3.5 Continuous gasifier

3.5.1 New system configuration

To solve the problem of char deposit on the bottom of the reactor and to turn the system from a semi-continuous gasifier to a continuous one, some modifications have been introduced. In details, the grid placed at the bottom of the reactor and the manual char discharging system has been replaced with an Archimedean screw. By means of the new screw, the char formed during the process fall down in a hopper located below the reactor (figure 3.19). The size of the screw (the discharge velocity) is the same of the biomass feeding screw. This allows the contemporary filling and empting of the reactor, at the same velocity. The switching "on and off" of the Archimedean screw and the operative time are controlled via pc. One of the air-pressure valves has been removed, because unnecessary.

Figure 3.19 Char collector with the Archimedean screw placed below the reactor

A catalytic filter has been also added to the system for tars and hydrogen sulphide (H_2S) abatement. The filter, filled with calcined dolomite and manganese oxides, is placed just after the reactor and the hot syngas goes directly thorough the catalytic filter. The filter has a cylindrical shape of 60.33 cm of diameter and 40 cm of length.
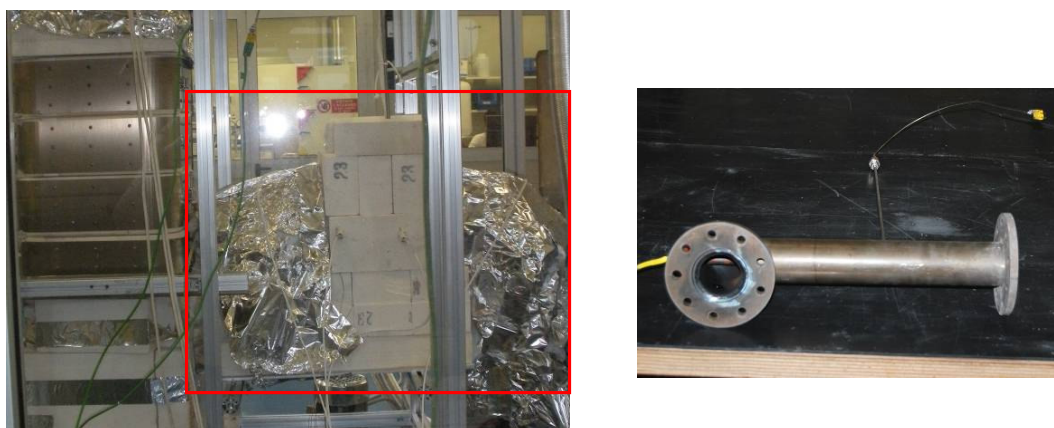
Figure 3.20 On the left the reactor plus the filtering system (in red); the electric ovens which heat up the filter are visible (placed inside them). On the right the catalytic filter.

At the beginning, the filter was heated by means of an electric resistance rolled up around the filter and, in spite of a thick layer of Alumina wool around it, the temperature reached inside the filter was around 500°C. This temperature is not high enough because the dolomite is efficient in tar cracking for temperature above 700°C. The heating system has been replaced with two electric ovens and, in this way, it is possible to reach 800°C inside the filter. A series of experiments have been performed at the University of Stockholm, to test different type of catalyst for tar cracking (See chapter 5), while the efficiency of dolomite for H_2S abatement has been tested in the laboratory at Mezzolombardo (Trento, Italy). As last step a SOFC stack have been connected to the gasifier and a few tests have been run coupling the gasifier with the fuel cells. The whole system is under a hood and the test can be controlled by an external pc to guarantee the safety of the operators. In figure 3.21 a picture of the entire system is reported. From the right is visible: the

steam generator plus the reactor (blue) and the feeding system above the reactor; the catalytic filtering part (green) and finally the fuel cells stack with all the controllers (red).
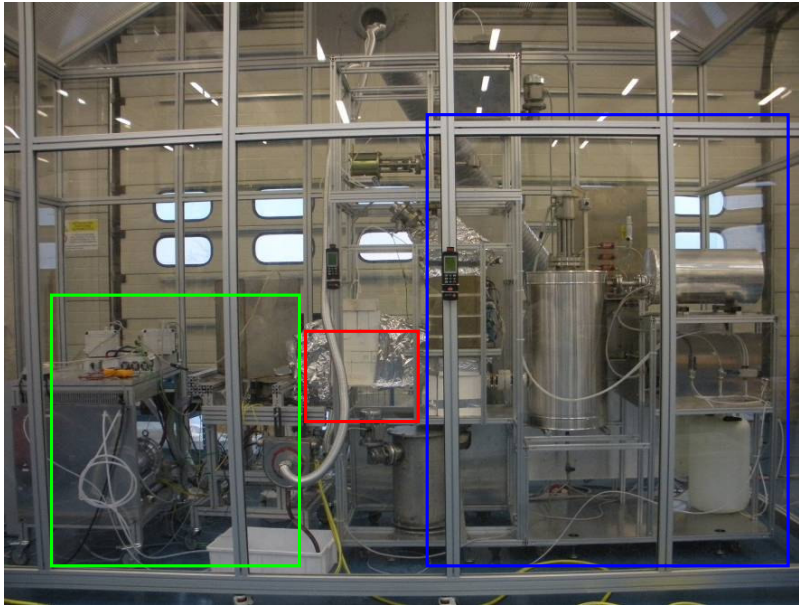
Figure 3.21 The whole system as is visible today

3.5.2 Experimental campaign and results

A new experimental campaign has been run with this system. The experimental activity now focuses on the coupling of the gasifier with a fuel cell stack. Thus, the gasification conditions have been kept fixed at:

- ➢   Gasification temperature: 800°C;
- ➢   Steam to Carbon =2.5;
- ➢   Steam temperature = 600°C;
- ➢   Feeding rate = 2 kg h^{-1} (0.2 kg every 6 minutes)

The modified system changes the gasifier from a semi-continuous to a continuous operative mode. The biomass and the char produced can be discharged at the same velocity and time. For a feeding rate of 2 kg h^{-1} a carbon residual of 0.35-0.4 kg h^{-1} has to be discharged. A new set of tests have been run with this new configuration summarized in table 3.14.

The height of the bed is controlled by means of the middle or the deepest thermocouple. For instance, in figure 3.22 the temperature profile of one of the tests performed is reported (all the tests have been run at the same conditions). The black square underlines the heating up phase, the blue square indicates the gasification process, and the green square shows the cooling of the system.
The temperature profile inside the reactor during the test differs completely from the previous configuration; the height of the biomass bed is kept constant and the deepest thermocouple remains

inside the bed. The temperature in the bed is, on average, 80-100°C lower then the reactor temperature measured by the highest thermocouple.

Table 3.14 Test in the second phase of the experimental activity

Test n°	T reactor	T steam	SC	Feeding	Catalyst	Gas analysis	Fuel cell
8	800°C	600°C	2.5	-	-	-	-
9	800°C	600°C	2.5	2 kg h^{-1}	-	H_2,CO,CO_2,CH_2,C_2H_2,C_2H_4,C_2H_6	-
10	800°C	600°C	2.5	2 kg h^{-1}	-	H_2,CO,CO_2,CH_2,C_2H_2,C_2H_4,C_2H_6	-
11	800°C	600°C	2.5	2 kg h^{-1}	-	H_2S,CO,CO_2,CH_2,C_2H_2,C_2H_4,C_2H_6	-
12	800°C	600°C	2.5	2 kg h^{-1}	Yes	H_2S,CO,CO_2,CH_2,C_2H_2,C_2H_4,C_2H_6	-
13	800°C	600°C	2.5	2 kg h^{-1}	Yes	H_2S,CO,CO_2,CH_2,C_2H_2,C_2H_4,C_2H_6	-
14	800°C	600°C	2.5	2 kg h^{-1}	Yes	-	Yes
15	800°C	600°C	2.5	2 kg h^{-1}	Yes	-	Yes
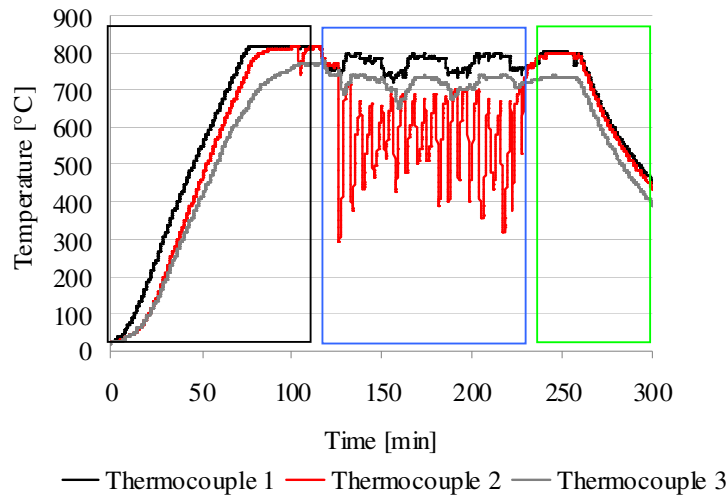
Figure 3.22 Temperature profile of one of the tests run with the continuous reactor

In figure 3.23 the syngas composition of the test number 9 is reported. The syngas production (calculated, as before, knowing the nitrogen flux fed from the biomass hopper through the system) and composition remain almost stable during the whole test.

The concentration of the gaseous species is slightly different from the previous tests; these variations are probably due to a more constant feeding and minor residence time of the gas inside the reactor. The gas composition measured by the GC, is:

C_2H_2 (%)	C_2H_4 (%)	C_2H_6 (%)	CH_4 (%)	CO (%)	CO_2 (%)	H_2 (%)	O_2 (%)
0.01	0.01	0.5	6.6	12	29.3	51.4	0.1

Respect to the first experimental results, the hydrogen concentration has decreased, and the methane and the carbon monoxide concentrations have risen. From the SOFC cell point of view the gas composition from the two systems are both suitable. In the first one, the hydrogen was higher

during the stable phase between two successive biomass loads, but not immediately after the feeding. This new configuration allows the production of a good quality gas, keeping almost constant operative conditions and gas production.
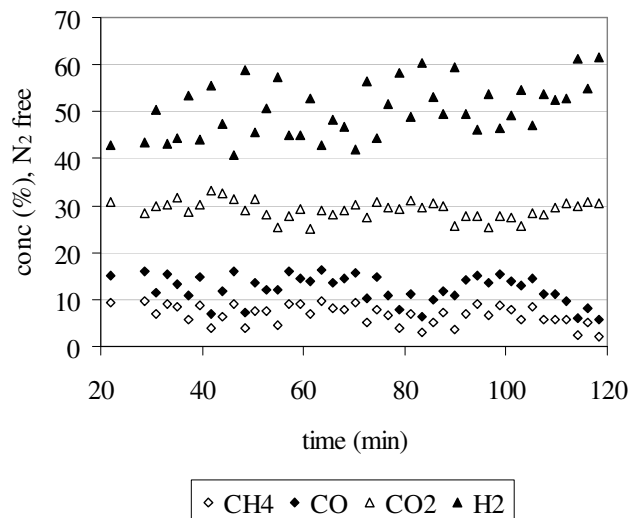
Figure 3.23 Syngas composition profile of the test number 9

On average, the gas production is around 24 NL min^{-1} or, respect to the biomass fed 0.75 Nm^3 kg^{-1} pellets. The low heating value has been calculated on the average gas composition reported above, and it is around 8 MJ Nm^{-3}.

3.5.3 Hydrogen sulphide measurements

A couple of tests have been carried out to measure the hydrogen sulphide which is the main problem for the fuel cells. Indeed, even if they can tolerate a certain level of tars in the gas, the H_2S is a dangerous poison for the cell, and the tolerated concentration is lower than 10 ppm. The measures have been performed with the same gas chromatograph used for the syngas analysis, changing the gas carrier from Argon to Helium; the Helium allows to detect the hydrogen sulphide but not the hydrogen and vice versa: this means that the GC measures the concentration of CH_4, CO, CO_2, N_2 and H_2S.

A first test without the catalyst has been run to measure the H_2S produced by the gasification process.

In figure 3.24 the temperature profile plus the hydrogen sulphide concentration is reported. For completeness, also the syngas composition has been reported (on the right). The hydrogen concentration, in this case, has been calculated for difference. A stop has occurred in the measurements system during the test. In this test, the reactor has been gradually filled up to the middle thermocouple, which is used to control the bed height. The H_2S amount is between 20 and

70 ppm. The sulphur concentration in the biomass adopted is very low (less then 0.01% from the elemental composition), however the H_2S produced is too high for a fuel cell.
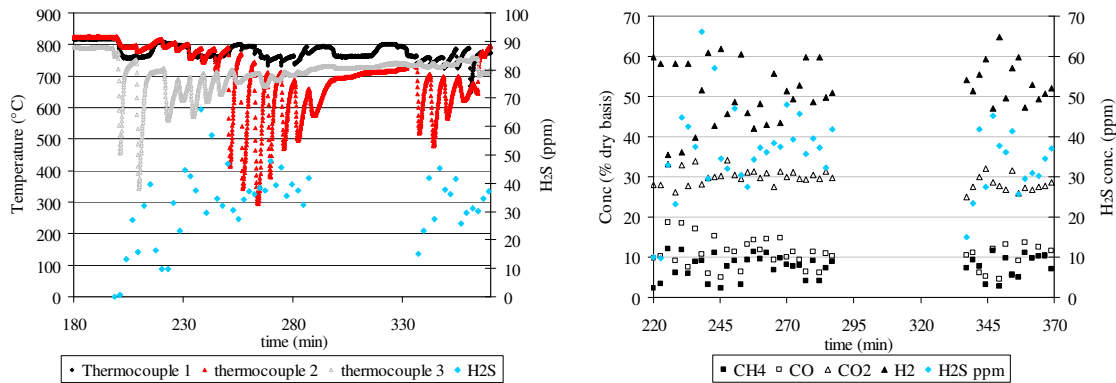
Figure 3.24 Temperature and H_2S concentration (left) and syngas composition (right) for test number 11

Before running the test with the catalyst, the efficiency of the catalyst itself has been tested in the lab. The catalyst is a mixture of dolomite with a small fraction of manganese oxides.

For the hydrogen sulphide abatement, several catalysts have already been proposed. At the moment, catalysts based on ZnO are commercially available but they are guarantee up to a temperature of 450°C. Moreover the ZnO, in a reduction environment, turns in metallic Zn which evaporates at 600°C. For process temperature between 600 and 1000°C several catalysts are under investigation, but nothing is still available for industrial and commercial applications. One of the main problems for the catalytic abatement of H_2S at high temperature is the regeneration time of the catalyst, which is usually greater than the deactivation time due to the catalyst saturation.

In this project a mixed catalyst of dolomite and manganese oxides have been tested. Dolomite and manganese oxides have separately show their efficiency in H_2S adsorption [Ko,2005], [Atimtay 1993]. Two tests have been done at 600°C. In the first one a mixture of H_2 (99.9%) and H_2S (0.1%) has been used. In the first test the catalyst has shown a high efficiency for 40 minutes (figure 3.25). This is a positive results considering that the sample of catalyst tested is very small (1 g) and the flux of hydrogen and sulphide acid has been changed from 40 to 60 to 200 NmL min^{-1}. From the lab tests, has been also noticed that the manganese oxides have a regeneration time comparable to the saturation time, instead the dolomite is harder to regenerate. For the second test, an artificial syngas has been used with the following composition: 49% of H_2, 28.7% of N_2, 7.24% of CO_2, 13% of CO, 2% of CH_4 and 342 ppm of H_2S. The total flux is kept constant at 107 NmL min^{-1} (figure 3.26). In this second case, the catalyst has shown longer performance, since the amount of H_2S in the mixtures was lower than before. The hydrogen sulphide has been completely removed for the first 80 minutes and than the level of H_2S on the gas has been kept around 12-13 ppm for 40 minutes more. Once the catalyst is poisoned, its efficiency rapidly decreases.

80
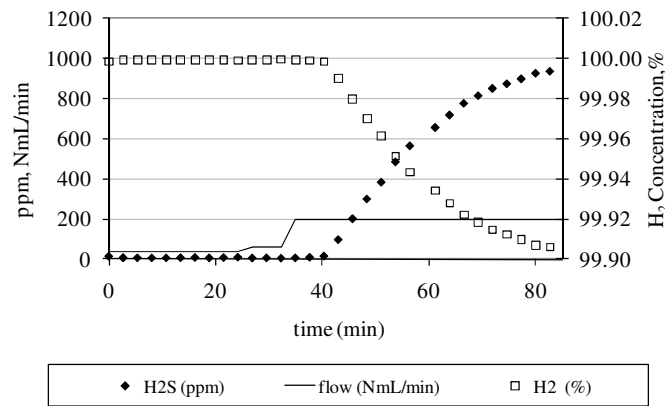
Figure 3.25 First lab test to verify the catalyst efficiency for H$_2$S abatement
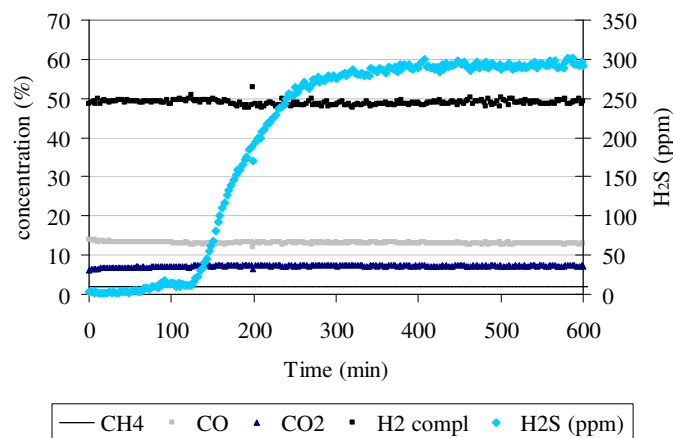
Figure 3.26 Second lab tests to verify the catalyst efficiency for H$_2$S abatement

The catalyst tested has shown promising results. Good performance are expected using the catalyst in the gasifier considering that, in the lab tests, the amount of catalyst was very small and that the H$_2$S content in the experimental syngas is lower than the concentration used in the lab (it ranges between 20 and 70 ppm, from test 11).

The gasification tests number 12 and 13 have been run with the presence of the catalyst. The catalytic filter has been filled with a mixture of calcined dolomite (300 g) and 300 g of silica support impregnated with manganese oxides.

In figure 3.27 the results of the first gasification test run with the catalyst are reported. On the left it is possible to see the temperature profile and on the right the syngas composition. On both charts, the hydrogen sulphide concentration has been reported. The reactor has been filled with char before the heating up of the system to verify the correct functionality even if the bed is controlled by the highest thermocouple (number 1). The beginning of the test can be seen from the first decreasing of temperature registered by the thermocouple (minute 179). The H$_2$S concentration starts from zero in

the first 10 minutes but then rises up to almost 100 ppm. Then the hydrogen sulphide ranges from 30 to 90 ppm. It is clear that the filter is not working properly except for the first 10 minutes. The main reasons are the low temperature inside the filter (around 500°C).

Thermocouple 1   Thermocouple 2   Thermocouple 3   H2S (ppm)

CH4   CO   CO2   H2   H2S [ppm]
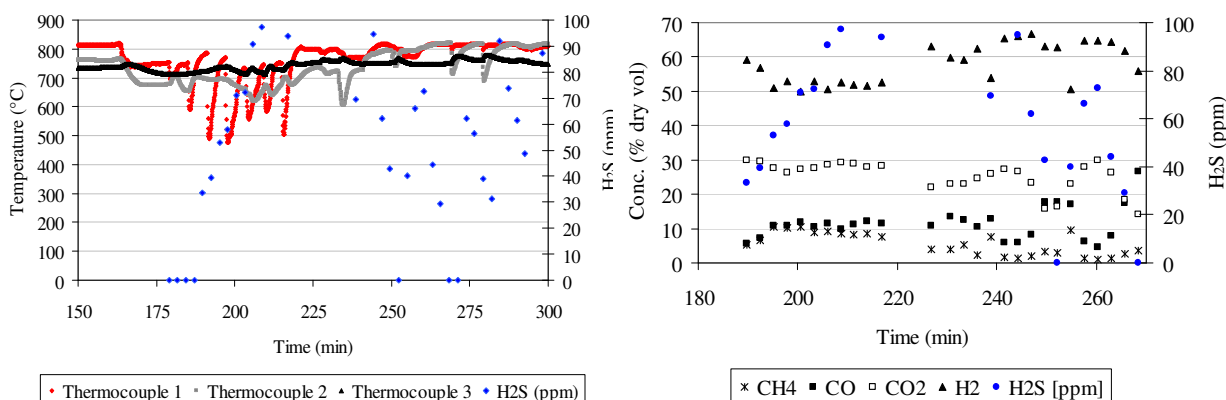
Figure 3.27 Gasification test with dolomite as catalyst

As said before, the dolomite is efficient in tar cracking for temperature above 700°C and, for H_2S, abatement a minimum temperature of 600°C should be reached. After the test the filter has been opened and, as shown in figure 3.28, the part of the catalyst closer to the syngas gasifier exit, has changed its colour from beige/white in grey/black. Instead, the final part of the catalyst, has kept almost its original colour (beige/white). When the catalyst works, it changes its colour in grey/black. This means that only a small fraction of the catalyst has worked. It has been also noticed that the connection tube between the gasifier and the catalyst was almost full of char.

Figure 3.28 Catalyst after the test at the beginning (left) and at the end of the filter (centre), the connection tube full of char (right)

A further test (test number 13) has been run at the same condition of this one, to confirm or contradict the observed results. The H_2S concentration of test number 13 is reported in figure 3.29.

In this test, the reactor has been completely emptied before the test, to avoid possible problem of back pressure due to char deposit. The biomass feeding started at minute 170 (the beginning of x-axis); the load is not immediately seen by the thermocouples because the reactor was completely

emptied, thus some minutes occurred for the growing of the biomass bed up to the deepest thermocouple which, in this test, has been used to control the bed height. From the hydrogen sulphide measurements, it can be seen that the catalyst has a good efficiency only at the beginning of the test. After the first ten minutes the H_2S concentration ranges between 10 and 30 ppm (anyway a lower concentration respect to the one measured in the test run without catalyst).
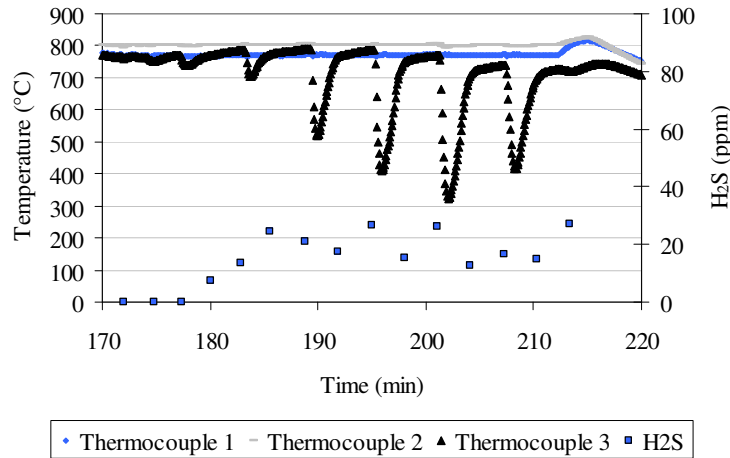
Figure 3.29 Gasification test with dolomite as catalyst

The average syngas composition measured (dry basis) is:

C_2H_2 (%)	C_2H_4 (%)	C_2H_6 (%)	CH_4 (%)	CO (%)	CO_2 (%)	H_2 (%)	O_2 (%)
0.06	-	0.99	8.39	20.89	28.77	40.37	0.53

With respect to the previous test, the filter seems to work partially, even if the level of hydrogen sulphide is still high to feed, for a long period, a SOFC stack. Anyway, the catalytic filter is working at too low temperature to be efficient in tar and hydrogen sulphide abatement.

After these three tests to measure the hydrogen sulphide and to test the catalyst, a first test coupling a SOFC stack with the gasifier has been done. The test has shown that the level of gas cleaning has to be improved because the SOFC stack gave up working in short time. Once open the stack, it has shown several point of carbon and tar deposition. Thus the heating system of the catalytic filter has been removed. The electric resistance has been changed with two electric ovens, able to keep the filter at 800°C.

3.5.4 Carbon and energy balance

For the test performed in this second experimental phase the carbon and energy balance has been estimated, as in the previous tests.

The carbon balance has been calculated, as before, knowing the moles of carbon fed, and the moles of carbon in gas and in solid phase. On average, 58% of the initial carbon moles exit from the gasifier in gas phase (of which 10% are tars) and the remaining 42 % in solid phase. The carbon

balance has been closed with and error of +/- 5%. As previously, the input and output energy fluxes have been considered and the overall system efficiency is around 45-50%.

A test with the empty reactor has been done to measure the system performances without the gasification process. For 30 minutes the consumptions of the empty system have been recorded. Then for 60 minutes the consumptions to keep the reactor at 800°C feeding only steam at 600°C have been measured. The average values are reported in table 3.15.

Looking at the data collected, 3.43 kW are needed to keep the reactor at 800°C. When the steam is fed at 600°C more energy is required to heat the steam up to 800°C: 4.47 kW. During the gasification process some of the reactions are endothermic and other exothermic; the need of energy during the steam gasification tests is approximately the same then when only steam is added.

Table 3.15 Energy consumption of the empty and working gasification system

Time	M1 (kW)	M2 (kW)	M3 (kW)	M4 (kW)	Steam generator (kW)	Ovens (kW)
			No steam, no biomass			
5 min	4.80	2.76	0.00	1.20	0.84	3.96
10 min	4.44	2.64	0.00	0.00	1.8	2.64
15 min	4.44	2.76	0.00	0.00	1.68	2.76
20 min	4.44	2.76	0.00	1.20	0.48	3.96
25 min	4.56	2.64	0.00	1.20	0.72	3.84
30 min	4.44	2.76	0.00	1.20	0.48	3.96
average	**4.54**	**2.71**	**0.00**	**0.72**	**1.10**	**3.43**
			Steam (3.6 kg h^{-1}) and no biomass			
5 min	9.36	2.64	1.2	0	3.84	5.52
10 min	9.12	2.64	0	1.2	3.84	5.28
15 min	7.8	2.64	1.2	1.2	5.04	2.76
20 min	8.04	2.52	0	1.2	3.72	4.32
25 min	8.4	2.64	0	0	2.64	5.76
30 min	8.28	2.64	1.2	1.2	5.04	3.24
60 min	8.34	2.6	0.4	0.8	3.80	4.54
average	**8.48**	**2.62**	**0.57**	**0.80**	**3.99**	**4.47**
			Steam (3.6 kg h^{-1}) and biomass (2kg h^{-1}= 200gr every 6 minutes)			
start	5.2	3	0	0	2.2	3
6 min	5.6	3.1	1	1	0.5	5.1
6 min	8.6	3.1	0	0	5.5	3.1
6 min	10.1	3.2	1	1	4.9	5.2
6 min	9.7	3.1	1	1	4.6	5.1
6 min	6	2.9	0	0	3.1	2.9
6 min	5.1	3	1	1	0.1	5
6 min	7.3	3	1	1	2.3	5
6 min	9.8	2.9	1	1	4.9	4.9
6 min	6.1	2.8	1	1	1.3	4.8
6 min	12.6	2.9	1	1	7.7	4.9
average	**7.83**	**3.00**	**0.73**	**0.73**	**3.37**	**4.45**

3.6 Gasifier coupled with a SOFC stack

At last, two of the preliminary tests performed coupling the system with a SOFC stack are here reported (number 14 and 15). In the test number 14 the gasifier has been coupled with a stack of 18 fuel cells. The nominal overall power is 250 W. In the test number 15 the gasifier has been coupled with a stack of 24 fuel cells for a global nominal power of 330 W.

The SOFCs have to work at high temperatures since their components are made of materials that became active at high temperature (electrically and as ions carrier). They have to be heated up to 600-1000°C. In a fuel cell the anode is where the oxidation reactions occur, and is the positive pole, instead in the cathode is the negative pole, where the reduction occurs.

The reactions which occur in a fuel cell working with syngas are:

Anode reactions:

$$H_2 + O^= \rightarrow H_2O + 2e^- \qquad\qquad (3.9)$$

$$CO + O^= \rightarrow CO_2 + 2e^- \qquad\qquad (3.10)$$

Cathode reaction:

$$\tfrac{1}{2}O_2 + 2e^- \rightarrow O^= \qquad\qquad (3.11)$$

Overall reactions

$$H_2 + 1/2\,O_2 \rightarrow H_2O \qquad\qquad (3.12)$$

$$CO + 1/2\,O_2 \rightarrow CO_2 \qquad\qquad (3.13)$$

In addition, considering that the syngas has also a percentage of methane, the oxidation and reforming of methane may also take place in the anode, using the available water.

$$CH_4 + 2O_2 \rightarrow 2H_2O + CO_2 \qquad\qquad (3.14)$$

$$CH_4 + 2H_2O \rightarrow 8H_2 + CO_2 \qquad\qquad (3.15)$$

For every mole of hydrogen one half mole of oxygen is needed for the fuel cell reaction, supplying 2 ions and 4 electrons. Likewise, combining the steam reforming and methane oxidation reaction, each mole of methane requires 2 moles of oxygen. It is then possible to calculate the number of oxygen moles required for 100% fuel utilization in the fuel cell:

$$\text{Mol of } O_2 = 0.5 \text{ (mol of } H_2) + 0.5(\text{mol of CO}) + 2 \text{ (mol of } CH_4) \qquad (3.16)$$

85

Considering the syngas composition and production measured during the experimental activity, the moles per hour yield are: H_2 = 31.6 mol h^{-1}; CO=7.42 mol h^{-1}; CH_4=3.9 mol h^{-1}; CO_2=17.3 mol h^{-1}, for a feeding rate of 2 kg h^{-1}. From the formula (3.16) the numbers of moles of oxygen needed for the full fuel utilization are 27.34 mol h^{-1} that means 0.66 Nm^3 h^{-1} of oxygen or 3.2 Nm^3 h^{-1} air.

The maximum attainable performance of the SOFC stack operating with the experimental syngas of the gasifier have been estimated using the Design performance data provided by Sofcpower (a local Fuel Cells production company) where this project has been developed. The stack is designed to have an efficiency of 45% (on the fuel LHV) at 70% of the fuel utilization. This fuel cell stack should achieve an areal power density of 0.3 W cm^{-2} of active area at a cell potential of 0.7 volts and a current density of 0.428 A cm^{-2}. The active area is 50 cm^2.

The total stack current at design conditions is then:

$$Current\ density \cdot active\ area = \left(0.428 \frac{A}{cm^2} \right)\left(50\,cm^2 \right) = 21.4\,A \tag{3.17}$$

Then, using this current, we estimate the required voltage of a 250 W stack:

$$\frac{stack\ power}{total\ stack\ current} = \left(\frac{250W}{21.4\,A} \right) = 11.69V \tag{3.18}$$

Using the designed potential of 0.7Volts/cell, the minimum number of cells is calculated as:

$$\frac{total\ voltage}{potential\ of\ the\ cell} = \left(\frac{11.69V}{0.7V\,/\,cell} \right) = 16.6\,cells \tag{3.19}$$

A cells stack is composed by several cluster of cells. Each cluster is composed by 6 cells. Thus, a stack of 3 cluster for a total of 18 cells has been assembled.

To examine if the current capacity of the gasifier is sufficient to supply fuel to a 250 W fuel cells stack, the assumption that each mole of oxygen supply two O$^=$ for ion conduction, and four electrons for electronic conduction is made. Considering a fuel utilization of 70 % the current capacity is:

$$\left(27.34 \frac{molO_2}{h} \right) \cdot \left(\frac{4e^-}{O_2} \right) \cdot (F) \cdot (0.7) \cdot \left(\frac{h}{3600s} \right) \cdot \left(\frac{1}{18cells} \right) = 113.9C \cdot s^{-1} = 113.9A \tag{3.20}$$

Where F is the Faraday constant = 96485 C/mol.

Since 113 is higher then the design current of 21.4 A, the fuel is widely more than the fuel needed for the stack. It is also possible to examine the reaction enthalpy of the fuel cell to determine the excess of energy produced. Considering the reaction enthalpy of the reactions (3.12), (3.13), (3.14) and the syngas moles in input the whole reaction enthalpy is around -11755 kJ per hour,

corresponding to an input power of 3.26 kW. For an output power of 250 W, and considering that the cell has a fuel utilization of 70%, the percentage of the syngas potential energy available utilized by the stack is:

$$\eta = \frac{Power_{out}}{Power_{in}} = \frac{0.25\,kW}{3.26 \cdot 0.7\,kW} = 10\% \qquad (3.21)$$

The maximum heat available for thermal integration is then 3.26 kW-0.25 kW = 3 kW. This heat can be used to generate superheated steam, or to heat the inlet air and supply heat to the gasification process. The same calculations have been performed for the stack of 24 cells. The current capacity is 85.48 A (greater then 21.4 A) and for a nominal output of 333 W, 14.5% of the fuel energy is utilized in the stack.

The temperatures in input and output of the fuel and of the air of test number 14 are shown in figure 3.30. The temperatures of the three clusters of the stack (6 cells for each cluster) are also reported. In figure 3.31 the current (A), the voltage (V) and the power (W) produced by the stack during the gasification test are reported.
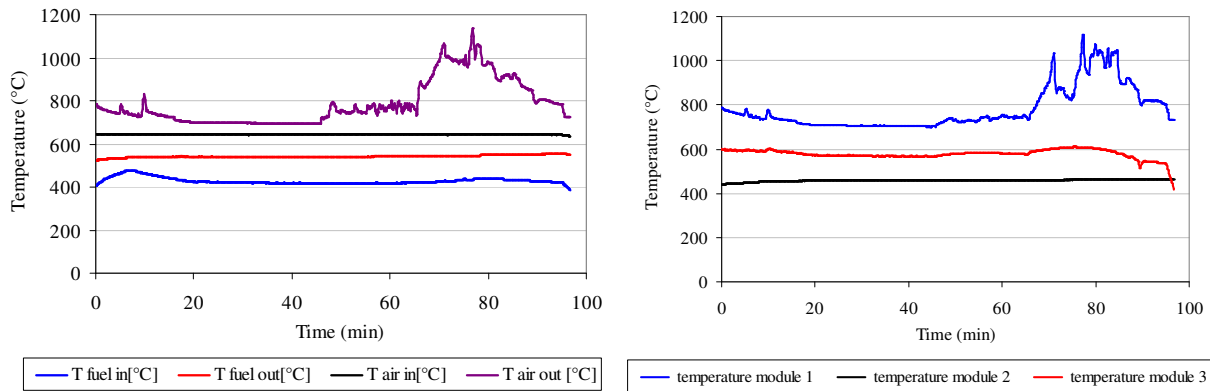
Figure 3.30 Air and fuel temperature (left) and temperature of the three modules (right)
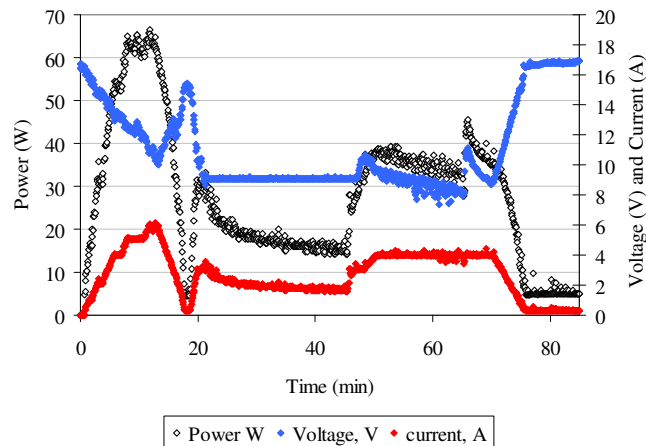
Figure 3.31 Voltage, current and power of the cells stack

The performance of the stack has not been constant. It has worked for approximately 80 minutes. Then the test has been stopped due to the poisoning of the cells. There has been a peak of power production of 65 W, after a period of increasing and decreasing of the power. Finally, for 20 minutes before the switching off, an almost stable period of operation has been registered, with a power production of 30-35 W. Considering that the nominal power of the stack is 250W (using pure hydrogen as fuel) the stack has worked, at 18% of its nominal power (considering the performance of the more reliable stable period). During the initial peak of production, the stack has worked at 24% of its nominal power, even if for a brief period.

In the last test (number 15) a stack of 24 cells has been coupled with the gasifier (4 clusters) for a nominal power of 333 W. In figure 3.32 the temperature profile inside the reactor is reported (left). As can be seen the bed height was controlled by the deepest thermocouple for 30 minutes (red dots), and then from the middle one (grey dots). In the same figure (right) the temperature of the syngas and air in input and output are shown. The stacks temperatures were between 800 and 1000°C for 3 of the 4 modules, instead one could reach only 400°C due to a problem of the cells module. It is important to consider that the fuel cells tested are prototypes of the local industry Sofcpower, thus some problems linked to the non-correct operation of the SOFCs can occur during the gasification tests.
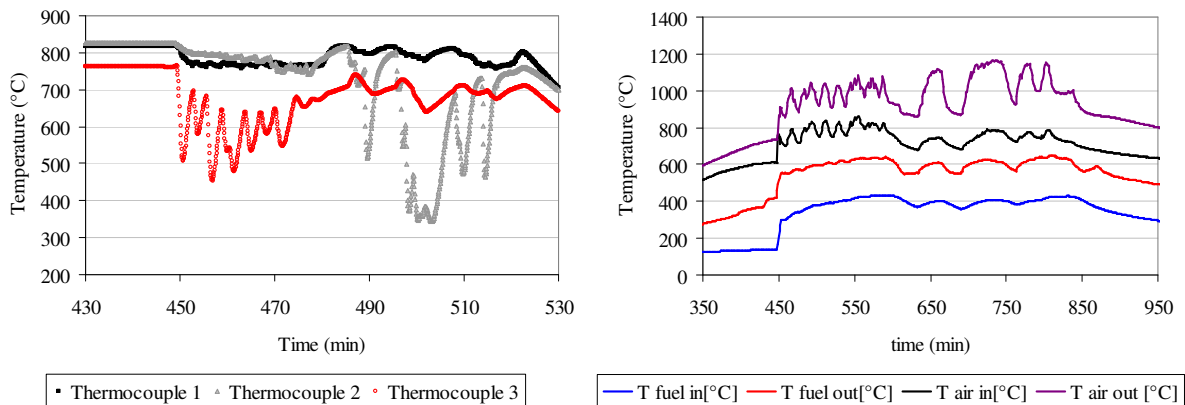
Figure 3.32 Temperature profile of the gasification reactor (left), temperature of the inlet and outlet air and syngas (right)

In figure 3.33 the power generated by the SOFC stack is shown. In the first phase 60 W have been generated for approximately 10 minutes, then the stack performance has rapidly decreased. The feeding of the syngas has been stopped for 10 minutes to clean the SOFCs with the so colled "forming gas" (nitrogen with 5% of hydrogen). In the second part of the tests 130 W have been produced for 15 minutes. Then the SOFCs performance has decreased again and test has been stopped. In this test, the cell efficiency has been of 18% during the first phase (60 W produced) and 40 % during the second phase (130-140 W produced).
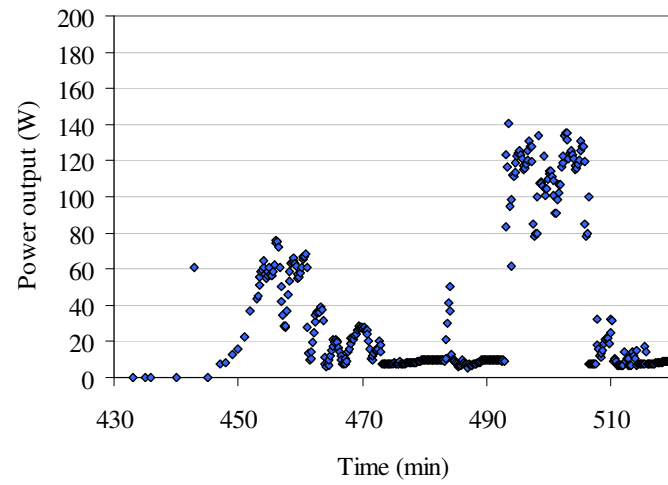
Figure 3.33 Power generation by the SOFC stack during test number 15

Chapter 4

Modelling activity

4.1 Introduction

In this chapter, the data collected during the experimental activity described in chapter 3, have been compared with the outputs of the thermodynamic equilibrium model described in chapter 3.2 and used in the preliminary phase of this project. The agreement between the experimental data and the outputs of the thermodynamic model is not satisfying. The model needs to be tuned up by means of experimental correlations. For this reason a simpler non-stoichiometric model that can be easily manipulate and adjusted according to the experimental data, has bee built. The new model has been tested and than modified in a quasi-equilibrium model. A satisfactory agreement has been observed between the modified model and the experimental data. In a second moment, the modifications have been applied also the the 2 phase, stoichiometric, equilibrium model. Finally, the temperature profile registered by the thermocouples placed inside the reactor described in the previous chapter, has been used to estimate the thermal conductivity coefficient of the biomass. The value found has been used to calibrate a 2D finite element model to simulate the temperature profile inside the reactor. Thanks to these two models, linked together, the temperature and gas composition inside the reactor have been modelled.

4.2 Model versus experimental results

4.2.1 Comparison of the syngas composition

A thermodynamic modeling approach allows the simulation of the gasification process at different temperature and SC values. In the first experimental campaign, the gasification tests have been run at 700 and 800°C for SC values equal 2 and 3.

In figure 4.1 the output of the stoichiometric equilibrium model for SC=2 and SC=3 at different temperature is reported.

In table 4.1 the average concentration of the four main gaseous compounds of the first seven tests are summarized. As can be seen, the hydrogen concentration is well predicted by the model, instead the CO is overestimated and the CO_2 underestimated. The predicted methane concentration is close to zero since it is not an equilibrium compound; anyway, the methane concentration in the syngas yield is quite low, because the residence time inside the reactor is long enough to reach almost equilibrium condition.
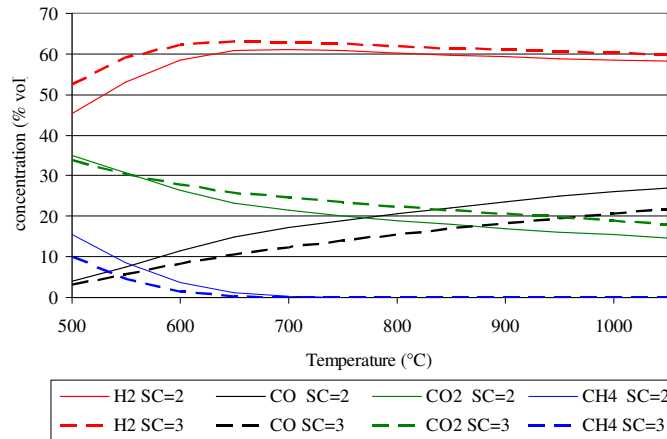
Figure 4.1 Output of the thermodynamic equilibrium model for SC=2 and SC=3

Table 4.1 Average composition of the syngas yield during the first set of tests

Test number	SC	CH_4 % vol	CO % vol	CO_2 % vol	H_2 % vol
1	2	1.3	4.2	29.2	63.4
2	2	1.5	7.0	28.2	63.1
3	3	1.4	3.7	30.0	64.9
4	2	1.9	6.6	27.2	64.3
5	2	2.9	3.6	30.4	63.0
6	3	2.9	3.6	30.4	63.0
7	3	3.5	4.0	28.4	64.0

The average syngas composition measured in the tests of the second experimental campaign (with the continuous configuration of the gasifier) is composed by hydrogen at 51%, CO at 12%, CO_2 at 29-30% and CH_4 at 6.5%. As noticed in the previous chapter, the continuous configuration of the gasifier reduces the residence time inside the reactor. Indeed the hydrogen concentration is lower and methane is higher respect to the model previsions. A better agreement exist between the measured carbon monoxide concentration and the predicted one, instead the carbon dioxide is still underestimated by the model.

The model, on the basis of the predicted syngas composition, calculates also the syngas low heating value.

The low heating value of the gas produced during the experimental tests is around 8 MJ Nm^{-3} both for the test performed at 700 and 800°C. Even if the gas composition is not predicted with good accuracy by the model, the correspondence between the predicted heating value and the experimental one is satisfying.

The model, as shown in chapter 3.2, is a two-phase model and, for SC values greater then 1.5, the model shows a complete conversion of biomass into syngas without any solid carbon formation (figure 3.4). In practice, during the experimental activity, a remarkable carbon formation has been measured (around 18-20% of the initial biomass weight). The carbon formation is quite common in fixed bed reactors due to the difficulties in mixing the solid biomass with the fluidizing agent;

91

instead, a very low carbon formation is usually measured for fluidized bed reactors which assure excellent mixing conditions and heat transfer. The particular type of feedstock chosen (pellets) due to its high density and low moisture, could be also a cause of the high solid residue.
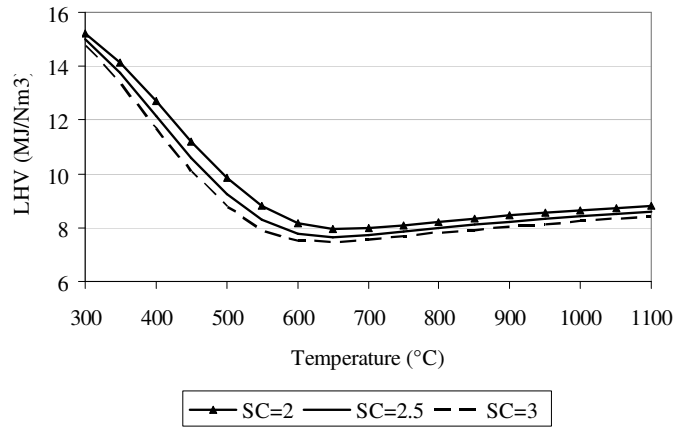
Figure 4.2 Syngas low heating value predicted by the model

4.2.3 Comparison: energy consumption

Thanks to the data collected by the energy meters, the comparison between the measured consumption and the theoretical one has been possible. The energy needed to produce superheated steam has been calculated according to the following scheme:
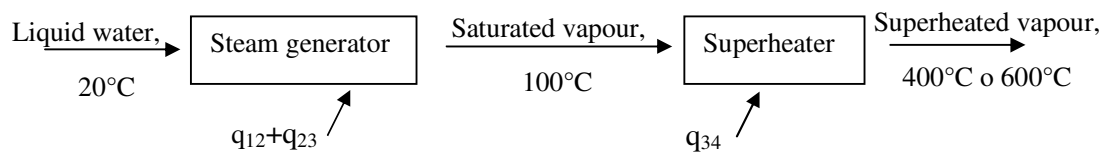
Figure 4.3 Energy needed for the steam generation.

State 1 to 2: water at 20°C to water at 100°C (saturated liquid);
State 2 to 3: saturated liquid to saturated vapour at 100°C;
State 3 to 4: saturated vapour at 100°C to superheated vapour at 400°C or 600°C.

From the theoretical calculation, the power needed for the steam generator and the super heater is reported in figure 4.4 (left). In figure 4.4 (right) the comparison between the calculated (lines) and the measured data (points) can be seen. The efficiency of the steam generator and super heater system is considered 75%. The measured values are close to the calculated ones.
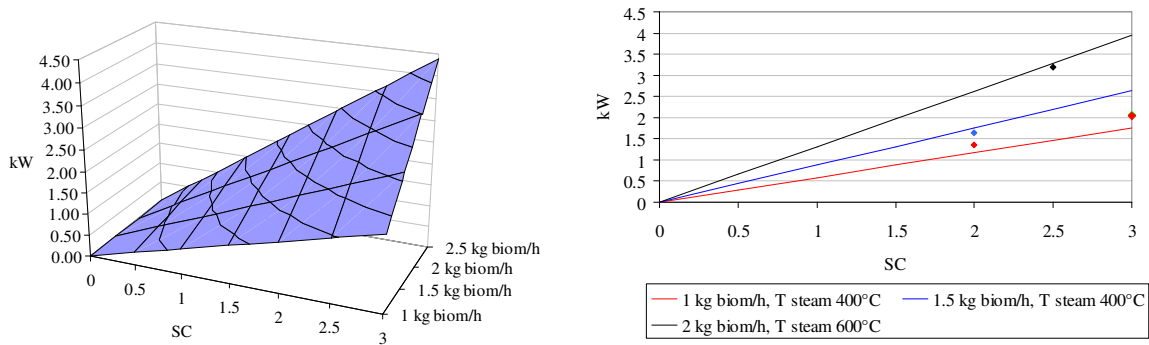
Figure 4.4 Theoretical estimation of the energy needed for the steam generator (left, in kWh) and comparison with the experimental value (right, in kW)

A subroutine of the two-phase thermodynamic model is dedicated to the analysis of the energy balance of the process to estimate the energy needed by the reactor. Two cases have been analyzed in the model:

➢ the reactor is externally heated: the whole enthalpy needed for the conversion process is provided as heat;

➢ part of the enthalpy needed is provided by the gasifying agent fed at high temperature, and the rest is provided externally.

The reactor tested is heated both externally and by means of steam fed at high temperature. Thus, the energy consumption measured during the experimental activity has been compared with the model results of the second case. The model simulations are reported in figure 4.5 considering different temperature of the gasifying medium: 100°C - 300°C - 600°C. The calculations are based on a feeding rate of 2.5kg h^{-1} and a gasification temperature of 800°C. The charts show that the higher is the steam to carbon value and the gasification temperature the higher is the energy required. However, increasing the steam temperature, the energy needed is less influenced by the amount of gasifying agent fed. Considering the experimental measurements for the tests run with a feeding rate of 2 kg h^{-1} and steam temperature of 600°C, the energy required by the ovens was, on average, 3.75 kW with ovens efficiency between 70-75%. The calculated values are close to the real one.
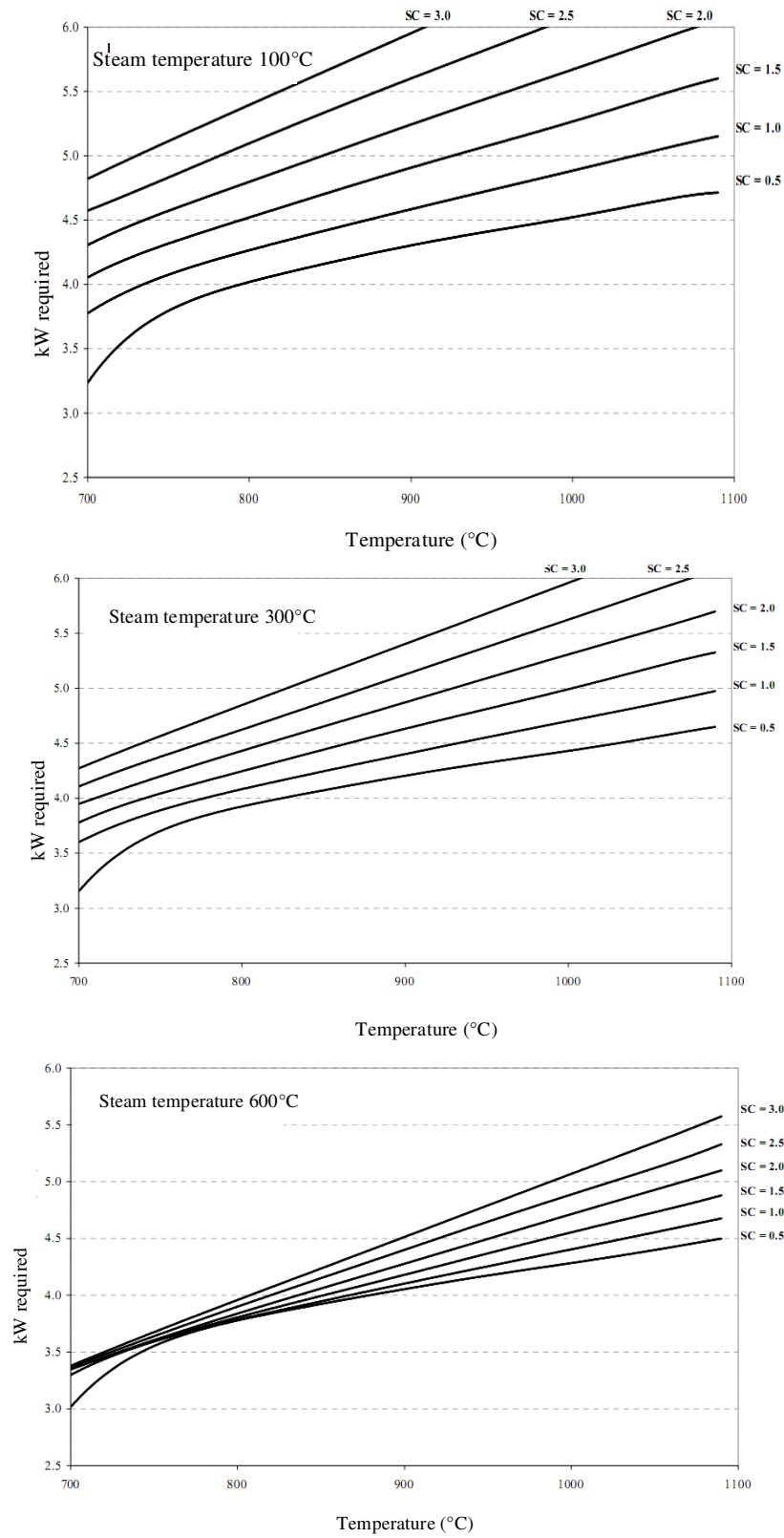
Figure 4.5 Energy needed by the system considering a gasification temperature of 800°C and different SC and steam temperature values: 100°C, 300°C and 600°C. [Baratieri, 2007]

94

The satisfying agreement between the calculated and the experimental data allows considering the present approach as reliable for the calculation of the energy required by the system during the reactors planning and designing. In this way, also alternative heating system can be considered, i.e. burning a fraction of the syngas produced or the residual char. In the tested gasifier, the char production is around 18-20% of the biomass fed. This means that for a feeding rate of 2kg h^{-1} there is a char formation of 0.36-0.4 kg h^{-1}. The char is carbon at 99% (measured during the experimental activity) and the carbon heating value is around 32 MJ kg^{-1}, thus, burning the char, 3.5kWh can be produced. The re-utilization of the char formed, theoretically, will drastically reduce the needed of the external electric energy.

4.3 Non Stoichiometric model

The deviation between the experimental data and the stoichiometric equilibrium model shows that the model needs to be tuned up by means of experimental correlations to improve the accuracy of the syngas composition predictions. A simpler non-stoichiometric equilibrium model, that can be easily modified, has been built. The 2-phase stoichiometric model has been used to verify the output of this new simpler model; the two models are both based on the Free Energy Minimization principles and they should return the same results.

The code is a one-phase model developed under the hypothesis that the biomass is composed only by C, H and O; S and N are considered negligible. Moreover, the model assumes that in the syngas produced five species can be formed: carbon monoxide, carbon dioxide, hydrogen, water and methane. The nitrogen is present only if air is used as gasifying agent. The code has been written in Matlab environment and the NASA [McBride,1993] databases have been used to evaluate the thermodynamic properties of the chemical species considered in the model.

The input data for the model are the gasification temperature and pressure, the ER or SC value (according to the gasifying agent), the input vector with the initial number of moles ($[n_C, n_H, n_O]$). Starting from the moles of C, H, O in the biomass chosen (known from the elemental analysis) and the amount of O_2 or H_2O added to the process, an initial gaseous mixture of CO, CH_4, H_2O, CO_2 and H_2 is guessed. The considered initial gaseous mixture respects the mass conservation constraint. The gasification products are modelled as a gaseous mixture (homogeneous phase) that represents the syngas. In output, the model returns the molar fraction of the gaseous compounds considered (CO, CO_2, CH_4, H_2O and H_2).

In the non-stoichiometric model, the minimization procedure applied to the (L) "Lagrangian" function (4.2) implies the computation of its partial derivatives with respect to the n_i mole number and gives the equilibrium condition (4.3), obtaining also the generic equation for the i-th component (4.4).

$$\sum_k \lambda_K \left(\sum_{i=1}^{N} n_i a_{ik} - A_k \right) + G^{TOT} = L \tag{4.1}$$

95

$$\left(\frac{\partial L}{\partial n_i}\right) = \left(\frac{\partial G^T}{\partial n_i}\right) + \sum_K \lambda_K a_{ik} = 0 \; i = 1,...,N \qquad (4.2)$$

$$\left(\frac{\partial L}{\partial n_i}\right) = \frac{\Delta G(T)}{RT} + \ln(y_i) + \sum_K \lambda_K a_{ik} = 0 \qquad (4.3)$$

By means of this procedure, it is possible to individuate N equations (one for each compound) that have to be solved simultaneously with the equations arising from the mass balance of the system. The unknowns are the n_i coefficients and the Lagrange multipliers. The obtained system is non-linear and it has been solved using the Newton-Raphson algorithm [Press,2007]. This method can be applied successfully if the initial values guessed for the unknowns are close to the final values. In this specific case, five unknowns are the molar fractions which surely range between 0 and 1, and one is the total number of moles, which is not far from the initial number of moles. For the other unknowns a first guess is made considering the typical syngas composition. Specific controls to guarantee the non-singularity of the Jacobian matrix and to avoid complex number are included.

In the 1-phase equilibrium model developed in the present work, the residual solid fraction has not taken into account. The moles of carbon in the feedstock are considered completely converted in gas (mainly in CO and CO_2).

4.3.1 Testing the model

The model has been tested with the data collected from a series of tests performed by Li et al. [Li, 2004]. Li et al. run several gasification tests in a CFB gasifier with both coal and biomass. The parameters and the experimental gas composition of some of the tests analyzed are reported in table 4.2.

Table 4.2 Syngas composition (case1-4): experimental data from a pilot CFB plant [Li et al. 2004].

Case number		1	2	4	5	6
Biomass		Coal	coal	hemlock	hemlock	hemlock
Pressure	Bar	1.6	1.65	1.19	1.19	1.19
Temperature	°C	810	780	815	772	787
Air / Biomass ratio	kg/kg	0.37	0.32	0.39	0.52	2.08
Steam / Biomass ratio	kg/kg	-	-	-	0.02	0.22
Measured dry gas composition- molar fraction						
H_2	%	10.4	13.0	3.0	4.0	3.8
CO	%	8.2	12.6	9.6	14.7	12.6
CO_2	%	16.3	13.5	17.1	16.5	15.7
CH_4	%	0.5	0.8	1.9	2.9	2.7
N_2	%	64.1	55.6	68.4	61.8	65.2
Elemental composition						
Coal (moisture:9%)	C:57.2	H:3.3	O:16.2	N:0.7	S:0.2	Ash:13.4
Hemlock (moisture 9.7%)	C:51.8	H:6.2	O:40.6	N:0.6	S:0.38	Ash:0.40

Both the models have been used to simulate the tests reported. In figure 4.6 the results for test number 1 and 2 and in figure 4.7 the results for test number 3 and 4 are reported.
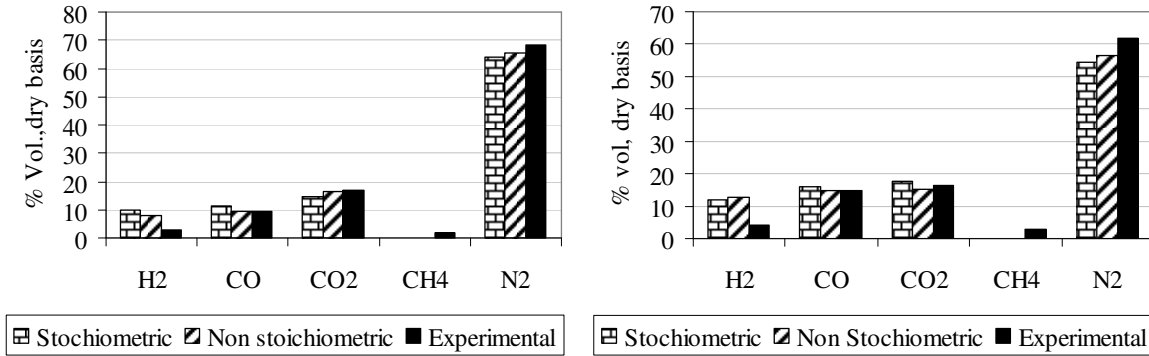
Figure 4.6 Comparison for Stoichiometric and non stoichiometric model for test number 1 and 2
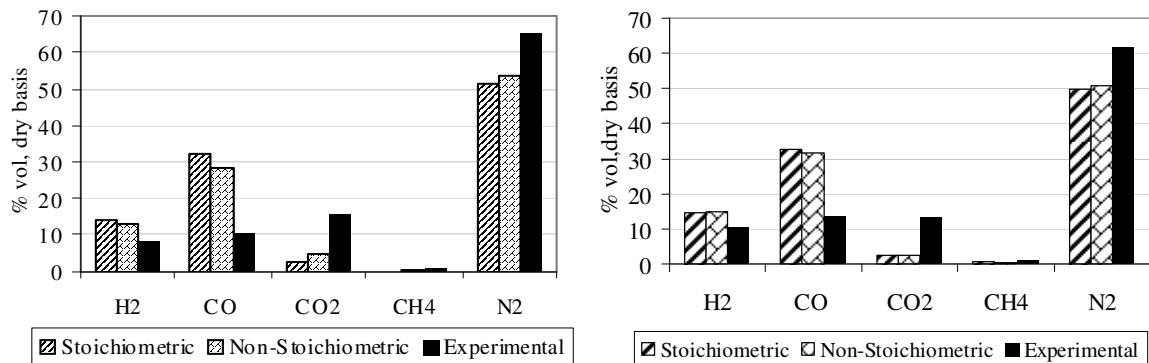
Figure 4.7 Comparison for Stoichiometric and non stoichiometric model for test number 3 and 4

From the comparison it can be seen that the two models return similar results. The slight differences between the predicted gas compositions can be due to the fact that the non-stoichiometric model is simpler and take into account only the C, H and O in input and five gaseous species in output. This model has been used to predict the syngas composition in the test run at the University of Stockholm (see chapter 5).

4.4 Quasi equilibrium model

Once verified the correspondence of the two models the cause of the non-total agreement between the predicted and the experimental data could be reconducted to the hypothesis under which the model works: the residence time in the reactor is long enough to reach equilibrium conditions. The models do not take into account that the kinetic and/or mass transfer influences real processes in a way that some elements never achieve the equilibrium. Many authors propose different methods in order to achieve a better agreement between model prediction and experimental data. A possible

approach is the application of empirical parameters in order to modify the carbon conversion or to correct directly the methane fraction in the syngas.

The high percentage of the residual fraction formed during the gasification process contains approximately 40% of the initial moles of carbon. These moles, which remain in solid phase, do not participate in carbon monoxide, methane and carbon dioxide formation. The model has been tuned according to the experimental data to take into account the residual solid phase and the methane production. The carbon conversion efficiency (i.e., the ratio between the number of carbon moles converted in gas and the total carbon moles fed) has been calculated:

$$\eta_c = \frac{C_{gas}}{C_{fed}} \tag{4.4}$$

Then the initial input vector of the model has been modified according to the η_c value.

$$N^0_{input} = [n_C, n_H, n_O] \quad \Rightarrow N^1_{input} = [\eta_C n_C, n_H, n_O] \tag{4.5}$$

The carbon conversion efficiency has been applied first to the non-stoichiometric and then to the stoichiometric model. In figure 4.8 and 4.9 the data collected during the first experimental campaign for SC=2 and 3 and gasification temperature of 700 and 800°C have been compared with the results of the quasi-equilibrium model. Now the carbon monoxide and dioxide concentration show a good agreement with the experimental data.
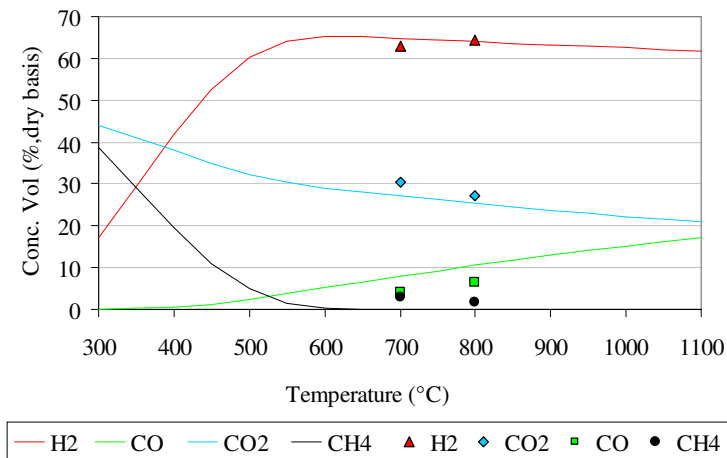
Figure 4.8 Comparison between the experimental data and the modified model for SC=2

As previously underlined, in the first part of the experimental activity, the methane production was very low, due to the high residence time. Instead, in the second part, a methane production of 6-7% has been measured. It is known that correct methane estimation by means of a thermodynamic model is a difficult task, since it is not an equilibrium compound [Linanki, 2001], [Prins, 2007].
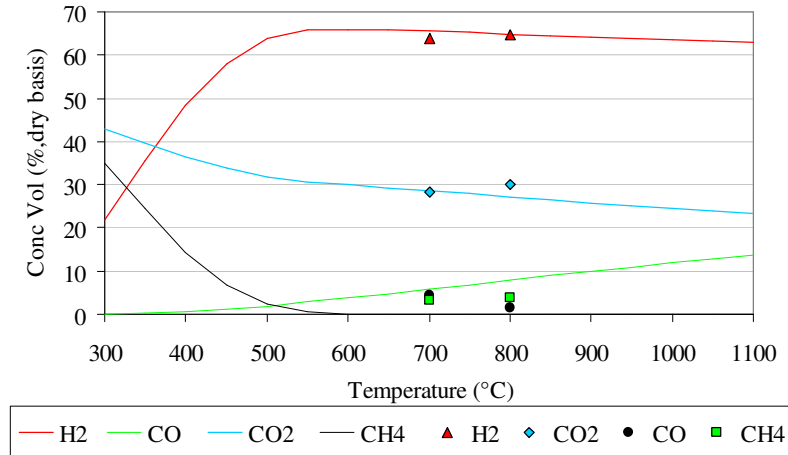
Figure 4.9 Comparison between the experimental data and the modified model for SC=3

In fact, the model does not predict the moles of carbon and hydrogen converted in methane, and this means an overestimation of hydrogen and carbon monoxide. Then, to consider also this non-equilibrium compound, a second modification has been applied to the model. The experimental gas composition has been used to evaluate the moles of carbon (n_1) and hydrogen (n_2) converted into CH_4 during the process; the initial composition is corrected considering the η_c and subtracting the moles of C and H arising from the previous calculation.

$$N^0_{input} = [n_C, n_H, n_O] \implies N^1_{input} = [\eta_C n_C, n_H, n_O] \implies N^*_{input} = [\eta_c n_C - n_1, n_H - n_2, n_O] \qquad (4.6)$$

The results of this second modification (MOD2) compared with the experimental data of the second part of the experimental activity are shown in figure 4.10.

Figure 4.10 Comparison between the experimental data and the modified model for SC=3. MOD1 is the model modified with the η_c parameter, and the MOD2 includes also the n_1, n_2 parameters.

The agreement between the experimental and the modelling data, considering the carbon conversion parameter (output of MOD1), has improved remarkably. However, to have a better correspondence, is necessary to also estimate the methane concentration, as clearly the output of the MOD2 shows. The experimental activity performed by means of this gasifier has not investigate a range of temperature and SC values wide enough to find out experimental correlation to estimate the methane and carbon conversion, as a function of the temperature or of the SC value. However, for extensive experimental campaigns found in the literature, it has been possible to find out experimental correlation, i.e. between the carbon conversion and the ER value [Li, 2001]. From one side the use of empirical correlation limits the predictive capability of the model to a specific reactor type and design; however, from the other side, the quasi equilibrium model becomes a useful instrument to know the gas composition and production with good accuracy for gasifier with similar configuration.

4.5 2D finite element model

For the purpose of the design of the gasifier a 2D finite element model has been built using a commercial software (Comsol Multiphysics ®) to integrate the thermodynamic analysis of the reactor.

The temperature field is calculated by means of the finite element method. The reactor has been modelled in a two dimensions domain and due to the axial symmetry of the reactor, only one side has been considered (Figure 4.11).

Figure 4.10 Reactor scheme used in the finite element model [Baratieri, 2007].

The software, uses the heat source calculated by the thermodynamic model as input, and solves two differential equations: the heat diffusion (4.8) and the Eulero equation (4.9) in stationary mode.

Since the simulated gasifier has a fixed bed configuration, the biomass is supposed to pass through the reactor at low velocity.

$$\nabla(\lambda\nabla T) = -H(T) \tag{4.7}$$

$$\rho(u\nabla u) = -\nabla p \tag{4.8}$$

The following boundary conditions have been imposed for the solution of the heat equation:

o   Fixed temperature on the external wall: T_{wall}

o   Adiabatic conditions on the top and the bottom surface of the reactor

o   Steam temperature on the internal wall: T_{steam}.

In the first iteration, the steam temperature is constant along the vertical axis; then, from the heat fluxes calculated by the model, the vertical temperature profile is re-calculated and utilized for the second iteration. The simulation stops when the difference of steam temperature between two successive iterations is smaller than a fixed tolerance.

For the Eulero equations the boundary conditions are:

o   Symmetry on the central axis

o   Slip condition on the reactor surface

o   Biomass input velocity on the inlet section and atmospheric pressure on the outlet section.

The heat source is function of the temperature, the SC and of the biomass treated. The heat source is calculated according to the equation (4.10).

$$H(T) = \Delta H(T) \cdot \dot{m}_b / V_b = -[H_{OUT}(T) - H_{IN}(T)] \cdot \dot{m}_b / V_b \tag{4.9}$$

Where m_b is the feeding rate (kg s^{-1}) and V_b the volume of the biomass treated. The ΔH is calculated with equation 4.11 and the values of A, B, C are listed in table 4.3.

$$\Delta H(T) = A \cdot T^2 + B \cdot T + C \tag{4.10}$$

Table 4.3 Values of A, B, C for the calculation of the heat source at different steam temperature

		SC=0	SC=1	SC=2	SC=3
T steam 200°C	A	-4.00E-06	-6.00E-06	-4.00E-06	-3.00E-06
	B	0.011	0.0151	0.01808	0.008
	C	-6.16011	-7.7242	-5.2391	-3.6418
T steam 400°C	A	-4.00E-06	-6.00E-06	-4.00E-06	-3.00E-06
	B	0.011	0.0151	0.01808	0.008
	C	-6.16011	-7.8083	-5.3781	-3.8626

T steam 600°C	A	-4.00E-06	-6.00E-06	-4.00E-06	-3.00E-06
	B	0.011	0.0151	0.01808	0.008
	C	-6.16011	-7.8845	-5.5208	-4.0967

The reactor has been divided in 10 elements along the z axis. Every element is 48 mm high. At every step, the finite element model calculates the radial temperature profile. This profile is used to estimate the syngas composition at each step by means of the equilibrium thermodynamic model. The thermodynamic model calculates also, at each step, a correction parameter (β_i), which represent the biomass converted in syngas (4.11). The β_i is function of the net power available for the process (calculated by the finite element model) and the integral average of the enthalpy variation during the conversion process, which is function of the radial coordinate due to the dependency with the process temperature (the radial temperature profile is calculated, at each step, by the finite element model).

$$\beta_i = \sum_{k=1}^{i} \frac{(Q_{in} - Q_{out})_k}{\frac{1}{R_d} \int_o^{R_d} \Delta H_k(T,r)dr} \tag{4.11}$$

This parameter is used to recalculate, every time, the heat source (4.12) and the biomass properties (porosity ϕ (4.13), density ρ (4.14), specific heat c_p (4.15), thermal conductivity λ (4.16)), considering the conversion in gas and char along the reactor [Baratieri, 2007].

$$H_{i+1}(T) = -\Delta H_i(T) \cdot \frac{\dot{m}_B}{V}(1 - \beta_i) \tag{4.12}$$

$$\phi_i = \phi_o \cdot (1 + \xi) \tag{4.13}$$

$$\rho_{i+1} = \phi_i \cdot \rho_g + (1 - \phi_i) \cdot \rho_b \tag{4.14}$$

$$c_{p_{i+1}} = \phi_i \cdot c_{p_g} + (1 - \phi_i) \cdot c_{p_b} \tag{4.15}$$

$$\lambda_{i+1} = \phi_i \cdot \lambda_g + (1 - \phi_i) \cdot \lambda_b \tag{4.16}$$

As initial values the following data has been used for the mass of pellets fed: porosity 0.49, density 1150- 1400 kg m^{-3}, bulk density 600-650kg m^{-3}, thermal conductivity 0.27 W m^{-1}K^{-1}, and specific heat 2380 J kg^{-1} K^{-1}. The physical properties vary considerably with the porosity, as shown in figure 4.11.
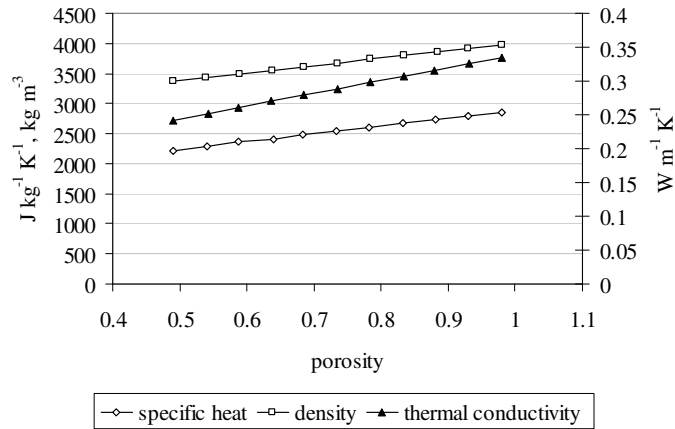
Figure 4.11 biomass physical properties versus biomass porosity [Baratieri,2007]

The 2D finite element model provides the radial temperature profile for each of the ten elements in which the reactor has been divided. Here the results for the simulation run at gasification temperature of 800°C, steam temperature of 600°C and SC values of 2.5 are reported. The feeding rate considered is 2 kg h^{-1}.

In figure 4.12 (left) the radial temperature profile simulated for the ten steps are reported. The x-axis starts from 16 mm, which is the distance of the external cylinder from the central axis of symmetry. From the model, the temperature inside the reactor is around 500-600°C. Looking back to the temperature profile measured during the experimental tests (chapter 3) the temperatures registered by the three thermocouples placed inside the reactor, at different radial position and height, are around 700 and 800°C. A difference of 200°C exists between the predicted and the measured data.
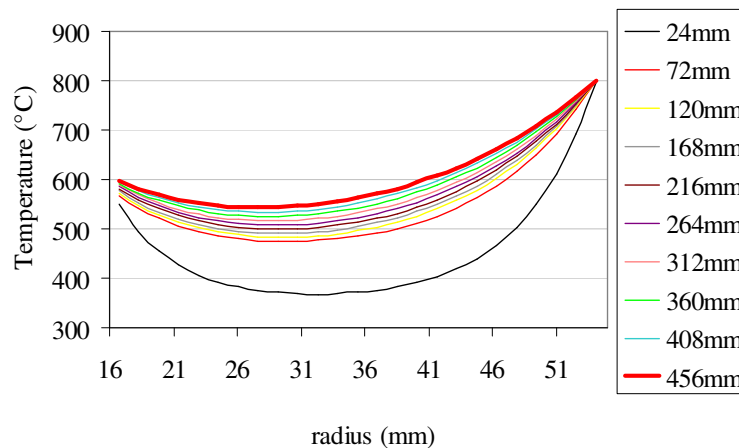
Figure 4.12 Reactor temperature profile simulated by the finite element model

The syngas composition at different steps, calculated by means of the thermodynamic model is reported in figure 4.13 (step 1, step 3, step 5, step 10). The theoretical evolution of the gas composition inside the reactor can be seen.
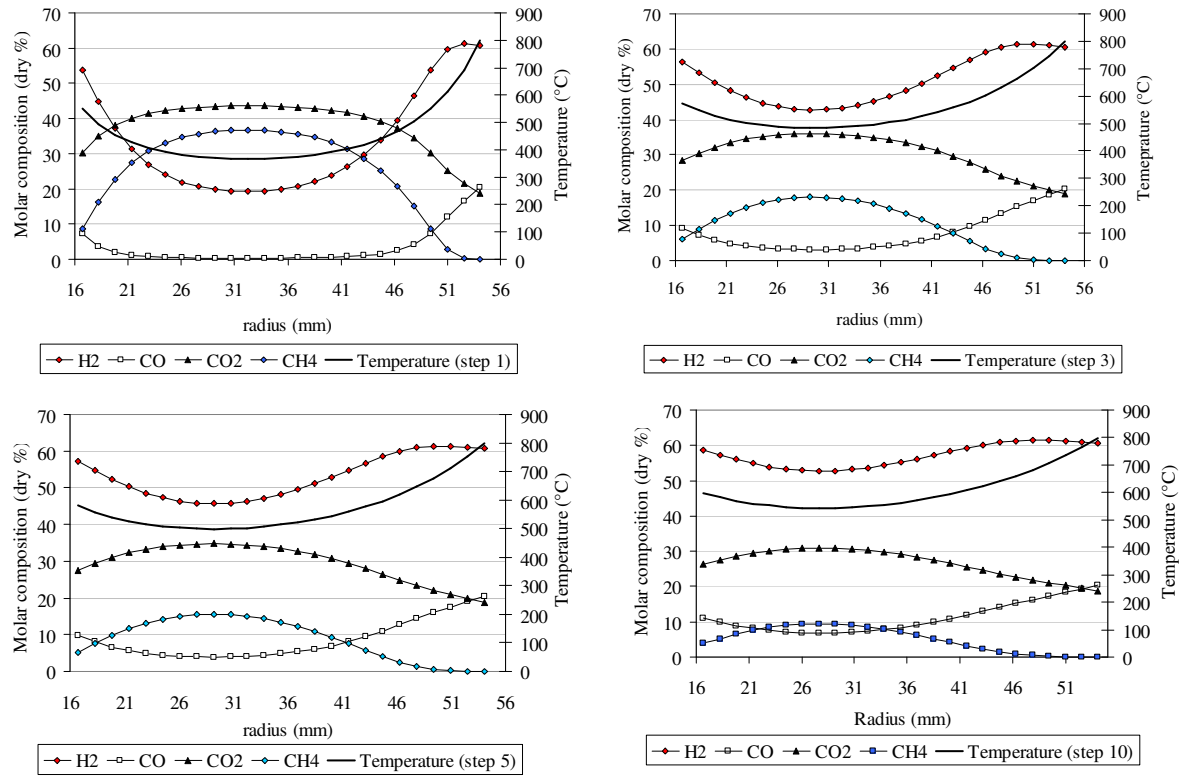
Figure 4.13 Evolution of the gas composition in the 2D reactor estimated with the original thermodynamic model [Baratieri, 2007]

4.5.1 Estimation of thermal conductivity

The finite element model takes into account only the heat transfer for conduction. However, the differences found between the experimental data and the model outputs, have underlined that heat exchanges through radiation and convection phenomena are not negligible. Therefore, the experimental data have been used to tune up the finite element model.

Instead of studying a complex problem considering the heat transfer for radiation and convection, the idea has been to go on considering only the conduction heat transfer but to estimate an a new thermal conductivity by means of the experimental data, which should include the contribution of the convection and radiation (we have called it "apparent thermal conductivity") . For this purpose, the Fourier equation for heat conduction (4.16) in one-dimensional case (4.17) has been used. The bed of biomass has been considered as a 1 dimensional body at uniform and initial temperature T_i dipped, at time $\tau=0$, in a field at constant temperature T_0 (T_0=gasification temperature) (4.18).

$$a\nabla^2 T = \frac{\partial T}{\partial \tau} \qquad (4.16)$$

$$a\frac{\partial^2 T}{\partial x^2} = \frac{\partial T}{\partial \tau} \tag{4.17}$$

Boundary conditions $T(x,0) = T_i \qquad T(0,\tau) = T_0$ (4.18)

To solve the problem of heat conduction in a semi-infinite solid body, the heat equation can be rewritten according to two dimensionless parameters: Θ and η. (4.19), with x the position inside the body.

$$\Theta = \frac{T - T_i}{T_0 - T_i} \qquad \eta = \frac{x}{2\sqrt{a\tau}} \tag{4.19}$$

The new dimensionless equation with the correspondent boundary conditions is reported in 4.20 and 4.21.

$$\frac{\partial^2 \Theta}{\partial \eta^2} + 2\eta \frac{\partial \Theta}{\partial \eta} = 0 \tag{4.20}$$

$$\Theta(\eta) \to 0 \ \text{for} \ \eta \to \infty; \quad \Theta = 1 \ \text{for} \ \eta = 0 \tag{4.21}$$

The solution of the equation 4.20 is the *error function* (erf function) (4.21).

$$\Theta = \frac{T - T_i}{T_0 - T_i} = 1 - \frac{2}{\sqrt{\pi}} \int_0^\eta e^{-z^2} dz = 1 - erf(\eta) \tag{4.22}$$

The solution of the integral of the *erf function* is not known in explicit form. The values of the error function can be found tabled.

Due to the thermocouple placed inside the biomass bed, the heating curve of the biomass has been registered, and it has been possible to calculate the time to heat the biomass from the initial temperature T_i to the final temperature T. In this way the Θ and the *erf(η)* values are easily calculated. Than the value of η has been extrapolated from the tables reported in [Guglielmini, 2004]. From the definition of η it is possible to come to λ, the thermal conductivity of the solid body (4.23)

$$\lambda = \left(\frac{x}{2\eta}\right)^2 \cdot \frac{\rho c_p}{\tau} \tag{4.23}$$

Since all the terms of the equation 4.23 are known, an apparent thermal conductivity has been estimated. The apparent thermal conductivity adopted in the finite element model is an average of the λ values calculated by means of the experimental data of five of the tests performed. The estimated thermal conductivity λ is 1.23 Wm^{-1} K^{-1}.

4.6 Linking the models

The 2D model – corrected with the apparent thermal conductivity - has been coupled with the modified equilibrium model, to take into account the biomass conversion in char and methane. The temperature profile is shown in figure 4.14. The thermocouples are placed in correspondence of the step number 3 (thermocouple 1), step number 5 (thermocouple 2) and step number 10 (thermocouple 3). Three points indicate the typical temperatures measured during the experimental tests. The predicted temperatures are close to the measured ones.
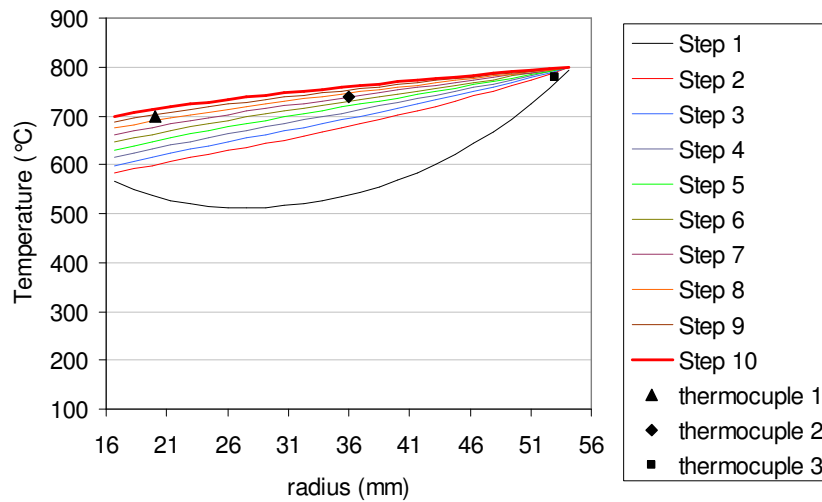
Figure 4.14 Reactor temperature profile simulated by the finite element model

In figure 4.15 the temperature of the biomass predicted by the model at each step is reported. The temperature is, on average, around 700°C, as the temperature registered in the experimental test by the thermocouple dipped in the biomass bed. On the right, the biomass consumption estimated by the correction parameter (ξ_i) is reported.
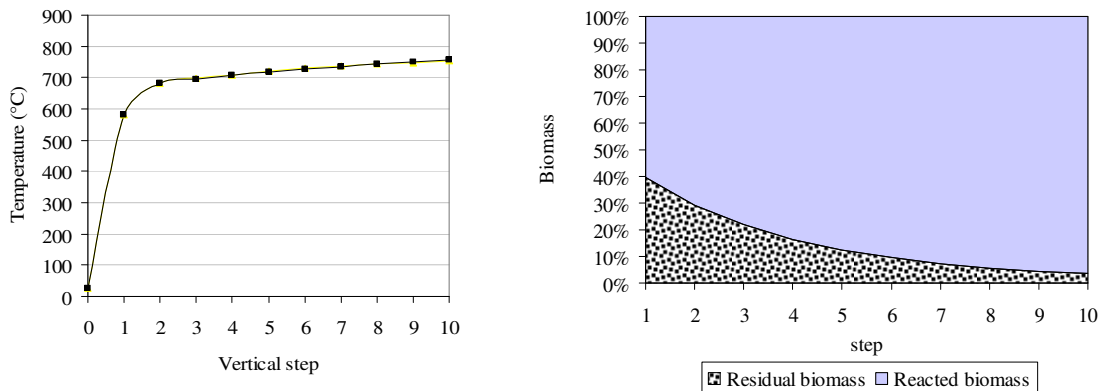
Figure 4.15 Predicted temperatures of the biomass bed (left) and biomass consumption (right)

The biomass is almost totally converted at the end of the reactor. This has no correspondence in the experimental results, even if, it should be considered that the high char residual in the experimental test can be due to the fixed bed configuration and the type of feedstock chosen (pellets).

The gas composition for step number 1, 3, 5 and 10 has been reported in figure 4.14.
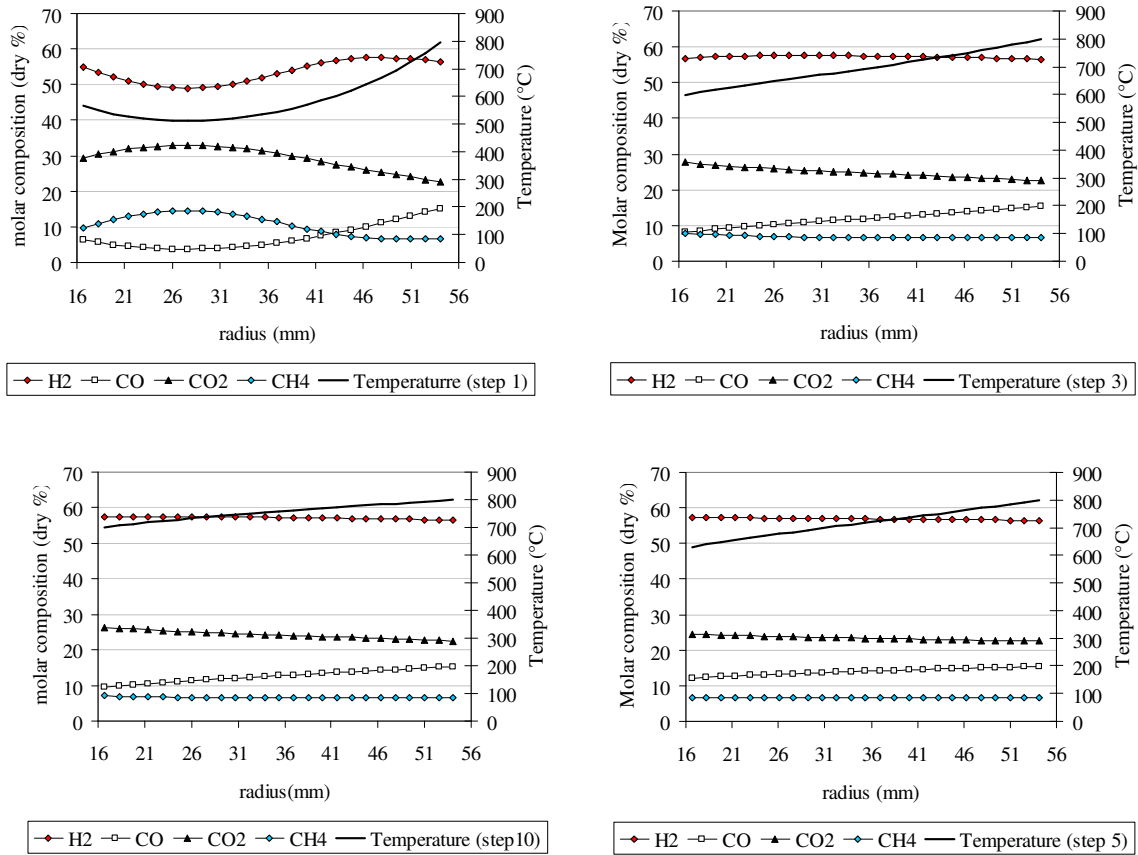
Figure 4.16 Syngas and temperature profile for step   1, 3, 5 and 10.

The gas composition predicted by the quasi equilibrium model changes significantly respect to the charts of figure 4.13. Due to a higher average value of the temperature (see radial profiles) predicted by the 2D model with respect to the previous simulation and to a lower carbon moles in input with respect to the model prediction, the syngas reaches a stable composition which is close to the experimental one (the average experimental gas composition is: H_2:51.4% CO:12%,CO_2: 29%, CH_4:6.6%).

To have a complete view, in figure 4.17, the temperature field predicted for the ten steps has been assembled (right) and the trend of the gas composition along the whole reactor has been reported. The simulated temperatures inside the reactor range between 700 and 800°C, as the measured ones. Finally, it is worth to compare the measurements of the hydrogen sulphide with the concentration predicted by the equilibrium model. The stoichiometric equilibrium model takes into account different sulphur compounds (C_2S, H_2S, SO_2, SO_3, S, COS) and the results is that, at equilibrium, the initial sulphur turns mainly in hydrogen sulphide.

In the experimental measurements, the hydrogen sulphide emissions have not a stable trend. The measured values jump between 30 and 70 ppm. This is probably due to a non uniform sulphur distribution in the feedstock composition. The elemental analyses have shown that the sulphur concentration is below 0.01%, but in some samples of crushed pellets no trace of S have been detected.

The equilibrium model, having in input a S content of 0.01%, foresee an H_2S concentration around 30-35ppm (as shown in figure 4.18). Even if the model does not foresee the highest concentration of H_2S measured (70ppm), it gives a reliable estimation of the minimum level that will be found in the syngas.
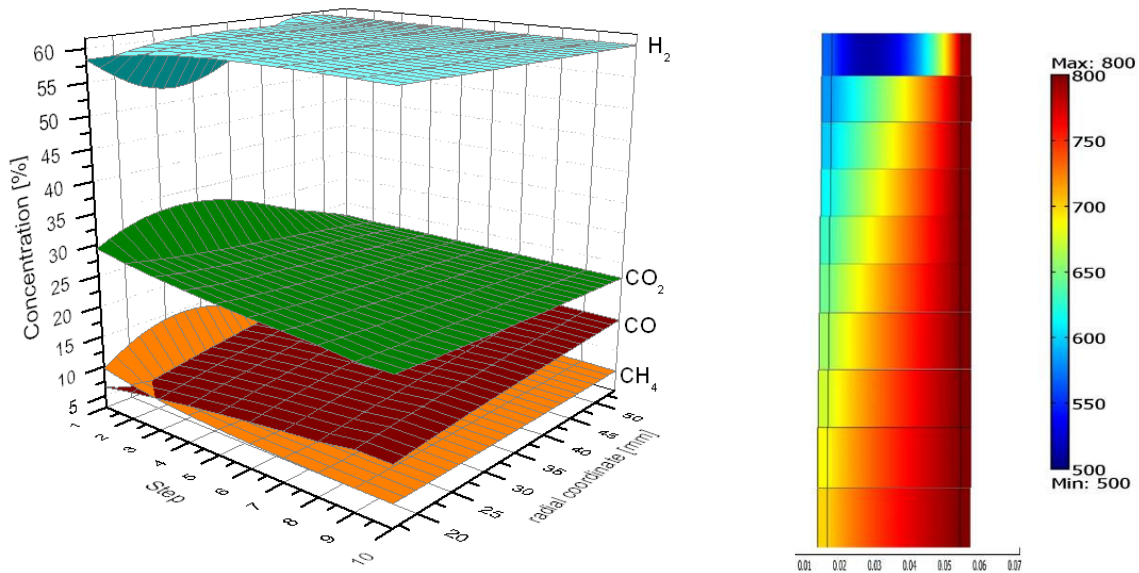
Figure 4.17 Temperature and gas composition predicted along the vertical and radial axis of the reactor.
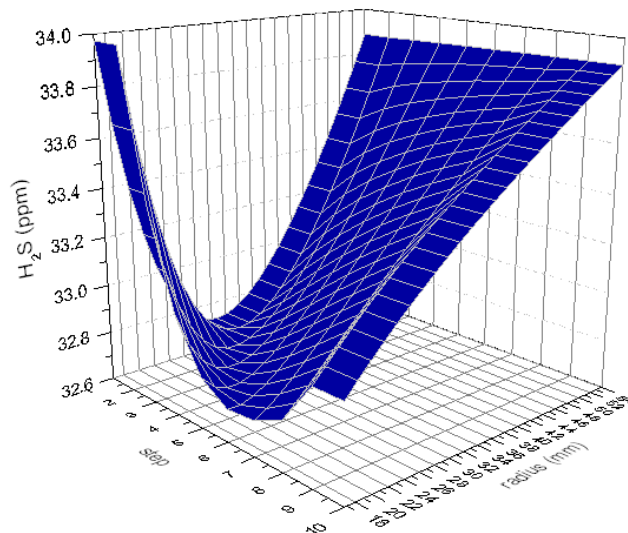
Figure 4.18 Model prediction of H_2S concentration for each step.

108

Chapter 5

Dolomite and iron efficiency in tar cracking

5.1 Introduction

The syngas produced via the steam gasification process has high hydrogen content, and it can be considered as a fuel with a high heating value quality. However, as mentioned above, the raw synthesis gas needs to be cleaned from tars before it may be upgraded to other commodities. That is because the reactors downstream, very often, are using catalysts to control the reactions. In most cases if tars deposit on the catalyst surface it will block the active sites i.e. carbon acts as catalyst poison. Furthermore, tars in the raw gas can also cause corrosion and blockage of pipes in downstream process equipment.

At present, the main challenge with respect to gasification of biomass is to minimize the tar content in the product gas and optimize the concentration of the permanent gases, increasing the H_2, CH_4, and CO contents. This may be achieved utilizing a tar cracking catalyst in a catalytic bed reactor. The most effective catalyst in tar cracking is traditionally nickel, but other alternatives have to be considered due to the high nickel cost [Baker, 1987], [Torres, 2007]. Several authors have reported about the catalytic tar cracking ability of dolomite [Olivares, 1997], and recently also the iron based catalysts have shown interesting abilities in tar cracking [Tamhankar, 1985], [Delgado 1996].

An extensive experimental campaign has been performed using a small-scale laboratory fluidized bed gasifier at the Royal Institute of Technology (KTH), Stockholm. The main goal has been the assessment of the tar cracking capability of different types of dolomite and of two types of iron based catalysts. The gas composition and tar concentration in the product gas have been analyzed. The modified non-stoichiometric equilibrium model has been used to predict the syngas composition and a good agreement with the experimental results has been found.

5.2 Experimental activity in an air fluidized bed gasifier

5.2.1 Experimental methods and procedures

The biomass gasification tests have been performed in an atmospheric fluidized bed gasification system available at the KTH laboratories [Heginuz, 1996]. The total system comprises a biomass feeder, a pre-heater, a fluidized bed reactor, a ceramic filter and a catalytic bed reactor. The reactor part that contains the fluidized bed has an inner diameter of 0.05 m and a height of 0.254 m. A cone is connecting the lower part of the reactor with the freeboard. The freeboard diameter is 0.10 m and the length is 0.508 m. The fluidized bed consists of 350g of Alumina, with a particle size of 63 – 125 μm. The fluidization medium is nitrogen while the oxidizing agent is pure oxygen. Before the

entrance of the fluidization medium in the reactor it is pre-heated to 650 °C. The syngas produced is cleaned from soot and bed particles in a ceramic filter (hot filtration). After the filter the hot gas is passed to the catalytic bed for tar cracking. Both the filter and the catalytic fixed bed reactor have a length of 0.70 m and an inner diameter of 0.05 m. All parts of the gasification system are heated with separated external heaters and the maximum temperature is 950 °C. This heating configuration makes it possible to simulate isothermal conditions.

The fuel is fed directly into the fluidized bed near the distribution plate by means of a screw feeder. The fuel hopper is provided with a purge gas of nitrogen. This is to prevent hot gases from entering in the hopper and making the fuel sticky. A detailed experimental setup has been described by Vriesman [Vriesman, 2001]. Figure 5.1 presents a schematic view of the gasification system.
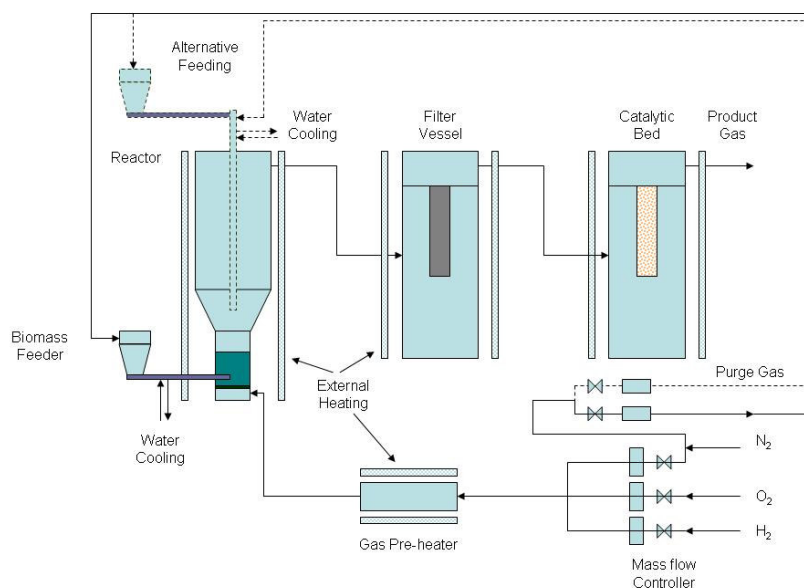
Figure 5.1 Schematic view of the KTH's gasification system

An extensive experimental campaign has been performed to examine the effect of the gasification temperature on gas, char and tar production. In the first stage nine runs have been conducted to investigate the efficiency of three types of dolomites (one from Sweden and two from China) in tar decomposition at different reaction temperatures (700, 750 and 800°C). Both the ceramic filter and the catalytic bed have been kept at 800°C. In a second stage eight tests to investigate the tar cracking efficiency of two metallic iron based catalysts have been run. Three different gasification temperatures have been tested (750-800-850°C) and the temperature of the catalytic filter has been moved between 750-800-850 and 900°C. For both series of tests birch wood has been used as feedstock. The elemental composition is reported in table 5.1. The biomass has been sieved before each test (particle sizes between 1-1.5 mm) to assure a constant feeding rate, that was approximately 4 g min^{-1} in all tests.

The cool, dry, clean gas composition has been analyzed with a gas chromatograph (Model Shimadzu, Japan), equipped with a flame ionization detector (FID) and a thermal conductivity detector (TCD). The tar sampling and analyses have been accomplished using the solid phase adsorption (SPA) method, described elsewhere [Brage, 1997]. Briefly, a 100 ml gas sample is manually drawn through a SPE tube during one minute. Later the SPE tubes are eluted using two different solvent mixtures to obtain an aromatic fraction and a phenolic fraction. The eluates were afterwards analyzed by gas chromatography.

Table 5.1 Elemental composition of the biomass employed

Elemental composition (% mass, dry sample)				
Birch wood				
C: 49	H: 6.1	O: 44.6	N: 0.1	S< 0.01
Moisture (% mass a.r.)				7.0
Ash (%mass a.r.)				0.4
PCI (MJ kg^{-1})				19.3

During the first series of tests, the ER value has been slightly changed between 0.21 and 0.26. To attain optimal fluidization conditions, 8.8 NL min^{-1} of nitrogen has been fed to the gasifier during the tests. The oxygen flow has been kept constant at 0.85 NL min^{-1}. The duration of tests has been between 1.5 and 2 hours. In table 5.2 the experimental parameters are summarized.

Table 5.2 Parameters of the tests run with dolomite as catalyst (SE= Swedish, Ch= Chinese dolomite)

Test num	T reactor (°C)	T ceramic filter (°C)	ER	dolomite type	T catalytic filter (°C)
1D	700	800	0.21	Sala $_{Se}$	800
2D	700	800	0.21	Zhejing$_{Ch}$	800
3D	700	800	0.21	Shanxi$_{Ch}$	800
4D	750	800	0.25	Sala $_{Se}$	800
5D	750	800	0.24	Zhejing$_{Ch}$	800
6D	750	800	0.24	Shanxi$_{Ch}$	800
7D	800	800	0.23	Sala $_{Se}$	800
8D	800	800	0.23	Zhejing$_{Ch}$	800
9D	800	800	0.22	Shanxi$_{Ch}$	800

In the second series of tests the fluidization conditions have been kept unchanged. The ER values have been changed for two of the tests run from 0.22 to 0.32. The experimental parameters of the second series of tests are summarized in table 5.3.

The tests have lasted for 1 hours and 30 minutes and during every test the temperature of the catalytic filter has been changed. In this way, for every run, the catalyst has been tested at two different temperatures.

Table 5.3 Parameters of the tests run with iron as catalyst (SE= Swedish, Ch= Chinese dolomite)

Test num	T reactor (°C)	T ceramic filter (°C)	ER	Iron type	T catalytic filter (°C)
1I	750	800	0.22	A	850/900
2I	800	800	0.22	A	750/800
3I	850	800	0.22	A	750/800
4I	800	800	0.32	A	800/850
5I	750	800	0.32	A	850
6I	800	800	0.22	A	850/900
7I	800	800	0.22	B	750/800
8I	800	800	0.22	B	850/900

5.3 Data Analysis

5.3.1 Gas composition

Gas and tar samples have been collected before and after the catalytic bed.

Figure 5.2 shows the average dry gas composition, nitrogen free, at different temperatures measured during the first series of test (dolomite) before and after the catalytic bed. It consists, before the catalyst, on 20-22% of hydrogen, 10% of methane and 30% of CO and CO_2. The nitrogen, used as fluidization medium, has a concentration of 68-70%. The influence of the reaction temperature has mainly effect on the carbon monoxide and carbon dioxide concentrations.
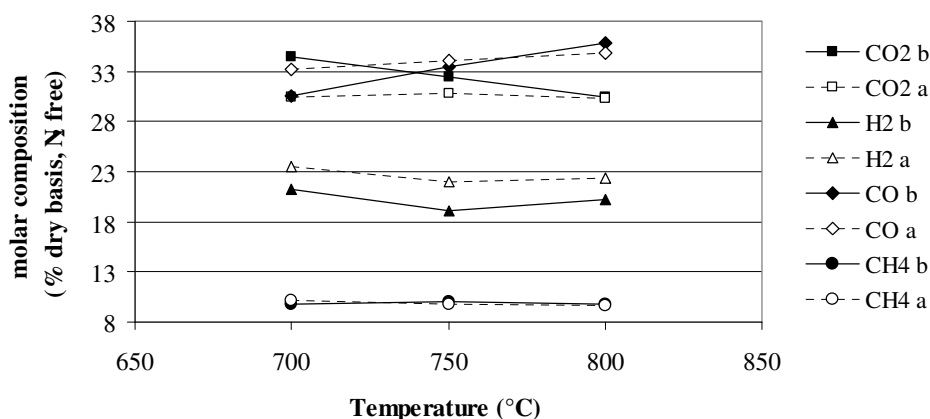
Figure 5.2 Syngas composition before (b) and after (a) the dolomite

The type and the presence of the catalyst does not influence significantly the gas composition, except for the hydrogen concentration. The hydrogen slightly increases (2-3%), for all the three dolomites and temperatures investigated. For the examinations at 700 and 750 °C there are small changes in the CO and CO_2 concentrations. Hence, the difference in syngas composition may be due to the temperature increase during the passage from the reactor (700-750 or 800°C) to the filter

112

and the catalytic bed (both the ceramic filter and the catalytic bed are kept at 800°C), and/or to the dolomite cracking of heavy hydrocarbons, which lead to hydrogen formation.

Figure 5.3 (right) shows the syngas composition measured before the Iron based catalyst, during the second series of tests. On the left, the gas composition after the catalyst, tested at different temperature, has been reported. The higher is the catalyst temperature the lower is the CO_2 and the higher is the CO.
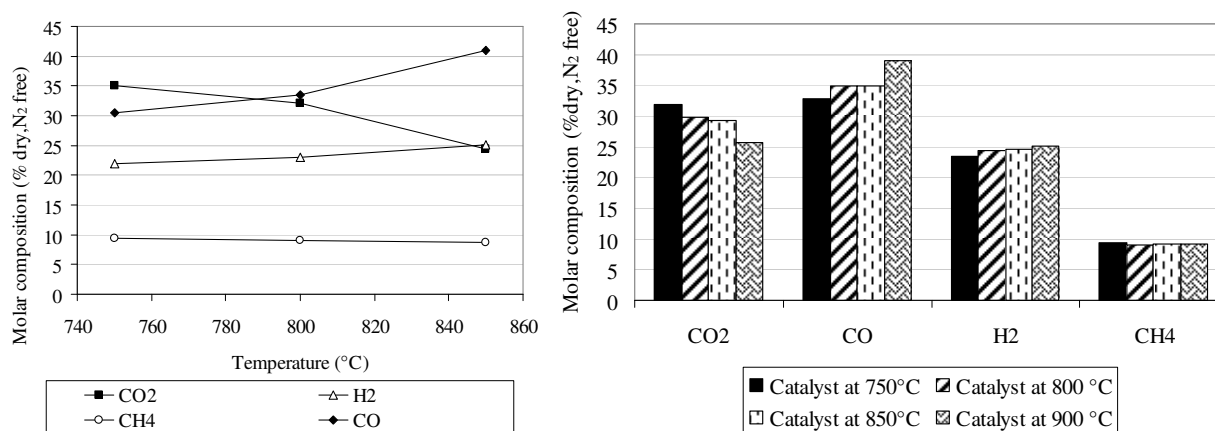
Figure 5.3 Syngas composition before (left) and after (right) the Iron catalyst

Knowing the nitrogen inlet flow, and under the hypothesis of no leakage through the system, the syngas production has been estimated. The syngas production increases after the passage through the catalytic bed, due to the conversion of heavy hydrocarbons. In table 5.4 the estimated syngas production is presented. The increase after the dolomite bed is almost constant for tests performed at the same gasification temperature, except for test number 8D, where something has not worked properly.

Table 5.4 Syngas production before and after the dolomite filter, N_2 free

Test number	Gasification Temperature (°C)	Syngas production before catalyst (NL min^{-1})	Syngas production after catalyst (NL min^{-1})	Increasing in gas production after dolomite (%)
1D	700	2.84	3.15	11%
2D	700	3.71	4.25	14%
3D	700	3.67	4.08	11%
4D	750	3.58	3.84	7%
5D	750	3.60	3.86	7%
6D	750	3.66	3.91	7%
7D	800	3.94	4.21	7%
8D	800	3.60	3.55	-1%
9D	800	4.05	4.29	6%

The same calculations have been done for the second series of test. No remarkable variations in the syngas production have been measured after the catalyst. The gas production, nitrogen free, remains stable between 3.8 and 4.2 NL min^{-1} (around 1 Nm^3 kg^{-1}).

During the first series of tests, the ER values have been moved from 0.21 to 0.26. The syngas heating value has been calculated (nitrogen free) as a weighted average of the gas composition. A plot of the gas heating values and the ER can be seen in figure 5.4. An almost linear trend has been noticed between the ER value and the calorific value of the gas before the catalyst, even though the correlation coefficient is about 0.7. In the gas composition, increasing the ER, lower H$_2$ and higher CH$_4$ and CO concentrations have been measured.
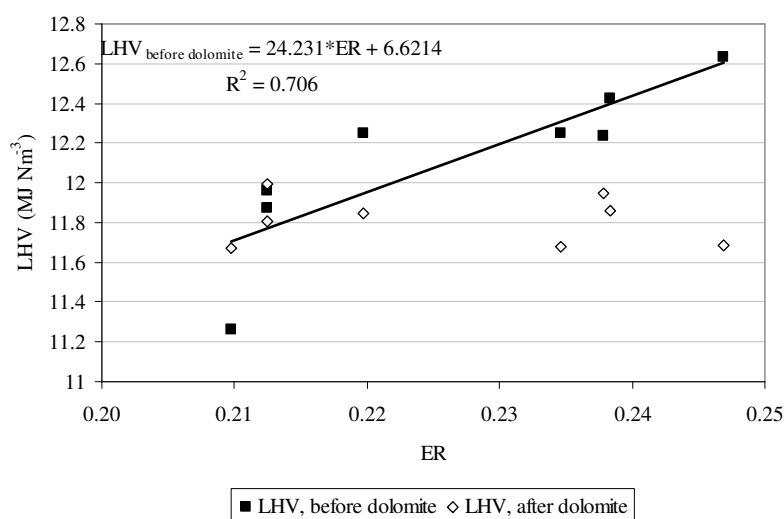
Figure 5.4 Gas heating value before and after the dolomite versus ER

After the dolomite bed, the syngas heating value has an almost uniform value in spite of different gasification temperatures and equivalent ratio values. This is may be due to both the tar cracking effect of the dolomite, and the influence of the temperature of the catalytic filter.

For the tests run with iron as catalyst, the ER value has been kept constant at 0.22 (except for tests number 4 and 5). The syngas heating value it is, on average, around 11-11.6 MJ Nm^{-3} (N$_2$ free).

5.3.2 Mass balance

For each test a known amount of biomass is loaded in the fuel hopper. After the test the char produced have been collected and weighted. From the syngas analysis and the amount of nitrogen fed in the gasifier, the gas production per kilogram of biomass has been estimated, considering nitrogen as an inert gas. The tar production before and after the catalytic bed is sampled, measured and analyzed. The carbon conversions in the gas, char and tar have been calculated and the overall mass balances have been closed with an error of +/- 5%. (The complete data of the tests run are reported in Appendix A).

The char production in fluidized bed is usually quite low. In figure 5.4 and 5.5 the percentage, as mass, of the produced char respect to the total biomass fed during the test, has been plotted against the gasification temperature and the ER value, respectively. A general trend can be noticed in both charts, even weather the correlation of figure 5.5 is stronger (correlation coefficient 0.88). The char production is remarkable influenced by the equivalent ratio.

The tests conditions, the gas and tar compositions, the mass balances are summarized in Appendix A.
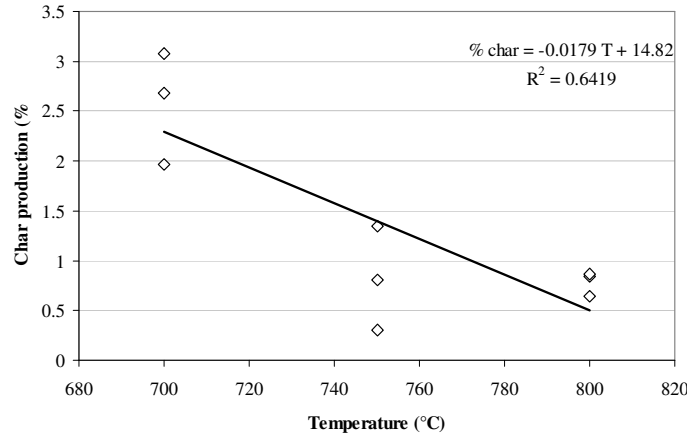
Figure 5.5 Empirical correlation between the reaction temperature and char production
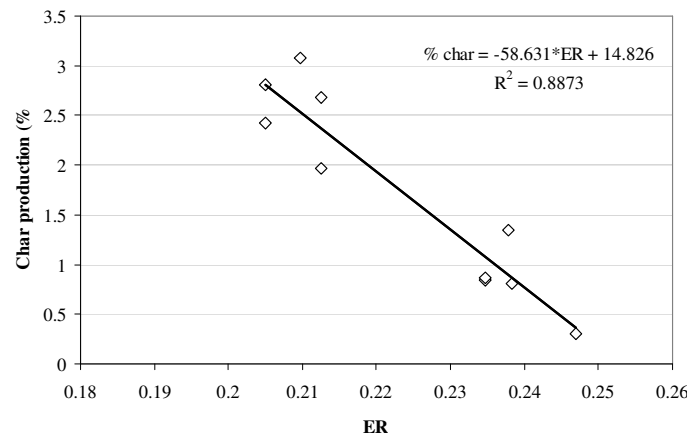
Figure 5.6 Empirical correlation between the ER value and % of char production on the amount of feedstock

5.3 Dolomite and Iron efficiency in tar cracking

Three types of dolomites have been tested, two from China and one from Sweden. From the analysis in the dolomite composition (table 5.5) no significant differences can be noticed; thus comparable efficiencies in tar cracking are expected for the three dolomites.

Table 5.5 Composition of the dolomite tested

Dolomite	CO_2	SiO_2	Al_2O_3	Fe_2O_3	CaO	MgO	K_2O	Na_2O	P_2O_5	MnO	TiO_2
Shanxi	50	0.25	0.14	0.48	26.14	22.39	0.01	0.01	0.02	0.007	0.01
Zhejing	48.61	0.35	0.14	0.03	30.72	20.12	0.02	0.01	0.01	0.002	0.00
Sala	44.80	1.94	0.36	0.53	30.1	20.9	0.04	0.02	0.01	0.07	0.01

For each test, a sample of 150 g of calcined dolomite has been added to the catalytic filter. The results on tar composition before and after the catalyst are reported in table 5.6 (for more details see appendix A).

Table 5.6 Tar reduction using calcined dolomite as catalyst

	1	2	3	4	5	6	7	8	9
Dolomite	Sala	Zhejing	Shanxi	Sala	Zhejing	Shanxi	Sala	Zhejing	Shanxi
T bed (°C)	700	700	700	750	750	750	800	800	800
T catalyst (°C)	800	800	800	800	800	800	800	800	800
ER	0.22	0.22	0.22	0.26	0.25	0.25	0.24	0.26	0.23
Feeding rate (g min^{-1})	4.17	4.17	4.23	3.59	3.72	3.73	3.78	3.58	4.03
Tar before (mg g^{-1}_{biom})	14.51	18.9	17.4	13.82	19.98	16.12	15.89	9	15.3
Tar after (mg g^{-1}_{biom})	4	5.38	4.99	4.92	7.06	6.64	5.34	4.9	7
% reduction	72	72	71	64	65	59	66	46	54

The dolomites, kept at 800°C, have shown a good efficiency in tar cracking. As expected, the tar production is higher at lower temperature. However, the higher dolomite efficiency in tar cracking is registered for the lowest gasification temperature (700°C). This means that dolomite has a good performance in cracking the tars compounds classified as "primary products" (the tar formed between 600- 800°C ,see 1.5.1). Anyway, in spite of the different gasification temperatures, the tar levels in the syngas after the catalyst are comparable.

Two iron based catalyst have been tested: Type A and type B. The tests on the iron based catalyst have been run as a part of a KTH project, and the results can be found in [Nemanova, 2011]. The results of the tests are reported in table 5.7. In two tests, the tar analyses have been omitted because the sampling conditions have not been considered reliable.

The measured tar cracking efficiency increases with the temperature of the catalytic bed filter. On average, the catalyst placed at 750°C has an efficiency around 24%, that rises up to 50-58% for catalyst temperature of 900°C.

Besides the good tar abetment shown by the iron based catalysts, better performances have been noticed for the calcined dolomite. For the steam gasification tests at Sofcpower (Trento, Italy), the

dolomite has been chosen as a suitable catalyst, not only for the higher efficiency, but also considering that the iron could be oxidized by the steam that does not react in the syngas produced via the steam gasification process.

In spite of the good tar abetment shows from the iron based catalysts, better performances have been noticed for the calcined dolomite. For the steam gasification tests at Sofcpower (Trento, Italy), the dolomite has been chosen as a suitable catalyst, for not only the higher efficiency showed, but also considering that the iron (which is in its metallic state) could be oxidized by the steam content that remains unreacted in the syngas produced via the steam gasification process. From the other side the steam could also react with the carbon that has precipitate on the iron surface but further investigations are planned at KTH in this field.

Table 5.7 Tar reduction for Iron based catalyst

test	T_{rector} (°C)	catalyst	T cat (°C)	ER	CO_2 %	CO %	H_2 %	CH_4 %	tar (mg/g_{biom})	% red
1I	750		-	0.22	34.0	31.1	22.5	9.1		
	750	iron A	850	0.22	30.6	33.7	24.3	9.3		
	750	iron A	900	0.22	27.0	38.2	25.1	8.8		
2I	800		-	0.22	32.1	33.5	23.0	9.1	6.68	
	800	iron A	750	0.22	30.5	33.7	24.2	9.5	4.91	26%
	800	iron A	800	0.22	29.8	34.9	24.3	9.1	5.05	24%
3I	850		-	0.22	24.3	40.9	25.1	8.7	2.81	
	850	iron A	750	0.22	26.3	38.7	25.4	8.7	2.03	27%
	850	iron A	800	0.22	24.6	41.0	25.4	8.2	2.34	17%
4I	800		-	0.32	39.8	30.0	20.6	7.8	3.07	
	800	iron A	800	0.32	36.7	31.0	23.0	7.8	1.94	37%
	800	iron A	850	0.32	33.3	35.2	22.5	7.7	1.34	56%
5I	800		-	0.32	42.5	30.4	19.0	6.6		
	800	iron A	850	0.32	25.9	36.0	25.8	10.3		
6I	800		-	0.22	31.6	33.4	23.2	9.5	5.63	
	800	iron A	850	0.22	29.2	35.0	24.6	9.2	4.37	22%
	800	iron A	900	0.22	25.8	38.9	25.0	9.2	2.37	58%
7I	800		-	0.22	32.3	32.7	23.4	9.2	6.52	
	800	iron B	750	0.22	31.9	32.8	23.4	9.5	5.08	22%
	800	iron B	800	0.22	31.7	32.6	24.4	9.0	4.96	24%
8I	800		-	0.22	31.6	33.4	23.2	9.5	5.69	
	800	iron B	850	0.22	29.2	35.0	24.6	9.2	3.86	32%
	800	iron B	900	0.22	25.8	38.9	25.0	9.2	3.04	47%

To test the dolomite efficiency even in presence of steam, four tests have been carried out different amount of steam directly in the catalytic filter, mixing it with the syngas yield. The tests have been performed keeping stable temperatures, 700°C in the reactor and 800°C in the ceramic and in the catalytic filter (with Sala dolomite). The results of these tests are summarized in table 5.8. The gas composition changes increasing the SC, since the steam added act as gasifying media and promote

the conversion in CO, CO_2 and H_2 of the compounds cracked by the dolomite. The dolomite shows a good efficiency even with high steam concentration.

Table 5.8 Tar reduction mixing steam with the catalytic bed of dolomite

Test	water(g min^{-1})	SC	ER	CO_2%	CO %	H_2%	CH_4%	Tar b. mg g^{-1}$_{biom}$	Tar a. mg g^{-1}$_{biom}$	Efficiency
A	0	0	0.22	28.9	23.1	23.1	10.0	9.88	3.62	63%
B	0.51	0.1	0.22	32.2	24.3	24.3	10.1	10.3	4.64	55%
C	1.24	0.4	0.22	35.4	25.6	25.6	9.6	9.1	5.32	42%
D	2.25	0.7	0.22	40.6	27.6	27.6	9.3	9.8	5.38	45%
E	3.56	2	0.22	45.1	27.9	27.9	9.1	10.1	5.63	44%

5.4 Modelling analysis

The 1 phase non-stoichiometric model described in chapter 4, has been used to predict the syngas composition of the tests described above. Both the equilibrium model and the quasi-equilibrium model, which takes into account the carbon conversion efficiency (η_c) and the moles of methane and hydrogen which participates to the methane and ethylene formation (n_1 and n_2), have been considered.

The carbon conversion efficiency has been calculated using the empirical correlation reported in figure 5.5.

From the carbon balance it has been estimated that approximately 20% of the initial moles of Carbon and 45% of the initial moles of hydrogen contribute to the formation of char (which is considered carbon at 97%), CH_4 and C_2H_4. These moles have been subtracted from the values of the input vector (N^0_{input}) .

The output of the modified model has been compared with the experimental data. The comparison between the model results and the test run with dolomite (in which both the ER and the gasification temperature have been changed) is presented in table 5.9.

Table 5.9 Predicted gas composition for the experimental test with the modified equilibrium model

Dolomite	Sala	Zhejing	Shanxi	Sala	Zhejing	Shanxi	Sala	Zhejing	Shanxi
Test num	1	2	3	4	5	6	7	8	9
CH_4	10.03	10.32	9.67	10.27	10.70	10.00	9.50	9.22	10.13
CO	33.08	32.52	35.07	34.35	32.60	35.01	36.82	36.76	37.30
CO_2	26.27	26.89	24.37	27.63	28.21	30.08	24.13	24.95	23.38
H_2	27.16	26.58	28.47	23.95	24.52	21.20	26.49	26.19	26.52
C_2H_4	3.46	3.69	2.42	3.80	3.96	3.70	3.07	2.88	2.67

As an example, figure 5.7, 5.8 and 5.9 show the comparison for the test performed with Zhejing dolomite - for three gasification temperatures (test number 2, 5, 8) - among the equilibrium model

(EQ_1), the modified model (EQ_MOD), the experimental gas composition before (Exp) and after the catalyst (Exp_dolomite). It appears clearly that the gas composition predicted predicted by the "pure" equilibrium model is quite far from the real composition. The concentration of the carbon monoxide is overestimated as well as the hydrogen one; vice versa the carbon dioxide is underestimated and the methane is almost zero. Thanks to some modifications, a closer agreement between the simulated and the experimental data has been achieved. In the last column, the gas composition measured after the catalytic filter has been also reported. As discussed in paragraph 5.3.1, the dolomite bed has a slight influence on the syngas composition, anyway the gas composition after the dolomite is in better agreement with the modelled one.
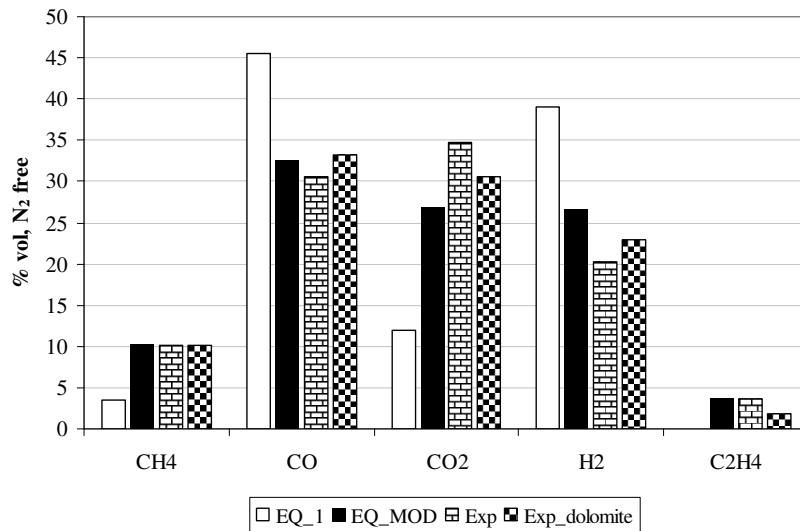
Figure 5.7 Comparison among the experimental gas composition (dry basis) and the output of the equilibrium models for the test number 2 (gasification temperature: 700°C)
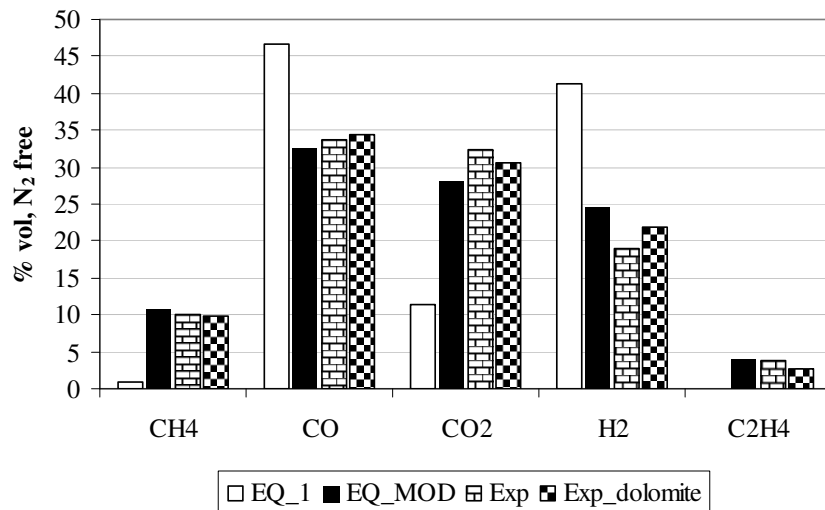
Figure 5.8 Comparison among the experimental gas composition (dry basis) and the output of the equilibrium models for the test number 5 (Gasification temperature: 750°C)
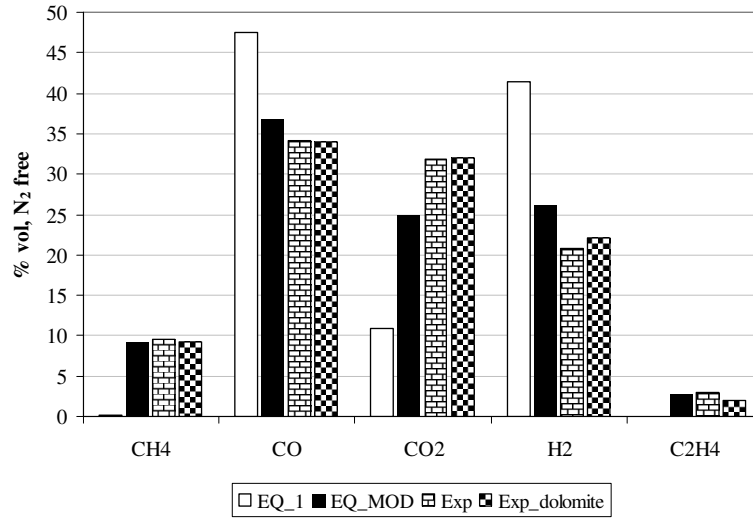
Figure 5.9 Comparison among the experimental gas composition (dry basis) and the output of the equilibrium models for the test number 10 (Gasification temperature: 800°C)

The syngas lower heating value (LHV) has been calculated both for modelled and experimental data. The values have been estimated as the weighted average of the gas composition. The results are summarized in table 5.10. A satisfying agreement between the experimental and the theoretical gas heating values has been assessed. It has also been noticed that, even using the output of the "pure" equilibrium model (EQ_1), the calorific value is not so far from the experimental one. This is probably due to the high concentrations of carbon monoxide and hydrogen predicted by the model that counterbalance the lack of methane.

Table 5.10 Low heating value estimated for modeling and experimental gas composition

	LHV (MJ Nm^{-3})			
Test number	EQ_1	EQ_MOD	Experimental	Exp_dolomite
1	11.2	12.6	11.5	12.0
2	11.2	12.7	11.8	11.8
3	11.2	12.3	11.1	11.7
4	10.5	12.7	12.2	11.7
5	10.6	12.8	12.1	11.9
6	10.6	12.4	11.8	11.9
7	10.7	12.6	12.1	11.7
8	10.5	12.4	11.6	11.2
9	10.8	12.7	11.9	11.8

Chapter 6

Conclusions and perspectives

At present, the biomass thermochemical conversion processes and their applications for heat and power generation are object of several research studies, to find out efficient systems to exploit the energy content of biomass, which is considered one of the most promising renewable energy sources.

The aim of the present work is to improve the understanding of the potential of the steam gasification process for power generation in small scale applications. The syngas produced via steam gasification process seems to be a suitable fuel both for gas engines and also for solid oxide fuel cells due to high hydrogen content.

The issues discussed in the previous sections, concern:

- the investigation on the current status of biomass gasification: the main operative plants at large, small and lab scale, and the analysis of the main parameters that influence the syngas quality (chapter 2);

- the design and development of a small scale fixed bed gasifier, with a semi continuous configuration and then with a continuous one, equipped with a steam generator and a hot gas cleaning line;

- the characterization of the syngas and the hydrogen sulphide produced via the steam gasification process as a function of the SC ratio and the gasification temperature (chapter 3);

- the comparison between the outputs of a two-phase thermodynamic equilibrium model, previously developed, and the experimental data. The non satisfactory agreement between the data and the model results have led to the development of a non stoichiometric equilibrium model that has been tuned up with the experimental data (chapter 4);

- the results of an extensive experimental activity performed in an oxygen fluidized bed gasifier at KTH, Stockholm, to investigate the tar cracking efficiency of different types of dolomites and two iron based catalysts. The data collected on the syngas composition have been compared with the outputs of the modified equilibrium model (chapter 5);

- the use of the experimental data to calibrate both the equilibrium model and a finite element model which solves the heat and Eulero equations and allows the simulation of the temperature profile inside the reactor.

Before the construction of any conversion systems, engineering models are usually applied to

design and evaluate the performances of these gasification systems. In this project there has been the opportunity to compare theoretical results with experimental data. A good agreement has been found in the evaluating the energy consumption required by the system.

A thermodynamic equilibrium model has been used in the preliminary phase of this project to estimate the syngas composition. The positive aspect of the thermodynamic approach is its applicability to several systems without a deep knowledge of the reaction mechanism. It can be successfully utilized to know the maximum theoretical performance of a biomass conversion process. A satisfactory agreement has been found between the experimental data and the equilibrium model simulations tuned with the data collected during the experimental activity on the steam gasifier. The same approach has been followed to predict the gas composition of the air gasifier tested at KTH in Stockholm, and a good agreement with the measured gas composition has been observed. Finally, a finite element model, tuned up with the experimental data, has been coupled with the quasi-equilibrium model with good results.

The experimental activity has included the building and testing of a continuous steam gasifier (11-13 kW_{th} in input) that can work for several hours. The syngas produced is characterized by a hydrogen content that ranges between 50-60% and a LHV of 8MJ Nm^{-3}. The obtained syngas seems to be a suitable fuel for fuel cells. The main problem is the gas cleaning: the Tar and the H_2S contained in the gas can rapidly decrease the life of the fuel cells. Since solid oxide fuel cells work at high temperature, a hot gas cleaning system has been built within the present project. The dolomite efficiency in tar cracking at high temperature (800°C) is well proved, as shown both in this project and in other experiences found in literature. A catalytic filter of a mixture of dolomite and manganese oxides, that recently has shown a good efficiency in H_2S abatement, has been prepared. However, the cleaning part is still the bottleneck of this experimental apparatus, since the optimum working conditions have not been found yet. Anyway, some preliminary tests have been done coupling the gasifier with a fuel cells stack and some promising results have been observed.

This project has shown the potential of the steam gasification process which is a promising way to obtain a gaseous fuel with high hydrogen content. It has also been confirmed that the gasification process, from a thermochemical point of view, is a complex phenomenon to be still studied in details. Anyway, the thermodynamic approach remains the simplest engineering tool to assess, with a good reliability, the theoretical performance attainable from a gasification system knowing only the main gasification parameters.

Therefore, further research activities are currently needed in this field:
- validating the application of the model to other power generating systems;
- extending the model with kinetic estimation of the methane production and/or the inclusion of the (third) liquid phase (i.e. including liquid vapor equilibrium);
- improving the laboratory apparatus tested (the steam gasifier plus the SOFC stack).

The first activity requires an extended state-of-art literature review focused on existing experimental activities, while the second one represents a (quite complex) enhancement of the proposed model,

that needs the coupling of a kinetic approach with the equilibrium one and/or the implementation of a further phase-equilibrium in the model code.

The last foreseen activity concerns the improvement of the small scale steam gasifier. For this purpose, an important issue is the changing of the reactor heating system. For example the char produced can be recovered and burned for the reactor heating. This is a compulsory step because the system must to be independent from the electric energy both for the small scale applications and for the scaling up of the plant. Moreover, the gas cleaning system has to be improved to get a higher gas quality. At the moment, a hot gas cleaning session is present. However a cold cleaning system has shown a better performance without needing the catalytic filter. On the other side a cold cleaning system implies the loss of the enthalpy content of the syngas coming out from the gasifier at high temperature.

The theoretical calculations show that an efficient solution would be the introduction of a regenerative heat exchanger coupled with a cold gas cleaning system. This configuration allows recovering the gas enthalpy content during its cooling from 800 to 100°C (the latent heat has not been considered in the heat exchanger) and using it for heating of the dry cleaned syngas from 25°C to 800°C. The calculations show that this solution works both for SC=2 and SC=3 and includes several advantages: avoids the heating of the catalytic filter, allows both a higher level of gas cleaning from tar and hydrogen sulphide and the removal of the water fraction present in the raw wet syngas. This configuration is recommended to improve the system efficiency and should be the next step in the improvement if the experimental apparatus.

References

Ahmed I., and Gupta A. K. "Syngas yield during pyrolysis and steam gasification of paper." *Applied Energy* 86, no. 9 (2009): 1813-1821.

Alderucci V., Antonucci P., Maggio G., Giordano N., and Antonucci V. "T hermodynamic analysis of a SOFC fuelled by biomass-derived gas." *International Journal of Hydrogen Energy* 19, no. 4 (April 1994): 369-376.

Altafini C., Wander P.R., Barreto R.M.. "Prediction of the working parameters of a wood waste gasifier through an equilibrium model." *Energy Conversion and Management* 44, no. 17 (October 2003): 2763-2777.

Atimtay A. T., Gasper-Galvin L.D., Poston J. A., "Novel supported sorbent for hot gas desulfurization." *Environmental Science & Technology* 27, no. 7 (July 1993): 1295-1303.

Babu B.V., Sheth P. N.. "Modeling and simulation of reduction zone of downdraft biomass gasifier: Effect of char reactivity factor." *Energy Conversion and Management* 47, no. 15-16 (September 2006): 2602-2611.

Baggio P., Baratieri M., Fiori L., Grigiante M., Avi D., and Tosi P., "Experimental and modeling analysis of a batch gasification/pyrolysis reactor." *Energy Conversion and Management* 50, no. 6 (June 2009): 1426-1435.

Bang-Moller C., Rokni M., "Thermodynamic performance study of biomass gasification , solid oxide fuel cell and micro gas turbine hybrid systems" *Energy Conversion and Management* 51,no.11 (2010): 2330-2339.

Baker E.G., Mudge L.K, Brown M.D., "Steam gasification of biomass with nickel secondary catalysts" *Ind.Eng.Chem.Res.* 26 (1987): 1335–1339.

Baratieri M., Pieratti E., Nordgreen T., and Grigiante M., "Biomass Gasification with Dolomite as Catalyst in a Small Fluidized Bed Experimental and Modelling Analysis." *Waste and Biomass Valorization,*no. 1, (2010):283-291.

Baratieri M., Baggio P., Fiori L., Grigiante M., "Biomass as an energy source: Thermodynamic constraints on the performance of the conversion process." *Bioresource Technology* 99 (2008): 7063-7073.

Baratieri M., Baggio P., "Sviluppo e progettazione di un sistema di piccola taglia basato sulla gassificazione di biomasse vegetali per la produzione di syngas atto ad alimentare pile a combustibile di tipo SOFC". Relazione Intermedia Progetto BioCheap (2007).

Beenackers A.A.C.M., "Biomass gasification in moving beds, a review of European technologies." *Renewable Energy* 16 (1999).

Brage C., Yu Q., Chen G., Sjöström K., "Use of amino phase adsorbent for biomass tar sampling and separation" *Fuel* 76(1997):137–142.

References

Brown D.W.M., Fuchino T., and Marechal F.M.A., "Stoichiometric equilibrium modelling of biomass gasification: validation of artificial neural network temperature difference parameter regressions*." Journal of chemical engineering of Japan 40*, no.3 (2007): 244-254.

Campoy M., Gómez-barea A., Vidal F. B., Ollero P., "Air – steam gasification of biomass in a fluidised bed: Process optimisation by enriched air." *Fuel Processing Technology* 90, no. 5 (2009): 677-685.

Channiwala S.A., and Parikh P.P., "A unified correlation for estimating HHV of solid, liquid and gaseous fuels." *Fuel* 81, no. 8 (May 2002): 1051-1063.

Chen G., Andries J., Spliethoff H., Fang M., Van de Enden P. J., "Biomass gasification integrated with pyrolysis in a circulating fluidised bed", *Solar Energy*, no. 76, (2004): 345-349.

Choren (2010) http://www.choren.com/en/carbo-v/carbo-v/

Cordiner S., Feola M. Mulone V., and Romanelli F., "Analysis of a SOFC energy generation system fuelled with biomass reformate." *Applied Thermal Engineering* 27, no. 4 (March 2007): 738-747.

Keith R. C., Brown R. C., "Ancillary equipment for biomass gasification." *Biomass and Bioenergy* no.23 (2002): 118- 128.

Delgado J., Aznar M.P., "Corella J., Calcined dolomite, magnesite, and calcite for cleaning hot gas from a fluidized bed biomass gasifier with steam: life and usefulness". *Ind. Eng. Chem. Res.* 35 (1996): pp. 3637-3643.

Demirbas M.F., Balat M., and Balat H., "Potential contribution of biomass to the sustainable energy development". *Energy conversion and Management*. no. 50, (2009): 1746-1760.

Dennis J., "The kinetics of combustion of chars derived from sewage sludge." *Fuel* 84, no. 2-3 (February 2005): 117-126.

DI Blasi C., "Dynamic behaviour of stratified downdraft gasifiers." *Chemical Engineering Science* 55, 15 (August 2000): 2931-2944.

Dogru M., Howarth C. R., Akay G., Keskinler B., Malik A. A., "Gasification of hazelnut shells in a downdraft gasifier", *Energy*, 27, 415-427 (2002).

Dogru M., Midilli A., Howarth C. R., "Gasification of sewage sludge using a throated downdraft gasifier and uncertainty analysis", *Fuel Processing Technology*, 75, 55-82 (2002).

Evans R.J., Milne T.A., "Molecular Characterization of the Pyrolysis of Biomass. 1. Fundamentals", *Energy & Fuels 1* , 2 (1987) pp.123–138

Evans R.J., Milne T. A., "Molecular Characterization of the Pyrolysis of Biomass. 2. Applications" *Energy & Fuels 1*, 4 (1987) pp. 311–319.

Evans R.J., Milne T.A., "Chemistry of tar formation and maturation in the thermochemical conversion of biomass". In: Developments in thermochemical biomass conversion. Bridgwater AV, Boocock DBG. DBG Ed., London, 2, (1997): 803-816.

References

Fermoso J., Gil M.V., Pevida C., Pis J.J., Rubiera F., "Kinetic models comparison for non-isothermal steam gasification of coal–biomass blend chars." *Chemical Engineering Journal* 161, no. 1-2 (July 2010): 276-284.

Fiaschi D., Michelini M., "A two-phase one-dimensional biomass gasiÿcation kinetics model." *Biomass and Bioenergy* 21 (2001): 121-132.

Franco C., Pinto F., Gulyurtlu I., Cabrita I., "The study of reactions influencing the biomass steam gasification process". *Fuel*, 82 (2003): 835–842.

García-Ibañez P., Cabanillas A., Sánchez J. M., "Gasification of leached orujillo (olive oil waste) in a pilot plant circulating fluidised bed reactor. Preliminary results", *Biomass & Bioenergy*, 27, (2004).183-194.

García-García A., Gregório A., Franco C., Pinto F., Boavida D., Gulyurtlu I., "Unconverted chars obtained during biomass gasification on a pilot-scale gasifier as a source of activated carbon production", *Bioresource Technology*, 88, (2003):27-32.

Gil J., Corella J., Aznar M. P., Caballero M. A., "Biomass gasification in atmospheric and bubbling fluidized bed: Effect of the type of gasifying agent on the product distribution", *Biomass & Bioenergy*, 17, (1999): 389-403.

Gil J., Aznar M.P., Caballero M.A., Frances E., Corella J., "Biomass gasifiction in fluidized bed at pilot scale with steam-oxygen mixtures. Product distribution for very different operating conditions", *Energy Fuels*, 11 (6), (1997): 1109 -1118.

Giltrap D. L., Mckibbin R., and Barnes G. R. G., "A steady state model of gas-char reactions in a downdraft biomass gasifier." *Solar Energy,* 74 (2003): 85-91.

Gøbel B., Henriksen U., Jensen T. K., Qvale B., and Houbak N., "The development of a computer model for a fixed bed gasifier and its use for optimization and control." *Bioresource Technology* 98 (2007): 2043-2052.

Gonzalez J., Roman S., Bragado D., and Calderon M., "Investigation on the reactions influencing biomass air and air/steam gasification for hydrogen production." *Fuel Processing Technology* 89, no. 8 (August 2008): 764-772.

Gordillo E.D., and Belghit A., "A two phase model of high temperature steam-only gasification of biomass char in bubbling fluidized bed reactors using nuclear heat." *International Journal of Hydrogen Energy* (October 2010): 1-8.

Granatstein D., "Case study on waste-fuelled gasification project Greve in Chianti,Italy." *IEA Bioenergy Agreeement*, Task 36.(2003).

Guglielmini G., Pisoni C., "Introduzione alla trasmissione del calore" Ed. CEA, 2004.

Guo B., Shen Y., Li D., and Zhao F., "Modelling coal gasification with a hybrid neural network." *Fuel* 76, no. 12 (October 1997): 1159-1164.

Guo B., Li D., Cheng C., and Shen Y., "Simulation of biomass gasi ® cation with a hybrid neural network model." *Bioresource Technology* 76 (2001).

Hall D.O., Overend RP 1978. Biomass, *Regenerable Energy*. Wiley, Great Britain.

References

Hannuala I., Lappi K., Simell P., Kukela E., Luoma P., and Haavisto I., "High efficiency biomass to power operation experiences and economical aspect of the novel gaisification process." In *15th European and biomass Conference and Exhibition(2007)*, 2252-2255.

Hasler P., and Nussbaumer T., "Gas cleaning for IC engine applications from fixed bed biomass gasification", *Biomass and Bioenergy*, 16 (1999): 385-395.

Heginuz E., Gregertsen B., Sorvari, Vriesman, Sjöström K., "Studies on solid fuel pyrolysis and fluidisation in a laboratory-scale, atmospheric, fluidised bed reactor", *Finnish-Swedish Flame Days, Proceedings*, Naantali, Finland, (1996).

Henriksen U., Ahrenfeldt J., Jensen T., Gobel B., Bentzen J., Hindsgaul C., and Sorensen L., "The design, construction and operation of a 75kW two-stage gasifier." *Energy* 31, no. 10-11 (August 2006): 1542-1553.

Herguido J., Corella J., Gonzalez-saiz J., "Steam gasification of lignocellulosic residues in a fluidized bed at a small pilot scale. Effect of the type of feedstock", *Industrial & engineering chemistry research*, no. 31, 5 (1997): 1274-1282.

Hofbauer H., Rauch R., Loeffler G.,Kaiser S., Fercher E., and Tremmel H., "Six years experience with the FICFB-Gasification process." *15th European and biomass Conference and Exhhibition* (2007).

Hornik K., "Approximation capabilities of multilayer feedforward networks." *Neural Networks* 4, no. 2 (1991): 251-257.

Jayah T. H., Aye L., Fuller R. J., and Stewart D. F., "Computer simulation of a downdraft wood gasiÿer for tea drying." *Biomass and Bioenergy* 25 (2003): 459 - 469.

Jarungthammachote S., and Dutta Ã., "Thermodynamic equilibrium model and second law analysis of a downdraft waste gasifier." *Energy* 32 (2007): 1660-1669.

Jarungthammachote S., and Dutta Ã., "Equilibrium modeling of gasification: Gibbs free energy minimization approach and its application to spouted bed and spout-fluid bed gasifiers." *Energy Conversion and Management* 49, no. 6 (June 2008): 1345-1356.

Kaushal P., Abedi J., and Mahinpey N., "A comprehensive mathematical model for biomass gasification in a bubbling fluidized bed reactor." *Fuel* 89, no. 12 (December 2010): 3650-3661.

Kelley K.K., "U.S. Bureau of Mines Bulletin" (1960), 584.

Kersten S. R. A., Prins W., Van der Drift B., Van Swaaij, W. P. M., "Principles of a novel multistage circulating fluidized bed reactor for biomass gasification", *Chemical Engineering Science*, no. 58, (2003): 725-731.

Kersten S. R. A., Prins W., Van der Drift B., Van Swaaij, W. P. M., "Interpretation of biomass gasification by "quasi" equilibrium models." *In Proceedings of the twelfth European Conference on biomass for energy, industry and climate protection* (2002).

Klass D.L., Biomass for renewable energy, fuels, and chemicals. San Diego: Academic Press. (1998)

References

Kikuchi R., Sato H., Matsukura Y., Yamamoto T., "Semi-pilot scale test for production of hydrogen-rich fuel gas from different wastes by means of a gasification and smelting process with oxygen multi-blowing", *Fuel Processing Technology*, no. 86, (2005):1279-1296.

Tzu-Hsing K., Chu H, and Lung-Kai C., "The sorption of hydrogen sulfide from hot syngas by metal oxides over supports." *Chemosphere* 58, no. 4 (January 2005): 467-74.

Kramreiter R., Url M., Kotik J., Hofbauer H., "Experimental investigation of a 125kW twin-fire ixed bed gasification pilot plant and comparison to the results of a 2MW comnbined heat and power plant (CHP)",*Fuel Processing Technolog,*no. 89,(2008): 90-102.

Li X., "Equilibrium modeling of gasification: a free energy minimization approach and its application to a circulating fluidized bed coal gasifier." *Fuel* 80, no. 2 (January 2001): 195-207.

Li X., "Biomass gasification in a circulating fluidized bed." *Biomass and Bioenergy* 26, no. 2 (February 2004): 171-193.

Linanki L., Lindman N., Sjoberg S.O., Strom E., "Methane yield from Biomass Gasification at high temperature and pressure". Royal institute of technology, Department of Chemical Technology, Stockholm, Sweden (2001).

Loha C., Chatterjee P. K., and Chattopadhyay H. "Performance of fluidized bed steam gasification of biomass – Modeling and experiment." *Energy Conversion and Management* 52, no. 3 (March 2011): 1583-1588.

Luo S., Bo X., Zhiquan H., Shiming L., Xianjun G., and Maoyun H., "Hydrogen-rich gas from catalytic steam gasification of biomass in a fixed bed reactor : Influence of temperature and steam on gasification performance." *International Journal of Hydrogen Energy* 34, no. 5 (2009): 2191-2194.

Lv, P. M., Xiong, Z. H., Chang, J., Wu, C. Z., Chen, Y., Zhu, J. X., "An experimental study on biomass air–steam gasification in a fluidized bed", *Bioresource Technology*, no. 95, (2004): 95–101.

Manyà, J. J., Sánchez, J. L., Ábrego, J., Gonzalo, A., Arauzo, J., "Influence of gas residence time and air ratio on the air gasification of dried sewage sludge in a bubbling fluidised bed", *Fuel*, no. 85, (2006): 2027–2033.

McBride B.J., Gordon S., Reno M.A., "Coefficients for Calculating Thermodynamic and Transport Properties of Individual Species", NASA Report TM-4513 (1993).

Mckendry P., "Energy production from biomass (part 1): overview of biomass." *Bioresource Technology* 83, no. July 2001 (2002): 37-46.

Mckendry P., "Energy production from biomass (part 2): conversion technologies." *Bioresource Technology* no. 83, July 2001 (2002): 47-54.

Mckendry P., "Energy production from biomass (part 3): gasification technologies." *Bioresource Technology* 83, no. July 2001 (2002): 55-63.

Midilli A., Dogru M., Howarth C. R., Ling M. J., Ayhan T., "Combustible gas production from sewage sludge with a downdraft gasifier*", Energy Conversion & Management*, no. 42, (2001): 157-172.

References

Mitta N.R., Ferrer-Nadal S., Lazovic A.M., Perales J.F., Velo E., Puigjaner L., "Modelng and simulation of a tyre gasification plant for synthesis gas production". In proceedings of *16th European symposium on computed aided process engineering and 9th international symposium on process system engineering* (2006): 1771-1776.

Nagel F. P., Künstle M., Biollaz S., "Link-up of a solid oxide fuel cell with a wood gasifier", *Proceedings of 14th European Biomass Conference*, 17-21 October 2005, Paris, France.

Nagel, F.P., S. Ghosh, C. Pitta, T.J. Schildhauer, and S. Biollaz. "Biomass integrated gasification fuel cell systems–Concept development and experimental results." *Biomass and Bioenergy* (September 2010):

Narvez I., Orio A., Aznar M. P., Corella J., "Biomass gasification with air in an Atmospheric bubbling fluidized bed. Effect of the six operative variable on the quality of the producer raw gas". *Ind. Eng. Chem. Res*., no.35 (1996): pp 2110–2120.

Nemanova V,, Nordgreen T,, Engvall K., Sjöström K., "Biomass gasification in an atmospheric fluidised bed: Tar reduction with experimental iron-based granules from Höganäs AB, Sweden." *Catalysis Today*, no. 2010 (January 2011): 8-12.

Tamhankar S.S., Tsuchiya K., Riggs J.B., "Catalytic cracking of benzene on iron oxide-silica : catalyst activity and reaction mechanism".*Appl.Catal*.16(1985): 103–121.

Torres W., Pansare S.S., Goodwin Jr. J.G., "Hot gas removal of tars, ammonia and hydrogen sulphide from biomass gasification gas" *Cat.Rev*.49 (2007) : 407–456.

Toshiaki H., Seiichi I., Seiji U., Tomoko O., Tomoaki M., "Effect of woody biomass components on air-steam gasification", *Biomass & Bioenergy*, no. 28 (2005) : 69-76.

Toman N., Review on hot gas cleans up, 2001.

Turn S., Kinoshita C., Zhang Z., Ishimura D., Zhou J., "An experimental investigation of hydrogen production from biomass gasification", *Hydrogen Energy*, no.8, (1998): 641-648.

Ocampo A., Arenas E., Chejene F., Espinel J., Londoño C., Aguirre J., Perez J. D., "An experimental study on gasification of Colombian coal in a fluidized bed", *Fuel*, no. 82, (2003):161-164.

Olivares A., Aznar M.P., Caballero M.A., Gil J., Frances E., Corella J., "Biomass gasification: produced gas upgrading by in-bed use of dolomite".*Ind. Eng. Chem. Res.* 36, 5220-5226 (1997).

Olofsson I., Nordin A., Söderlind U., "Initial review and evaluation of process technologies and systems suitable for biomass to liquid fuels." (2005) http://www.biofuelregion.se/dokument/5_95.pdf

Omosun A. O., Bauen A., Brandon N. P., Adjiman C. S., Hart D., "Modelling system efficiencies and costs of two biomass-fuelled SOFC systems." *Journal of Power Sources* 131, no. 1-2 (May 2004): 96-106.

Pankratz L.B., "U.S. Bureau of Mines Bulletin" ,(1982), 672.

Parikh J., Channiwala S., and Ghosal G., "A correlation for calculating HHV from proximate analysis of solid fuels." *Fuel* 84, no. 5 (March 2005): 487-494.

References

Pathak B.S., Patel S.R., have A.G., Bhoi P.R., Sharma A.M., Shah N.P., "Performance evaluation of an agricultural residue-based modular throat-type down-draft gasifier for thermal application", *Biomass and Bioenergy*, no.32 , (2008):72-77.

Pengmei L., Zhenhong Y., Longlong M., Chuangzhi W., Yong C., Jingxu Z., "Hydrogen-rich gas production from biomass air and oxygen/steam gasification in a downdraft gasifier", *Renewable Energy*,no. 32, (2007): 2173-2185.

Pieratti E., Patuzzi F., Baratieri M., Baggio P., Grigiante M., "Parametric analysis of small scale biomass gasification plant" *Proceedings of 16th European biomass conference,* Valencia (2008).

Pieratti E., Baratieri M., Baggio P., Grigiante M., Ceschini S., "A biomass steam gasification pilot plant: syngas suitability for SOFC stacks" Proceedings of *3rd International Conference on Engineering for Waste and Biomass Valorisation*, 17-19 (May 2010), Beijing, China.

Pindoria R. V., Megaritis A., Messenböck R. C., Dugwell D. R., Kandiyoti R., "Comparison of the pyrolysis and gasification of biomass: effect of reacting gas atmosphere and pressure on Eucalyptus wood", *Fuel*, no.77, 11, (1998): 1247-1251.

Pinto F., Franco C., André R. N., Miranda M., Gulyurtlu I., Cabrita I., "Co-gasification study of biomass mixed with plastic wastes", *Fuel*, no. 81, (2002): 291-297.

Phyllis, database for biomass and waste, http://www.ecn.nl/phyllis Energy research Centre of the Netherlands

Press W.H., Teukolsky S.A., Vetterling W.T., Flannery B.P., "Numerical Recipes 3rd Edition: The Art of Scientific Computing". Cambridge University Press, (2007).

Prins M. J., Ptasinski K. J., Janssen F., "From coal to biomass gasification: Comparison of thermodynamic efficiency". *Energy* 32, 1248-1259 (2007).

Rapagnà S., Jand N., Kiennemann A., Foscolo P.U., "Steam-gasification of biomass in a fluidised-bed of olivine particles", *Biomass & Bioenergy*, no. 19, (2000): 187-197.

Rostami A., "Modeling of smoldering process in a porous biomass fuel rod." *Fuel* 83, no. 11-12 (August 2004): 1527-1536.

Ruggiero M., Manfrida G., "An equilibrium model for biomass gasification processes." *Renewable Energy* 16 (1999): 1106-1109.

Salo K., Horvath A., "Biomass Gasification in Skive: Opening Doors in Denmark" Articles of *Renewable Energy World* (2009)

http://www.renewableenergyworld.com/rea/news/article/2009/01/biomass-gasification-in-skive-opening-doors-in-denmark-54341.

Sharma A., "Equilibrium and kinetic modelling of char reduction reactions in a downdraft biomass gasifier: A comparison." *Solar Energy* 82, no. 10 (October 2008): 918-928.

Sheng C., Azevedo Ã. "Estimating the higher heating value of biomass fuels from basic analysis data." *Biomass and Bioenergy* 28 (2005): 499-507.

Babu S., "Workshop No. 1: perspective on biomass gasification". *IEA bioenergy agreement Task 33: Thermal gasification of biomass*. (May 2006).

References

Shoko E. Mclellan B. Dicks A. and Dacosta J.,"Hydrogen from coal: Production and utilisation technologies." *International Journal of Coal Geology* 65 (August 2005): 213 - 222.

Smith W.R., Missen R.W., "Chemical Reaction Equilibrium Analysis: Theory and Algorithm." Wiley - Interscience, New York (1982).

Spencer H.M. *Ind.Eng.Chem* 40 (1948):2152-54.

Srivastava V.J., "Manufactured gas plant sites: characterization of wastes and IGT's innovative remediation alternatives." *Hazardous and Environmentally Sensitive Waste Management in the Gas Industry Proceedings*, (1993) Albuquerque.

Turare C., "Biomass gasification technology and utilization".Report, ARTES Institute of Glucksburg, Germany.

Umeki K., Yamamoto K., Namioka T., Yoshikawa K., "High temperature steam-only gasification of woody biomass", *Applied Energy* 87, (2010):791-798.

Van Krevelen D.W., Coal—Typology—Physics—Chemistry—Constitution (3rd ed.), Elsevier, Amsterdam (1993).

Van Kasteren, J. M. N., "Co-gasification of wood and polyethylene with the aim of CO and H_2 production", *Mater Cycles Waste Managment*, no. 8 (2006): 95-98.

Valin S., Ravel S., Guillaudeau J., Thiery S.. "Comprehensive study of the influence of total pressure on products yields in fluidized bed gasification of wood sawdust." *Fuel Processing Technology* 91, no. 10 (October 2010): 1222-1228.

Vervaeke P., Tack F. M. G., Navez F., Martin J., Verloo M. G., Lust N., "Fate of heavy metals during fixed bed downdraft gasification of willow wood harvested from contaminated sites", *Biomass & Bioenergy*, no. 30, (2006): 58-65.

Vriesman P., "Nitrogen conversion in a biomass fuelled atmospheric fluidised bed gasifier", Licentiate of engineering thesis, KTH, (2001).

VVBGC, 2010 http://www.vvbgc.se

Waldheim L., Nilsson T., "Heating value of gases from biomass gasification" Report prepared for IEA Bioenergy Agreement, Task 20-Thermal gasification process. (May 2001).

Wang Y., and Kinoshita C. M., "kinetic model of biomass gasification." *Solar Energy* 51, no. 1 (1993): 19-25.

Wojcik A., Middleton H., Damaopoulos I., Van Herle J.. "Ammonia as a fuel in a solid oxide fuel cells." *Journal of Power Sources* no.118 (2003): 342-348.

Wu W., Kawamoto K., Kuramochi H., "Hydrogen-rich synthesis gas production from waste wood via gasification and reforming technology for fuel cell application", *Mater Cycles Waste Manag*, 8, 70-77 (2006).

Yan F., Zhang L., Hu Z., Cheng G., Jiang C., Zhang Y., Xu T., He P., Luo S., Xiao B.. "Hydrogen-rich gas production by steam gasification of char derived from cyanobacterial blooms (CDCB) in a fixed-bed reactor: Influence of particle size and residence time on gas yield and syngas

composition." *International Journal of Hydrogen Energy 35*, no. 19 (October 2010): 10212-10217.

Yang Y. "Effects of fuel devolatilisation on the combustion of wood chips and incineration of simulated municipal solid wastes in a packed bed★." *Fuel* 82, no. 18 (December 2003): 2205-2221.

Yu Q.-Z., Brage C., Nordgreen T., Sjstrom K., "Effects of Chinese Dolomites on tar cracking in gasification of birch", *Fuel,* no 88, (2009):1922-1926.

Zainal Z. A., Rifau A., Quadir G. A., Seetharamu K. N., "Experimental investigation of a downdraft biomass gasifier", *Biomass & Bioenergy*, no.23, (2002):283-289.

Zainal Z. A., Ali R., Lean C. H., Seetharamu K. N., "Prediction of performance of a downdraft gasifier using equilibrium modeling for different biomass materials." *Energy* 42 (2001).

Zevenhoven-Onderwater M., Backman R., Skrifvars B., Hupa M., Liliendahl T., Rose C., "The ash chemistry in ̄ uidised bed gasi ® cation of biomass fuels . Part II : Ash behaviour prediction versus bench scale agglomeration tests." *Chemical Engineering,no.* 80 (2001): 4-7.

Zanzi R., Björnbom E., Soria S., Grimm A., "Fixed bed updraft gasification of biomass", *14th European Biomass Conference*, 17-21 October 2005, Paris, France.

Appendix A

Report of the tests run at KTH

In Appendix A the results of the experimental test performed at KTH, Stockholm are reported. The first table shows the test run with dolomite as catalyst, instead the second and third tables report the results for the test run with iron based catalyst. The gas and tar composition, and the carbon balances are summarized.

Appendix A

Summary of parameters and results of the tests run with dolomite as catalyst.

Catalyst	1D		2D		3D		4D		5D		6D		7D		8D		9D	
	Sala		Zhejing		Shanxi		Sala		Zhejing		Shanxi		Sala		Zhejing		Shanxi	
Temperature Bed (°C)	700		700		700		750		750		750		800		800		800	
Temperature Catalyst (°C)	800		800		800		800		800		800		800		800		800	
ER	0.21		0.21		0.21		0.25		0.24		0.24		0.23		0.23		0.22	
feeding (g min^{-1})	4.17		4.17		4.23		3.59		3.72		3.73		3.78		3.58		4.03	
Char in bed (g tot)	15.10		10.00		15.80		1		3		6.2		3		3.2		2.3	
Gas product (N$_2$ free(vol%))	**before**	**after**	**before**	**after**	**before**	**after**	**before**	**after**	**before**	**after**	**before**	**after**	**before**	**after**	**before**	**after**	**before**	**after**
reaction time (min)	60	75	55	68	45	75	40	50	50	50	55	51	40	54	45	45	30	61
CO$_2$	34.19	30.02	34.73	30.51	34.59	30.92	31.88	31.19	32.42	30.60	33.19	30.50	29.73	29.26	31.82	31.95	29.73	29.62
C$_2$H$_4$	3.39	2.63	3.65	1.79	2.49	0.00	3.93	2.24	3.84	2.66	3.73	2.86	3.19	1.89	2.96	1.99	3.19	2.37
C$_2$H$_6$	0.00	0.00	0.00	0.64	0.00	1.98	0.00	0.00	0.00	0.00	0.00	0.00	0.10	0.08	0.00	0.00	0.10	0.00
C$_2$H$_2$	0.66	0.22	0.00	0.00	0.00	0.00	0.52	0.22	0.44	0.18	0.50	0.22	0.00	0.00	0.17	0.13	0.00	0.19
H$_2$	22.05	24.20	20.27	22.98	21.54	23.15	18.06	21.87	18.93	21.93	20.20	22.08	19.87	22.53	20.75	22.18	19.87	22.49
CH$_4$	9.54	9.92	10.18	10.15	9.76	10.23	10.19	10.00	10.02	9.72	9.84	9.54	9.81	9.93	9.50	9.16	9.81	9.72
CO	29.87	32.76	30.61	33.30	31.29	33.46	34.83	33.92	33.69	34.28	31.92	34.15	36.63	35.71	34.16	33.95	36.63	34.94
Low Heating value	11.96	11.99	11.87	11.81	11.26	11.67	12.63	11.69	12.43	11.86	12.24	11.95	12.25	11.68	11.82	11.23	12.25	11.84
Syngas production (Nm^3 /kg$_{biom}$)	0.64	0.76	0.89	1.02	0.87	0.97	1	1.07	0.97	1.04	0.98	1.05	1.04	1.12	1.01	0.99	1.01	1.06
Tar																		
Tar without benzene(mg g^{-1}$_{biom}$)	14.51	4.00	18.90	5.38	17.40	4.99	18.42	5.32	19.98	7.06	16.12	6.64	15.89	5.38	10.5	4.9	15.3	7
Benzene (mg g^{-1}$_{biom}$)	8.94	12.36	12.41	17.40	11.53	14.99	13	16.17	19.09	20.36	16.38	19.08	21.2	18.59	16.74	17.2	18.8	18.75
Indene (mg g^{-1}$_{biom}$)	1.36	0.00	1.93	0.00	1.46	0.00	1.45	0	1.6	0	1.19	0	0.28	0	0.28	0	0.24	0
Napthalene (mg g^{-1}$_{biom}$)	1.78	1.97	2.65	2.80	2.38	2.81	3.12	2.42	4.53	3.95	3.76	3.56	5.36	3.04	4.01	3.54	4.6	3.28
Toluene (mg g^{-1}$_{biom}$)	4.59	2.02	5.80	1.70	5.52	1.57	4.72	2	5.8	2.26	5.23	2.07	2.11	0.88	1.49	0.75	1.8	0.76
Carbon conversion																		
to gas (%wt)	60.0	64.0	81.0	89.0	80.0	85.1	94.5	94.59	94.87	91.22	92.80	93.7	96.0	98.0	86.0	87.0	91.0	94.0
to char (%wt)	6.0	6.0	4.0	4.0	7.0	7.0	4	0.65	0.65	1.46	1.46	1.9	1.8	1.8	1.8	1.8	1.3	1.3
to tar (%wt)	1.0	1.1	1.0	1.1	1.0	1.1	1.5	1.55	1.09	1.98	1.44	1.3	2.0	1.5	1.4	1.0	1.5	1.5
mass balance %	67.0	71.1	86.0	94.1	88.0	93.2	100	96.80	96.62	94.67	95.70	96.9	99.8	101.3	89.2	89.8	93.8	96.8

Appendix A

Summary of parameters and results of the tests run with iron as catalyst.

Test number	1I			2I			3I			4I		
Catalyst	Iron A			Iron A			Iron A			Iron A		
Temperature Bed (°C)	750			800			850			800		
Temperature Catalyst (°C)	850/900			750/800			750/800			800/850		
ER	0.22			0.22			0.22			0.22		
feeding (g min^{-1})	3.70			3.70			3.70			3.70		
Char in bed (g tot)	20.00			9.80			11.00			7.00		
Gas product (N$_2$ free(vol%))	before	Iron 850°C	Iron 900°C	Before	Iron 750°C	Iron 800°C	Before	Iron 750°C	Iron 800°C	Before	Iron 800°C	Iron 850°C
CO$_2$	34.99	32.50	26.95	32.15	30.47	29.78	24.35	26.27	24.57	39.79	36.71	33.33
C$_2$H$_4$	0.00	0.00	0.00	0.00	0.00	0.00	0.00	0.00	0.00	0.00	0.00	0.00
C$_2$H$_6$	2.58	1.75	0.74	1.80	1.62	1.43	0.58	0.58	0.47	1.37	1.09	0.84
C$_2$H$_2$	0.29	0.10	0.00	0.11	0.21	0.16	0.01	0.09	0.06	0.07	0.09	0.04
H$_2$	21.91	24.98	25.10	22.96	24.16	24.35	25.14	25.35	25.43	20.58	22.98	22.55
CH$_4$	9.49	6.18	8.78	9.10	9.48	9.06	8.72	8.72	8.17	7.79	7.81	7.74
CO	30.46	34.38	38.19	33.53	33.69	34.90	40.91	38.69	41.01	30.04	30.96	35.17
Low Heating value	11.44	10.44	11.16	11.20	11.42	11.30	11.39	11.17	11.19	9.73	9.95	10.21
Syngas production (Nm^3 kg^{-1})	1.03	0.99	1.04	0.99	1.09	1.07	1.19	1.17	1.15	1.08	1.16	1.18
Tar												
Tar without benzene(mg g^{-1}$_{biom}$)	-	-	-	6.68	4.91	5.05	2.21	2.03	2.34	1.34	1.11	3.07
Benzene (mg g^{-1}$_{biom}$)	-	-	-	10.20	10.49	10.25	10.75	10.11	10.31	7.92	8.47	8.57
Indene (mg g^{-1}$_{biom}$)	-	-	-	0.31	0.23	0.20	0.17	0.16	0.37	0.08	0.12	0.20
Napthalene (mg g^{-1}$_{biom}$)	-	-	-	2.95	2.33	2.43	0.66	0.72	1.16	0.02	0.60	1.26
Toluene (mg g^{-1}$_{biom}$)	-	-	-	0.66	0.49	0.33	0.11	0.07	0.06	0.30	0.16	0.11
Carbon conversion												
to gas (%wt)	80%	79%	78%	78%	84%	82%	90%	88%	86%	87%	90%	92%
to char (%wt)	10%	10%	10%	5%	5%	5%	5%	5%	5%	3%	3%	3%
to tar (%wt)	2%	0%	0%	3%	3%	3%	2%	2%	2%	2%	2%	2%
mass balance %	92%	89%	88%	86%	92%	90%	98%	96%	94%	92%	96%	97%

Test number	5I		6I			7I			8I		
Catalyst	Iron A		Iron A			Iron B			Iron B		
Temperature Bed (°C)	800		800			800			800		
Temperature Catalyst (°C)	850		850/900			750/800			850/900		
ER	0.32		0.22			0.22			0.22		
feeding (g min^{-1})	3.70		3.70			3.70			3.70		
Char in bed (g tot)	10.00		14.00			14.00			10.50		
Gas product (N$_2$ free(vol%))	**Before**	**Iron 850°C**	**before**	**Iron 850°C**	**Iron 900°C**	**Before**	**Iron 750°C**	**Iron 800°C**	**Before**	**Iron 850°C**	**Iron 900°C**
CO$_2$	25.94	42.53	31.60	29.24	25.75	32.30	31.90	31.72	34.02	32.11	27.33
C$_2$H$_4$	0.00	0.00	0.00	0.97	0.00	0.00	0.00	0.00	0.00	0.00	0.00
C$_2$H$_6$	1.56	1.15	1.87	0.66	0.81	1.92	1.91	1.74	2.41	1.85	0.63
C$_2$H$_2$	0.12	0.06	0.10	0.07	0.01	0.14	0.17	0.19	0.22	0.10	0.00
H$_2$	25.77	18.99	23.16	24.62	25.04	23.40	23.45	24.39	22.12	25.32	26.76
CH$_4$	10.26	6.56	9.53	9.17	9.17	9.24	9.46	9.04	9.65	9.32	8.69
CO	35.95	30.35	33.41	34.96	38.91	32.67	32.80	32.59	31.13	35.21	37.37
Low Heating value	12.08	9.01	11.40	11.40	11.44	11.28	11.39	11.22	11.45	11.77	11.13
Syngas production (Nm^3 kg^{-1})	0.82	1.20	1.04	0.99	1.09	1.01	1.06	1.03	1.07	1.02	1.08
Tar											
Tar without benzene(mg g^{-1}$_{biom}$)	-	-	5.63	4.37	2.37	5.99	5.50	4.96	5.69	4.22	3.04
Benzene (mg g^{-1}$_{biom}$)	-	-	9.61	8.53	7.98	8.99	9.61	8.54	7.46	8.80	6.96
Indene (mg g^{-1}$_{biom}$)	-	-	0.39	0.19	0.05	0.30	0.19	0.19	0.17	0.20	0.20
Napthalene (mg g^{-1}$_{biom}$)	-	-	1.97	2.06	1.43	2.29	2.35	2.12	2.25	2.05	1.52
Toluene (mg g^{-1}$_{biom}$)	-	-	0.59	0.18	0.13	0.61	0.53	0.42	0.49	0.18	0.09
Carbon conversion											
to gas (%wt)	97%	81%	82%	76%	82%	79%	83%	80%	87%	90%	92%
to char (%wt)	5%	5%	7%	7%	7%	5%	5%	5%	5%	5%	5%
to tar (%wt)	2%	2%	2%	2%	2%	2%	2%	2%	2%	2%	2%
mass balance %	104%	88%	91%	85%	91%	87%	91%	87%	95%	98%	99%